



# **BRNO UNIVERSITY OF TECHNOLOGY**

VYSOKÉ UČENÍ TECHNICKÉ V BRNĚ

## **FACULTY OF MECHANICAL ENGINEERING**

FAKULTA STROJNÍHO INŽENÝRSTVÍ

## **INSTITUTE OF SOLID MECHANICS, MECHATRONICS AND BIOMECHANICS**

ÚSTAV MECHANIKY TĚLES, MECHATRONIKY A BIOMECHANIKY

## **STRESS-STRAIN ANALYSIS OF THE RAILWAY BRIDGE IN ZAHRÁDKY NEAR ČESKÁ LÍPA**

NAPJATOSTNĚ DEFORMAČNÍ ANALÝZA ŽELEZNIČNÍHO MOSTU V ZAHRÁDKÁCH U ČESKÉ LÍPY

### **BACHELOR'S THESIS**

BAKALÁŘSKÁ PRÁCE

### **AUTHOR**

AUTOR PRÁCE

Abdul rahman Abdul moghni

### **SUPERVISOR**

VEDOUCÍ PRÁCE

doc. Ing. Vladimír Fuis, Ph.D.

**BRNO 2021**

# Assignment Bachelor's Thesis

Institut: Institute of Solid Mechanics, Mechatronics and Biomechanics  
Student: **Abdul rahman Abdul moghni**  
Degree program: Applied Sciences in Engineering  
Branch: Mechatronics  
Supervisor: **doc. Ing. Vladimír Fuis, Ph.D.**  
Academic year: 2020/21

As provided for by the Act No. 111/98 Coll. on higher education institutions and the BUT Study and Examination Regulations, the director of the Institute hereby assigns the following topic of Bachelor's Thesis:

## **Stress–strain analysis of the railway bridge in Zahrádky near Česká Lípa**

### **Recommended bibliography:**

JANÍČEK, P., ONDRÁČEK, E., VRBKA, J. a BURŠA, J. Mechanika těles: Pružnost a pevnost I, Akademické nakladatelství CERM, s.r.o., Brno, 2004, ISBN 80-214-2592-x.

FLORIAN, Z., PŘIKRYL, K. a ONDRÁČEK, E. Mechanika těles - statika. Vyd. 3. Brno: PC-DIR, 1995, ISBN 80-214-0694-1.

Deadline for submission Bachelor's Thesis is given by the Schedule of the Academic year 2020/21

In Brno,

L. S.

---

prof. Ing. Jindřich Petruška, CSc.  
Director of the Institute

---

doc. Ing. Jaroslav Katolický, Ph.D.  
FME dean

# Zadaní bakalářské práce

Ústav: Ústav mechaniky těles, mechatroniky a biomechaniky  
Student: **Abdul rahman Abdul moghni**  
Studijní program: Aplikované vědy v inženýrství  
Studijní obor: Mechatronika  
Vedoucí práce: **doc. Ing. Vladimír Fuis, Ph.D.**  
Akademický rok: 2020/21

Ředitel ústavu Vám v souladu se zákonem č.111/1998 o vysokých školách a se Studijním a zkušebním řádem VUT v Brně určuje následující téma bakalářské práce:

## **Napjatostně deformační analýza železničního mostu v Zahrádkách u České Lípy**

### **Stručná charakteristika problematiky úkolu:**

Prutové soustavy se běžně používají k modelování chování mostů, jeřábů, stožárů a ostatních technických objektů, které jsou vyrobeny z prutových těles a splňují předpoklady kladené na prutové soustavy.

U obce Zahrádky na trati mezi Litoměřicemi a Českou Lípou se nachází železniční most přes Robečský potok. Tento most bude v bakalářské práci řešen z hlediska napjatosti a deformace.

### **Cíle bakalářské práce:**

1. Rešerše a získání vstupních údajů o železničním mostě.
2. V případě nutnosti úprava topologie mostu tak, aby byly splněny předpoklady kladené na prutovou soustavu.
3. Vytvoření 2D výpočtového modelu prutové soustavy mostu a provedení napjatostně deformační analýzy při různém statickém zatěžování.
4. Posouzení změny napjatosti a deformace mostu při změně míry statické neurčitosti uložení.
5. Verifikace vybraného 2D analytického výpočtu numerickým řešením.
6. Vytvoření 3D výpočtového modelu prutové soustavy mostu v ANSYSu a srovnání výsledků napětí a deformace s výsledky získanými pro 2D model.

### **Seznam doporučené literatury:**

JANÍČEK, P., ONDRÁČEK, E., VRBKA, J. a BURŠA, J. Mechanika těles: Pružnost a pevnost I, Akademické nakladatelství CERM, s.r.o., Brno, 2004, ISBN 80-214-2592-x.

FLORIAN, Z., PŘIKRYL, K. a ONDRÁČEK, E. Mechanika těles - statika. Vyd. 3. Brno: PC-DIR, 1995, ISBN 80-214-0694-1.

Termín odevzdání bakalářské práce je stanoven časovým plánem akademického roku 2020/21

V Brně, dne

L. S.

---

prof. Ing. Jindřich Petruška, CSc.  
ředitel ústavu

---

doc. Ing. Jaroslav Katolický, Ph.D.  
děkan fakulty



## **Abstract**

In this Bachelor thesis, the main goal was applying Stress-strain analysis of the railway bridge in Zahrádky near Česká Lípa. The structure of the Bridge was simplified and modeled as a truss construction. The first section of this bachelor thesis was dedicated to searching and obtaining the input data and essential information from the technical documentation of the Bridge. Then truss models for the Bridge were created with various levels of simplification. Therefore we split the analytical section into two parts. The first one was dedicated to statically indeterminate structure the second one was dedicated to the statically determinate structure. Also, every part contains both, self-bridge load and a passing trainload. However, because these equations were quite long, we have used Maple software to help us with calculations. The limit state of buckling was also checked for both structures, but we chose just two variants the lightest, which is self-load, and the heavies, which is the fourth Phase of a passing train. After accomplishing the analytical section, it was essential to verify the results. Therefore, we used the finite element method using Ansys software in the numerical section to verify the analytical part. All calculations were done in 2D. The only exception is in the numerical section, where we added a 3D model to compare with the 2D model.

## **Abstrakt**

Cílem této bakalářské práce je využití deformačně napěťové analýzy na Železniční most v Zahrádkách u České Lípy. Konstrukce mostu byla zjednodušena a vymodelována jako nosníková konstrukce. První část bakalářské práce byla věnována získávání vstupních dat a základních informací z technické dokumentace mostu. V nosníkovém modelu bylo využito několik zjednodušení. První model považujeme za staticky neurčitý, zatímco druhý jako staticky určitou konstrukci. Každý model tedy obsahuje zátěž z důvodu vlastní váhy a zatížení způsobeno projíždějícím vlakem. Z důvodu objemnosti rovnic, využíváme k výpočtu software Maple. Zkontrolovali jsme i mezní stav vzpěru pro oba modely, avšak jsme uvažovali pouze zatížení vlastní váhou a zatížení způsobeno vlakem. Po získání analytických dat bylo důležité tyto výsledky ověřit. Toto bylo docíleno využitím metody konečných prvků za pomoci programu Ansys. Veškeré výpočty byly provedeny pro 2D modely. Jediná výjimka je numerická sekce, kde byl přidán 3D model za účelem porovnání s 2D modelem.

## **Keywords**

Node, bar, structure, tension, compression, buckling, statically determinate structure, statically indeterminate structure, strain analysis, stress analysis.

## **Klíčová slova**

Styčník, prut, soustava, tah, tlak, vzpěr, staticky určitá soustava, staticky neurčitá soustava, napětostně analýza, deformační analýza.

### **Bibliographic citation:**

ABDUL MOGHNI, Abdul Rahman. *Stress-strain analysis of the railway bridge in Zahrádky near Česká Lípa*. Brno, 2021. Bachelor's Thesis. The Brno University of Technology, Faculty of Mechanical Engineering, Institute of Solid Mechanics, Mechatronics and Biomechanics. Supervisor doc. Ing. Vladimír Fuis, Ph.D.

### **Bibliografická citace:**

ABDUL MOGHNI, Abdul Rahman. *Napjatostně deformační analýza železničního mostu v Zahrádkách u České Lípy*. Brno, 2021. Bakalářská práce. Vysoké učení technické v Brně, Fakulta strojního inženýrství, Ústav mechaniky těles, mechatroniky a biomechaniky. Vedoucí bakalářské práce doc. Ing. Vladimír Fuis, Ph.D.

### **Declaration**

I declare that I have written my bachelor thesis with the subject of (**Stress-strain analysis of the railway bridge in Zahradky near Česká Lípa**) individually with the instructions of the supervisor. I was using sources and literature listed in the appendix to this work.

25 April 2021

.....  
Abdul Rahman Abdul Moghni



### **Acknowledgment**

I would like to express my gratitude to my supervisor, **doc. Ing. VLADIMÍR FUIS Ph.D.** for imparting his knowledge and experience, advice, and comments in this thesis.

I would also like to thank **Ing. Novák Pavel**, who provided me with technical documentation for the Bridge and answered my questions.

I would also like to thank **Ing. Jaroslav Kovář**. for helping me develop the computational program.

I would like to sincerely thank **Mrs. Zdráhalová Michaela** for guiding and advising me with correct and legal form citation.

It is my privilege to thank my fiancé **Dr. Sabrin Altashi**, for her constant encouragement throughout my thesis period.

I am extremely thankful to my friend **Bc. Ali Al-Qubati** for providing me with the necessary suggestions during my thesis period.

I would like to thank my friend **Bc. Zaid Al-Daylami** and **Abu Asad Mohammad** who helped me to accomplish this thesis.

Last but not least, I would like to express my deep and sincere gratitude to my parents, my father, **Dr. Hassan Abdulmoghni**, my mother, **Mrs. Zerina Abdulmoghni**, and family members who encouraged and supported me all the time to complete this thesis.

## Contents

|   |    |
|---|----|
| 1 Introduction.....   | 10 |
| 1.1 History of the Bridge.....                              | 10 |
| 2 Objectives .....  | 11 |
| 3 Theory .....  | 12 |
| 3.1 Bar .....   | 12 |
| 3.1.1 Bar Assumptions .....                                 | 12 |
| 3.2 Geometrical characteristic of a cross-section.....      | 15 |
| 3.2.1 Cross-section area .....                              | 15 |
| 3.2.2 Linear static moment.....                             | 15 |
| 3.2.3 Quadratic moment of a cross-section $\psi$ .....      | 16 |
| 3.2.4 Saint Venant's principle.....                         | 16 |
| 3.2.5 Saint venant's principal Advantages. ....             | 16 |
| 3.3 System of bars .....                                    | 17 |
| 3.3.1 Types of bars system .....                            | 17 |
| 3.4 Methods solving system of bars .....                    | 18 |
| 3.4.1 Method of nods.....                                   | 18 |
| 3.4.2 Method of sections .....                              | 18 |
| 3.5 Tensil, compressive stress acting on a bar .....        | 18 |
| 3.5.1 Abslute tenion and compression .....                  | 18 |
| 3.5.2 Geometrical relations .....                           | 19 |
| 3.5.3 Tension .....   | 19 |
| 3.5.4 Determination of stress-energy and displacements..... | 19 |
| 3.6 Castigliano's theorem .....                             | 20 |
| 3.7 Limit states .....                                      | 20 |
| 3.7.1 Limit state of deformation.....                       | 21 |
| 3.7.2 Limit state of elasticity.....                        | 21 |
| 3.7.4 Limit state of buckling .....                         | 22 |
| 4 Analytical calculations.....                              | 24 |
| 4.1 Statically indeterminate assignment.....                | 24 |
| 4.1.1 The main descriptions of the bridge.....              | 24 |
| 4.1.2 The main dimensions .....                             | 24 |

|   |    |
|---|----|
| 4.1.3 Numbering the bars .....  | 25 |
| 4.1.4 The names of nods.....  | 25 |
| 4.1.5 Coloring the bridge for better orientation of cross-sections..... | 29 |
| 4.2 Static analysis.....  | 30 |
| 4.2.1 External static analysis .....                                    | 30 |
| 4.2.2 Internal static analysis .....                                    | 31 |
| 4.3 Bridge's self-weight load.....                                      | 31 |
| 4.3.1 Free body diagram.....  | 32 |
| 4.3.2 Solving the system of equations.....                              | 38 |
| 4.3.3 Checking the limit state of elasticity .....                      | 42 |
| 4.4 Load acting on the Bridge from Train plus self-load of Bridge.....  | 42 |
| 4.4.1 Train specifications .....  | 42 |
| 4.4.2 Phase 1.....  | 43 |
| 4.4.3 Phase 2.....  | 44 |
| 4.4.4 Phase 3.....  | 45 |
| 4.4.5 Phase 4.....  | 46 |
| 4.4.6 Conclusion of the four phases .....                               | 48 |
| 4.5 Statically Determinate assignment .....                             | 49 |
| 4.5.1 The main descriptions of the bridge.....                          | 49 |
| 4.5.2 The main dimensions .....   | 49 |
| 4.5.6 The naming of nods and numbering of bars.....                     | 49 |
| 4.5.7 Cross-sections.....   | 50 |
| 4.6 Static analysis.....  | 50 |
| 4.6.1 External static analysis .....                                    | 51 |
| 4.6.2 Internal static analysis .....                                    | 51 |
| 4.7 Bridge's self-weight load.....                                      | 51 |
| 4.7.1 Free body diagram.....  | 52 |
| 4.7.2 Solving the system of equations.....                              | 52 |
| 4.7.3 Checking the limit state of elasticity .....                      | 55 |
| 4.8 Load acting on the Bridge from Train plus self-load of Bridge.....  | 55 |
| 4.8.1 Train specifications .....  | 55 |
| 4.8.2 Phase 1.....  | 56 |

|  |    |
|--|----|
| 4.8.3 Phase 2.....   | 57 |
| 4.8.4 Phase 3.....   | 58 |
| 4.8.5 Phase 4.....   | 59 |
| 4.9 Conclusion of the four phases .....  | 60 |
| ❖ Phase1.....  | 60 |
| ❖ Phase2.....  | 60 |
| ❖ Phase3.....  | 61 |
| ❖ Phase4.....  | 61 |
| 4.10 Checking the buckling stability limit state of the bridge. ....   | 62 |
| 4.10.1 Self-weight load .....  | 62 |
| 4.10.2 Load acting on the Bridge from Train plus self-load of Bridge.....  | 63 |
| a) Safety for a static indeterminate structure.....  | 63 |
| b) Safety for a static determinate structure .....   | 63 |
| 5 Numerical Calculations using finite element method.....  | 63 |
| 5.1 Statically indeterminate structure 2D.....   | 64 |
| 5.1.1 Self-weight bridge analyzing displacement and normal forces .....  | 64 |
| 5.1.2 Comparison between Numerical and Analytical results .....  | 65 |
| 5.1.3 Train's-weight phase 4 analyzing displacement and normal forces .....  | 66 |
| 5.1.4 Comparison between Numerical and Analytical results .....  | 67 |
| 5.2 Statically indeterminate structure 3D.....   | 67 |
| 5.2.1 Load acting on the Bridge from passing Train in phase 4 plus self-load of Bridge<br>analyzing displacement and normal forces ..... | 69 |
| 5.2.2 Comparison between 3D and 2D structure Numerically .....   | 70 |
| 5.2.3 Model modification .....   | 70 |
| 6 Conclusion .....   | 71 |
| List of resources .....  | 74 |
| Figures list.....  | 75 |
| List of tables .....   | 78 |
| List of used symbols.....  | 79 |
| List of attachments .....  | 79 |



# 1 Introduction

## 1.1 History of the Bridge

It is a steel structure bridge which is located in Česká Lípa Zahrádkách. The first operation of the bridge started in 1898, and the bridge was constructed to connect between two hills as we can see in fig.1., where the figure on the left shows the bridge before reconstruction, and the figure on the right shows the bridge after reconstruction.



**FIG. 1.2 LOCATION OF THE BRIDGE ON THE MAPS.[3]**



**FIG. 1.1 LOCATION OF THE BRIDGE ON THE MAPS.[4]**

Replacement and reconstruction for the whole bridge took place in 2013, as we can see the difference between fig. 1.1 and fig. 1.2. the bridge is used for railways only, where trains can only move in one direction at once. The bridge is divided into two parts, and the structure is made of steel bars and nodes of steel material which made it a strong structure. The bridge is located south of Česká Lípa more in fig.1.3, 1.4, 1.5.



**FIG. 1.3 LOCATION OF THE BRIDGE ON THE MAPS. [5]**

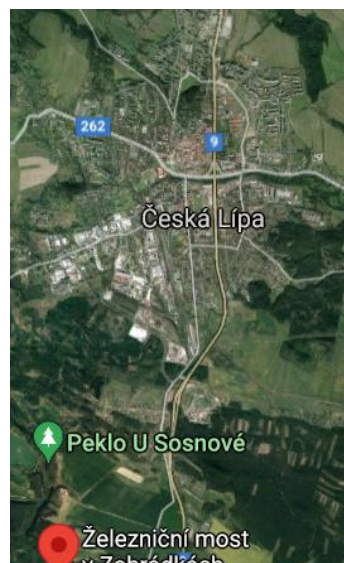


**FIG. 1.4 LOCATION OF THE BRIDGE ON THE MAPS. [5]**





**FIG. 1.5 LOCATION OF THE BRIDGE ACCORDING TO THE CZECH REPUBLIC ON THE MAPS.[5]**

In this thesis, we will analyze the deformation and stress of this bridge using two methods, analytical by using Maple software and numerical by using Ansys software.

## 2 Objectives

The first step we considered in this thesis was finding input data, which were taken from the Railway and transport administration. The second step was to make deformation and stress analysis. The loading applied on the bridge are static, and they are two types of loadings, the first type is generated by the weight of the bridge itself, and the second type is generated by the weight of a passing train on the bridge. The analysis of both cases has been performed separately using two methods, analytical with Maple and numerical using finite element method with Ansys, at the end, both methods will be compared in each case to discriminate that there are no mistakes with the analytical approach. Moreover both cases will be compared to distinguish which case will have more minor deformation and fewer stresses. As we can see in fig. 2.1, we chose just one part of the bridge because they are identical where each has its own supports, which means the results will be for sure the same in both parts, so when we mention the word bridge in the thesis, it means just the one part.



**FIG. 2.1 CHOOSING ONE PART OF THE BRIDGE.[6]**

### 3 Theory

The theoretical part of this thesis is taken from resources [8] unless it is mentioned.

#### 3.1 Bar

The bar is the simplest model of a real body which must fulfill assumption geometry, deformation, loads, supports, and stress states. And these assumptions will be labeled as Bar Assumption.

##### 3.1.1 Bar Assumptions

The bar assumptions are geometry, deformation, loads, supports, and stress states:

###### A) Geometrical assumption

The geometrical definition of a bar is a centerline  $\Upsilon$  that is defined by a cross-section  $\psi$  in each point of it as in fig. 3.1.

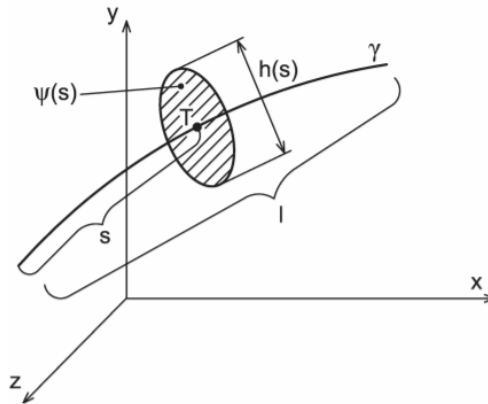


FIG. 3.1 CENTERLINE AND BARS CROSSSECTION.

- The centerline  $\Upsilon$  has a finite length, and it must be smooth. It cannot be 90 degrees curved more as shown in fig. 3.2.
- The cross-section must be a continuous plane region.

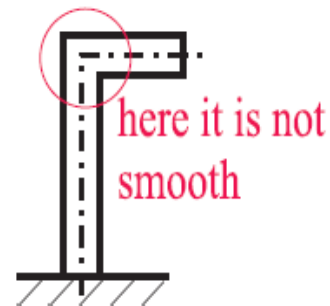


FIG. 3.2 CENTERLINE AT A BENT BAR.



### B) Deformational Assumption

- During deformation, the centerline doesn't change its continuity and smoothness, as in fig.3.3.

It doesn't matter which type of deformation acts on a bar. The important thing is that the cross-sections remain perpendicular to the centerline and planar. Moreover, the types of deformation affecting a bar are described below more in figures 3.4, 3.5, 3.6, 3.7.

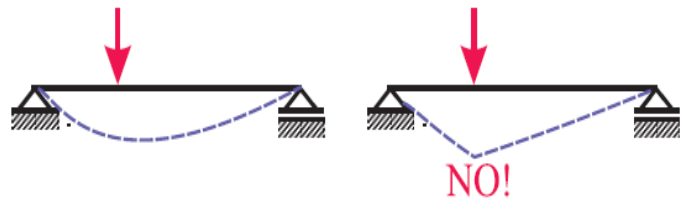


FIG. 3.3 MAINTAINING THE SMOOTHNESS OF THE CENTERLINE.

#### a) Tension

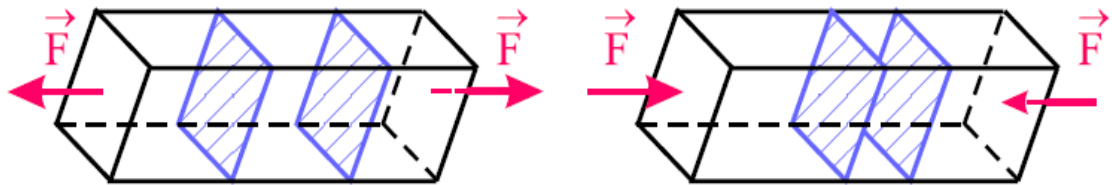


FIG. 3.4 TENSION IN A BAR.

#### b) Flection

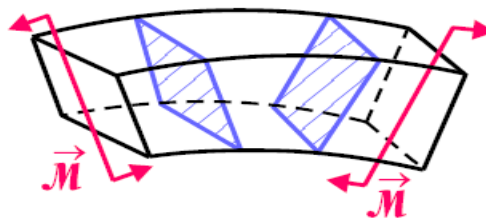


FIG. 3.5 FLECTION IN A BAR.

#### c) Torsion

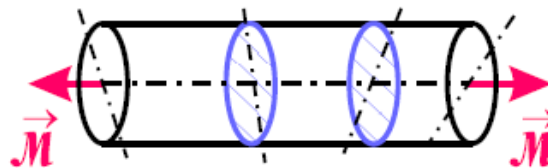


FIG. 3.6 TORSION IN A BAR.

d) Shear

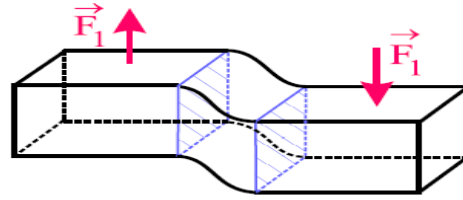


FIG. 3.7 SHEAR IN A BAR.

C) Loadings Assumption

- Supports restrict displacement and rotation.
- All external loading acts only on the centerline of the bar.
- We model supports and loadings to make them act on the centerline. In that Place, according to the saint-venant's principle, there is a different state of stress act on the centerline, which leads to break bar assumptions more in fig. 3.8.

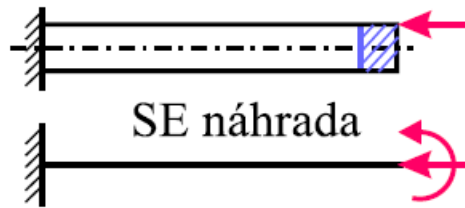


FIG. 3.8 SIMPLIFICATION FROM A BAR INTO CENTERLINE.

D) Stress state Assumption

Normal and shear stresses in the cross-section determine the state of stress, and thanks to symmetry, remaining stresses are equal to zero as in fig. 3.11.

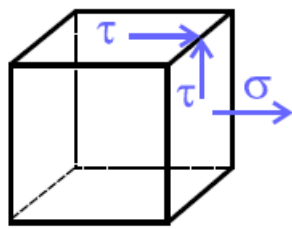


FIG. 3.10 BAR STATE OF STRESS DISPLAYED ON A UNIT CUBE.

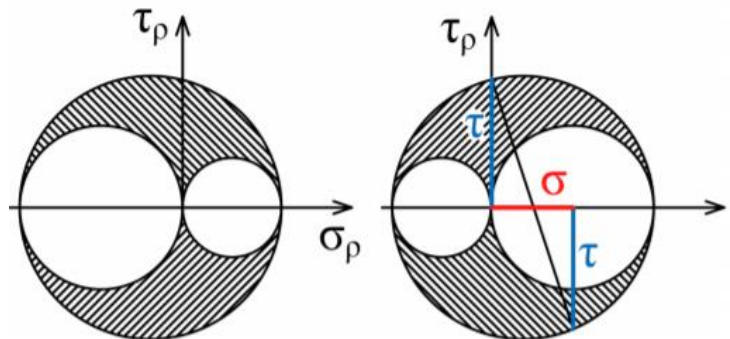


FIG. 3.9 BAR STATE OF STRESS DISPLAYED ON A MOHR'S CIRCLE.

$$T_{\sigma} = \begin{pmatrix} \sigma_x & \tau_{xy} & 0 \\ \tau_{yx} & 0 & 0 \\ 0 & 0 & 0 \end{pmatrix} = \begin{pmatrix} \sigma & \tau & 0 \\ \tau & 0 & 0 \\ 0 & 0 & 0 \end{pmatrix}$$

FIG. 3.11 STRESS TENSOR FOR BAR IN

### 3.2 Geometrical characteristic of a cross-section

To calculate stress and deformation, we will have to use a formula that contains a quantity called geometrical characteristic of the cross-section, which characterizes cross-sections. These characteristics are divided into two groups dependent on the characteristics and independent of the choice of the coordinate system.

#### 3.2.1 Cross-section area

As you can see in fig.3.12, the body does not depend on the coordinate system. Because of that, we will use the following formula.

$$S = \int_{\psi} dS = \iint_{\psi} dydz \quad [\text{m}^2]$$

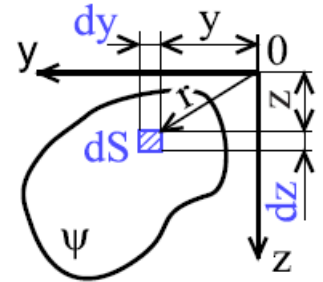


FIG. 3.12 CROSS-SECTIONAL AREA.

#### 3.2.2 Linear static moment

By using these formulae, we can calculate the static moment, which depends on the coordinate system.

$$Q_x = \int_A y dA$$

$$Q_y = \int_A x dA$$

Arbitrary Cross Section

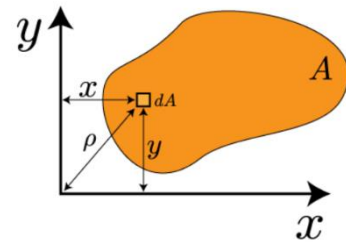


FIG. 3.13 ARBITRARY CROSS-SECTION AREA.

- The following formula is to determine the center of gravity of a given body in the x and the y axis.

$$\bar{x} = \frac{Q_y}{A} = \frac{\int_A y dA}{\int_A dA} = \frac{\sum_i \bar{x}_i \bar{A}_i}{\sum_i \bar{A}_i}$$

$$\bar{y} = \frac{Q_x}{A} = \frac{\int_A x dA}{\int_A dA} = \frac{\sum_i \bar{y}_i \bar{A}_i}{\sum_i \bar{A}_i}$$

### 3.2.3 Quadratic moment of a cross-section $\psi$

The axial quadratic moment, this type of moment is always calculated to the coordinate axis as we can see in the following formula it is calculated to the y-axis. the unite we use here is  $m^4$ . The quadratic moment is primarily used in bending cases which we don't need in our analysis except in buckling limit state analysis. Therefore, we add the  $J_y$  Into our theoretical part and the formula is as follows.

$$J_y = \int_{\psi} z^2 dS$$

### 3.2.4 Saint Venant's principle

In a real-life, we cannot determine the distribution of forces acting on the surface of a body, so to make this problem solvable, we simplify it into a model of a substituted force interaction acting on the exact same place causing the same effect and same stress. The model for sure is statically equivalent to the original problem more in fig. 3.15.

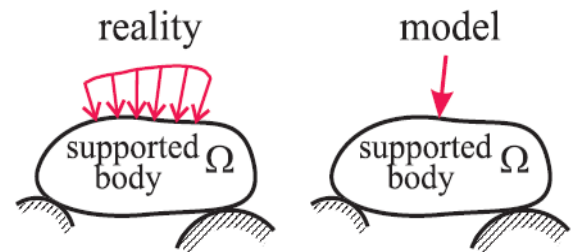


FIG. 3.14 LOADING IN REALITY VS IN MODEL.

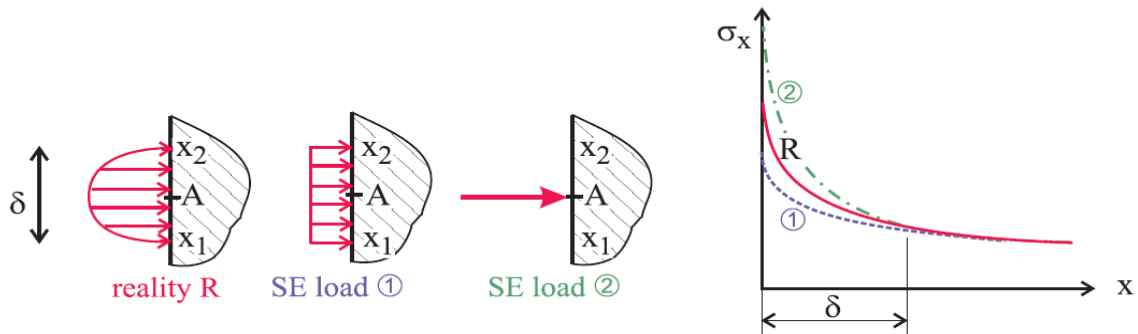


FIG. 3.15 LOAD DISTRIBUTION ACCORDING TO THE VENANT PRINCIPLE.

- As you can see in fig. 3.14 is a comparison between the real problem and a substituted model the graph shows the relation between the stress sigma x and the deformation; as we can see, the is an insignificant difference which is not a problem for calculations.

### 3.2.5 Saint venant's principal Advantages.

- It enables us to use computational models of loads (volume and area forces) correctly.

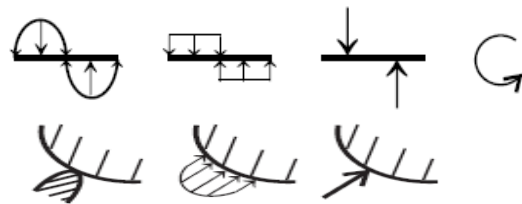


FIG. 3.16 APPLICATION OF S.V. PRINCIPLE.  
[9]

- It enables us to introduce computational models of contact between bodies correctly.
- It proves the incorrectness of some substitutes (commonly used in statics ) for stress analyses.

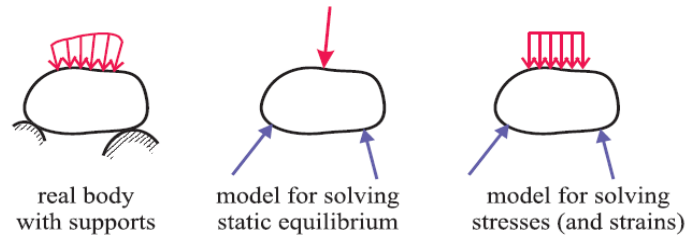


FIG. 3.17 COMPUTATIONAL MODELS.

### 3.3 System of bars

The bar system is a computational model for lattice structures, where straight slender bodies are modeled by bars and they are connected in the reality by elements (rivets, welds ...), but in the computational models are replaced by so-called joints (pins), which realize rotational or spherical bonds. These adjustments are made to facilitate the analytical calculation. Prerequisites for using the bar system model. [10]

The system of bars is the most simple method used in modeling bridges, it consists of bars and joints, also called nodes.

- The main idea of this method is that there is a bar connected to a node, the internal bar is modeled as rotary, thanks to that, we can neglect the bending moment, which means that the bars are loaded just by tension and compression.
- To apply that the bars are loaded just by tension and compression, we have to consider the following facts.
  - The loading is applied just on the nodes nowhere else.
  - The system of bars are at least connected to two nodes which leads to that the bars are not movable.
  - The bar has to be as we already defined it in chapter 3.1.
- Before starting to design the structure, we must check the limits state of elasticity for bars that are loaded by compression. In some cases, buckling may occur, which leads to loss-of stability.

#### 3.3.1 Types of bars system

- In order to solve a certain system, we have to know if the system is statically determinant or statically indeterminate, thanks to that, we can determine how many we will have deformation conditions for the system.

##### a) External Statically determinant

It relates to the determination of external unknown contact forces released of the bar body from the usable conditions of static equilibrium, the external static equilibrium is given by the relation.

$$V_{ext} = \mu_{ext}$$

Where  $V_{ext}$  is the application of equilibrium condition, and  $\mu_{ext}$  is the number of unknown parameters of external contact forces. The degree of external uncertainty is given by the formula.

$$S_{ext} = \mu_{ext} = V_{ext}$$

### **b) Internal statically determinant**

It relates to the determination of axial forces in members, conditions of static equilibrium bar systems are linearly dependent on a system of static equilibrium conditions joints, in other words, for the system to be solvable, the number of unknown internal parameters must equal the number of equations, the condition of the internal static equilibrium is given by the following formula.

$$3K - 6 = P \dots\dots \text{For 3D systems of bars.}$$

$$2K - 3 = P \dots\dots \text{For 2D systems of bars.}$$

Where K is the number of nodes and P is the number of bars.

### **c) Statically indeterminant**

The system becomes statically indeterminate. When the number of unknowns exceeds the number of equations, so to solve this problem, we have to add boundary conditions, the relation to calculate the boundary conditions is as follows.

$$3K = P + \mu_{ext} \dots\dots \text{For 3D systems of bars.}$$

$$2K = P + \mu_{ext} \dots\dots \text{For 2D systems of bars.}$$

## **3.4 Methods solving system of bars**

There are so many methods to solve a system of a bar, but the more useful are two Methods, method of nodes and method of sections.

### **3.4.1 Method of nodes**

In order to apply this method, we have to draw a free body diagram for all nodes in the system after that, we establish applicable static equilibrium conditions, then we will get a set of linear algebraic equations after that, we can put the equations into a matrix and use a software to solve it, this is the universal method.

### **3.4.2 Method of sections**

In order to apply this method, we draw a free body diagram for certain nodes that are statically determinate, this method concentrates on the easier type of problems because that this method is not viable, it is better to use the Method of nodes.

## **3.5 Tensile, compressive stress acting on a bar**

### **3.5.1 Absolute tension and compression**

Simple tension/compression is a type of loading a straight prismatic bar if the following conditions are applied.

- a) Bar assumptions are satisfied.
- b) Cross-sections mutually draw away (near) and consequently deform isotropically (i.e., they change their magnitude but not the shape).
- c) Normal force N is the only non-zero component of the inner resultant,
- d) Deformations are not substantial from the viewpoint of the static equilibrium of an element. “.

### 3.5.2 Geometrical relations

The geometric relations are showing us the dependence between the displacement and the deformation if we assumed that we make a cut and which is further analyzed due to the load and the element is stretched, and at the same time, its cross-section decreases as shown in fig. 3.18 the right angels remain the same even after deformation, and therefore, the bevels are zero, the angular length is calculated by the equation  $\epsilon_x = \frac{du}{dx}$ , where  $du$  is displacement and  $\epsilon_x$  is the strain in the X-direction.

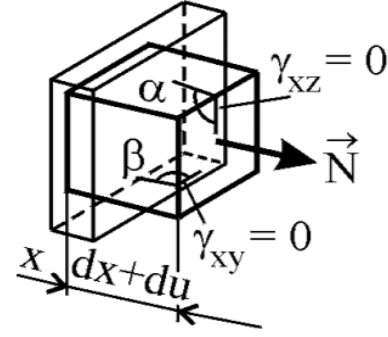


**FIG. 3.18 DEFORMATION OF AN ELEMENTARY ELEMENT BY SIMPLE TENSION.**

For tensile-compressive stress, it is possible to express the strain tensor as follows.

$$T_{\epsilon} = \begin{bmatrix} \epsilon_x & 0 & 0 \\ 0 & \epsilon_y & 0 \\ 0 & 0 & \epsilon_z \end{bmatrix}$$

### 3.5.3 Tension

Because the bevels are zero and the stress is uniaxial, there is only one non-zero stress tensor component at a non-zero loading force. The stress is constant across the cross-section. Therefore, all points have the same safety to the limit state of elasticity. Since the only non-zero component of the resulting internal effects is the normal force, the stress can be determined.

$$\sigma = \frac{N}{S}$$

This relationship only applies to the central coordinate system. Therefore, all loads must act on the centerline axis.

### 3.5.4 Determination of stress-energy and displacements

When there is a load applied on a body, the body deforms, the applied forces do work. This energy can be translated to work, and it is stored in the deformed body as stress energy.

$$w = \frac{1}{2} \int_Y \frac{N^2}{S \cdot E} dx$$

The stress-energy per unit volume is the specific stress-energy.

$$\Lambda = \frac{dW}{dV} = \frac{\sigma^2}{2 \cdot E} = \frac{1}{2} \cdot E \cdot \epsilon^2$$

The deflection on the part of a bar of length can be expressed as.

$$u_R = \int_0^{x_R} \epsilon dx = \int_0^{x_R} \frac{N}{E \cdot S} dx$$

Where  $E$  is the cross-sectional stiffness, similarly, the displacement can be expressed using Castigliano's theorem.

$$w_R = \frac{\partial W}{\partial F} = \int_0^{x_R} \frac{N}{E S} \cdot \frac{\partial N}{\partial F} dx$$

### 3.6 Castigliano's theorem

„ Castigliano’s theorem is the most important theorem of the linear theory of elasticity from the viewpoint of practical application because it enables us to calculate deformation characteristics of any linear elastic body, provided that we are able to formulate a relation for its strain energy. The whole system of bodies must be included in the strain energy if the deformations of the neighboring bodies (or of the frame) are not negligible in comparison with the deformations of the investigated body. “.

, A negative sign of the displacement (or turning angle) means that the orientation of this displacement (angle) is opposite to the orientation of the corresponding force (a couple of forces). Castigliano’s theorem is independent of sign conventions because a positive work always means that the displacement is oriented according to the orientation of the acting force.“.

Castigliano's theorem is a powerful tool to solve static indeterminate structures (truss system) because, in this type of problem, we always end with inequality between the number of equations and unknown parameters, so in this system that many equations miss as many, the system is statically indeterminate. By using the Castigliano theorem, it is possible to compile deformation conditions that complete the missing equations. Deformation conditions compile at the point of displacement or rotation, which means at the supports. We release as many supports to make the system statically determinate, and by assembling the deformation, conditions mean partial releasing. Castigliano’s theorem can also be used to determine the displacements or rotations in a place no force or moment acts on by considering an additional force or moment that has zero magnitudes.

### 3.7 Limit states

Generally, this is a state when a body is under load stops fulfill its function; in other words, when a functionally permissible deformation of failure changes into functionally impermissible, so it's all about how the body is loaded according to that limit states can be divided into two groups. [2]

- a) Limit state associated with deformation.
  - Limit state of deformation.
  - Limit state of elasticity.
  - Limit state of buckling.
  - Limit state of fracture.
- b) Limit states associated with the violation.
  - Limit state of crack initiation.
  - Limit state of fracture.
  - Fragile.
  - Malleable.
  - Fatigue.
  - Creep.



### 3.7.1 Limit state of deformation

„ All parts deform under any load, i.e., they change their shape, dimensions, tolerances between them (clearance or interference). If these changes do not disturb the function of the equipment, as defined in specifications and technical standards valid for the equipment (concerning the accuracy of production, mobility of the components, etc.), we call them admissible deformations. “.

### 3.7.2 Limit state of elasticity

The limit state of elasticity is the state in which the first microplastic deformation begins to occur, and it is measurable. We can describe this limit state using a stress value which is called the yield strength, therefore up to this limit state, the material behaves elastically after unloading the material returns to its original condition, but if the ultimate yield strength has been exceeded, the material will be permanently deformed. The yield strength can be obtained from the tensile test. The output of this test will be a tensile diagram. This diagram is showing the relationship between stress and strain the force can be converted to stress using the original cross-section of the tested specimen.

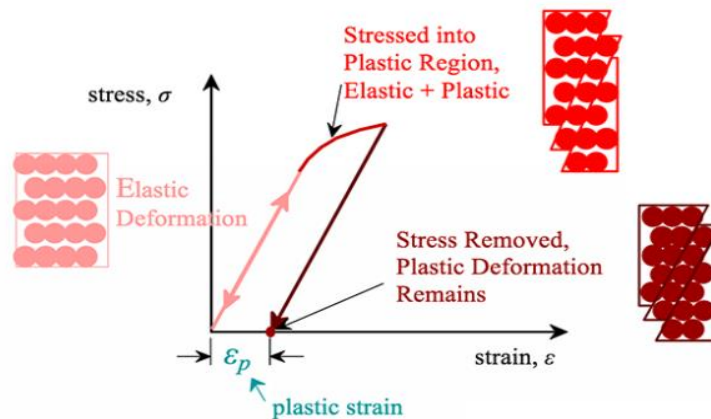


FIG. 3.19 ELASTIC AND PLASTIC DEFORMATION.[12]

So, to indicate if a specimen is safe or not, we have to calculate the factor of safety according to the limit state of elasticity, and it is as the following formula.

$$K_k = \frac{\sigma_k}{\sigma_{max}}$$

Where  $K_k$ ... factor of safety.

$\sigma_k$ ... yield stress.

$\sigma_{max}$ ... maximum stress calculated of the specimen.

So, if the factor of safety is greater than one, the specimen did not exceed the limit state, and it is safe. Still, if the safety factor is smaller than one, it means that the sample exceeded the limit state, and plastic deformation for sure will occur.

### 3.7.4 Limit state of buckling

, Limit state of buckling is such a state among the operational states of the body when the equilibrium shape of the body becomes unstable, and a stepwise shape change to another stable geometrical configuration can occur.”

so the bar has to be under a compressive force which means a negative magnitude of a normal force to occur buckling. In addition to compression, there is a sudden deflection in the bar that leads to a change from compressive stress into bending stress. So this limit state is sensitive because a situation can happen where we can continue in compressive loading, and we get a sudden loss of stability (buckling). Between these two states is a critical point called a Bifurcation point, more in fig. 3.20.

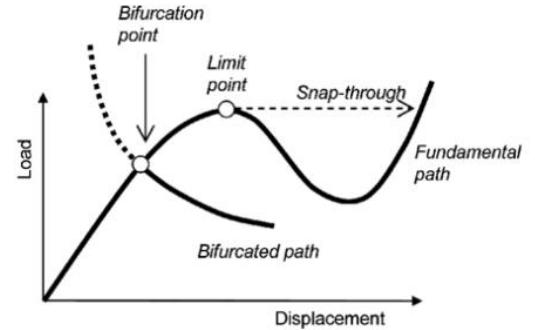


FIG. 3.20 BIFURCATION POINT IN BUCKLING.[11]

as we can see in fig. 3.21 the critical force  $F_{kr}$  is the interface between the pressure and bending and the critical force is defined at this point which indicates the loss of stability and is given by the following relationship.

$$F_{kr} = \frac{\alpha^2 \cdot E \cdot J_2}{l^2}$$

Where parameter  $\alpha$  depends on the type of support of the bar more in fig. 3.22,  $E$  is Young's modulus of elasticity,  $J_2$  is the minimum quadratic moment, and  $l$  is the length of the bar.

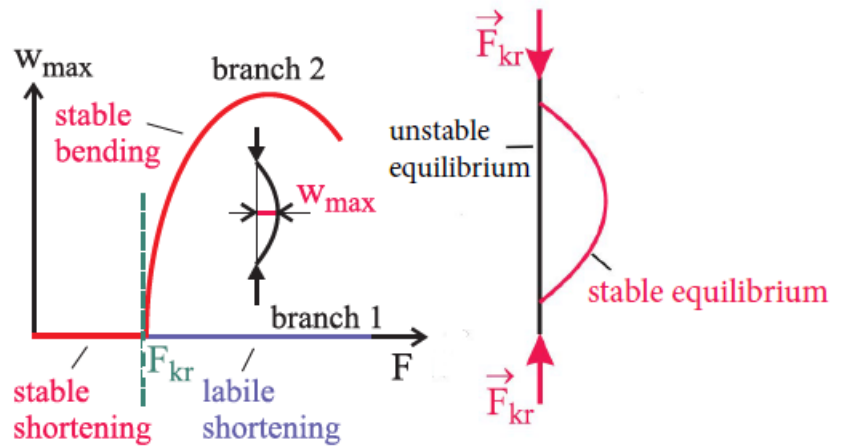


FIG. 3.21 VALUES OF COEFFICIENTS A DEPOSITS.

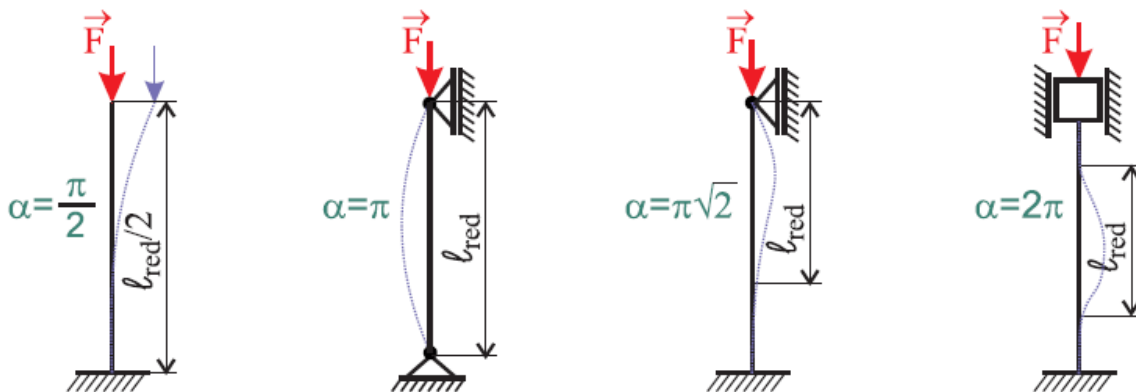


FIG. 3.22 VALUES OF COEFFICIENTS A DEPOSITS.

For an ideal bar under an ideal load, we can check the factor of safety by the following formula.

$$K_V = \frac{F_{kr}}{F}$$

Therefore, if the force that compresses the bar greater than the critical force, the bar is bent, and if the force is smaller than the critical force, the bar is stable the deflection did not occur, it can also be that the force equals the critical force and this is the critical point which is called the Bifurcation point.

What we dealt with was an ideal bar with ideal assumptions, but in real-life application, it can be different since the limit state of elasticity can occur before the buckling stability limit state, therefore to deal with this situation, the quantity slenderness and critical slenderness of bar are introduced, however easily if the magnitude of bar's slenderness is greater than the magnitude of critical slenderness, it means that the limit state of buckling has been exceeded, but if the situation was the opposite it means that the limit state of elasticity will occur before the limit state of buckling. To calculate the slenderness and the critical slenderness of a bar, the following formula can be used.

- The slenderness of a bar.

$$\lambda = \frac{l}{\sqrt{J/S}}$$

- The critical slenderness of a bar.

$$\lambda_{Kr} = \alpha \cdot \sqrt{\frac{E}{R_e}}$$

- To calculate the Normal stress at the buckling limit state.

$$\sigma_{Kr} = \frac{F_{kr}}{S} = \frac{\alpha^2 \cdot E \cdot J}{S \cdot l^2} = \frac{\alpha^2 \cdot E}{\lambda^2}$$

- The dependence of the stress at which the limit state of loss of buckling stability on slenderness occurs is called the Euler hyperbola fig. 3.23.
- ❖ So, to conclude, the limit states are assessed as follows.
  - If  $\lambda < \lambda_{Kr}$ , then the limit state of elasticity occurs first, therefore, to check the safety, we have to use this formula  $K_k = \frac{\sigma_k}{\sigma_{max}}$ .
  - If  $\lambda > \lambda_{Kr}$ , then the buckling stability limit state occurs first, therefore, to check the safety, we have to use this formula  $K_V = \frac{F_{kr}}{F}$ .

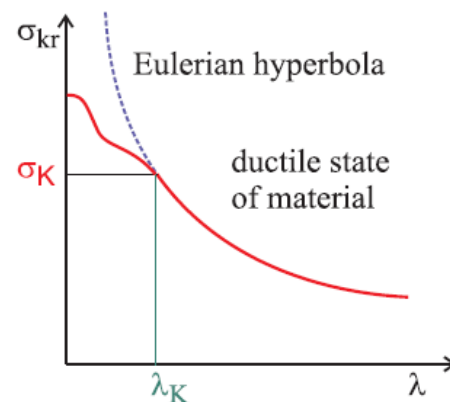


**FIG. 3 23 DEPENDENCE OF COMPRESSIVE STRESS  $\sigma_{Kr}$ . ON THE SLENDERNESS  $\lambda$  FOR A TOUGH MATERIAL.**

## 4 Analytical calculations

### 4.1 Statically indeterminate assignment

The bridge we are analyzing, Contains 71 bars and 32 nodes, and they are affected by simple tension and compression because it is a truss system, The bridge is made of steel and individual bars connected by nodes, the total length of the part is  $4140 \times 10$  which means it'll be 41400 mm long, with a width of 3000 mm, and a height of 4000 mm, This part of the bridge is supported by two supports, on the left pin support which allows just rotation on Z-axis (perpendicular) and the right is supported by roller support which means that the part of the bridge can move horizontally and rotate around the Z-axis (perpendicular).

#### 4.1.1 The main descriptions of the bridge

The bridge was simplified from the real-life bridge more in fig. 4.1 and described as simple as possible As it is shown in fig. 4.2, to make it accessible in calculations and orientations, using an alphabet system and numbering.



FIG. 4.1 BRIDGE IN THE REAL-LIFE.  
[6]

#### 4.1.2 The main dimensions

The main dimensions describe the full length of the part of the bridge, which is 41400 mm, the height, which is 4000 mm, the length of one block, which is 4140 mm, the length of inner bars which is 5757 mm, and the angle between the bars which is  $44.01^\circ$ .

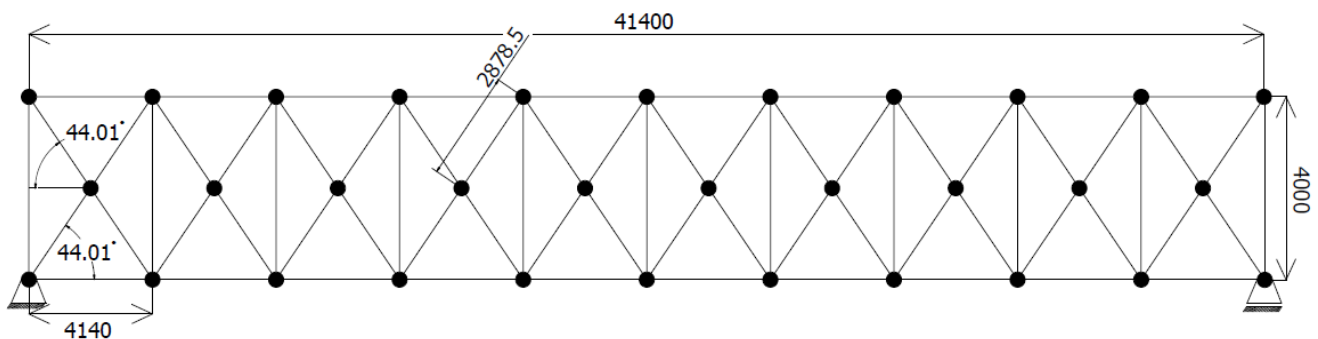


Fig. 4.2 Bridge's dimensions.

### 4.1.3 Numbering the bars

This part of the bridge contains 71 bars separated by nodes, so they were numbered from 1 to 71, starting from the bottom left, then the top part, then the middle part, as in fig. 4.3.

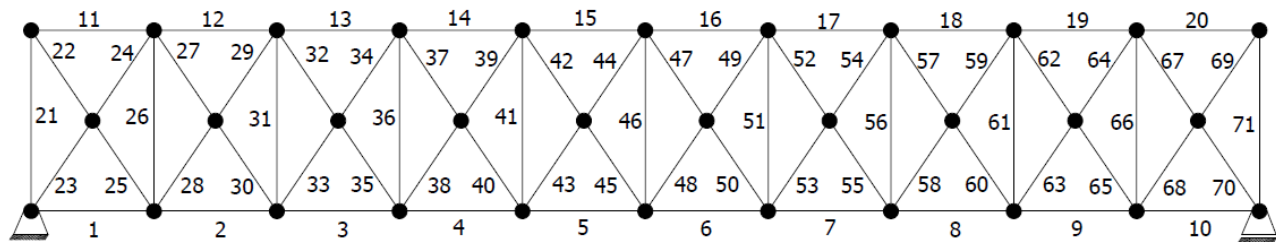


FIG. 4.3 NUMBERING THE BARS.

### 4.1.4 The names of nodes

This part of the bridge contains 32 nodes, so they were named alphabetically, starting from bottom left by letter A to the bottom right by letter K, the upper part of the bridge was copied from the bottom, but with adding one like this (A1) and so on, the nodes which are in the middle of the bridge were named starting by L ending with V, skipping the letter U, as in fig. 4.4.

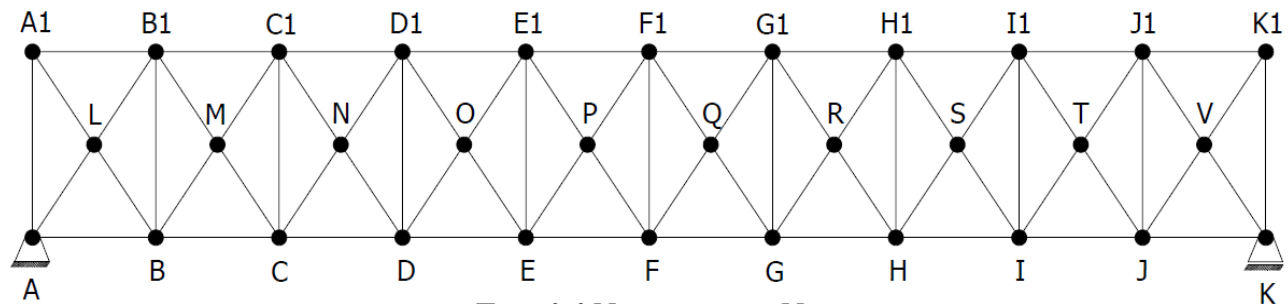


FIG. 4.4 NAMING THE NODES.

### 4.1.5 Cross-sections

For the construction of the bridge, 19 different types of cross-sections were used, and they are as follows.

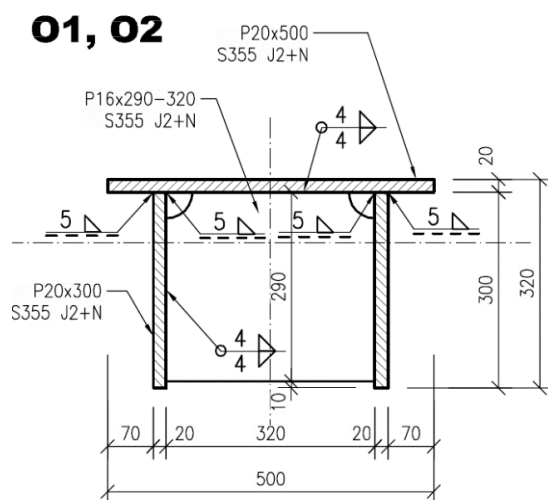


FIG. 4.5 CROSS-SECTION O1, O2. [1]

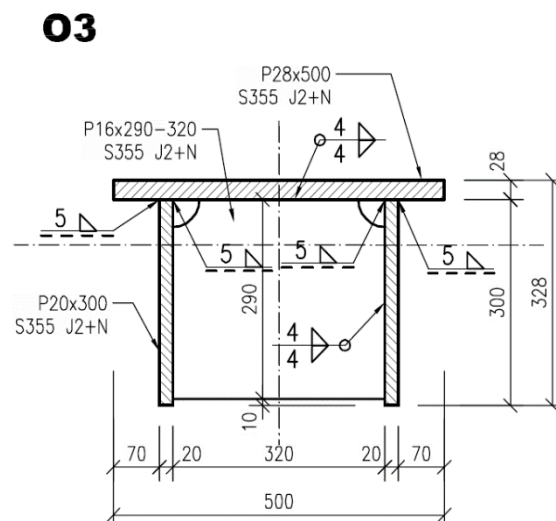


FIG. 4.6 CROSS-SECTION O3.[1]

## O4, O5

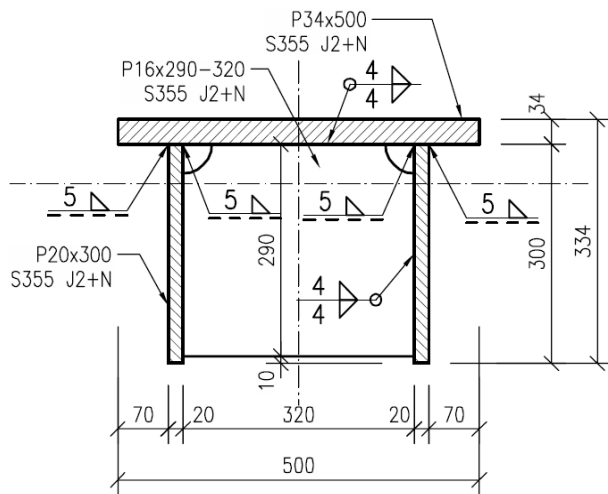


FIG. 4.8 CROSS-SECTION O4, O5.

[1]

## U1, U2

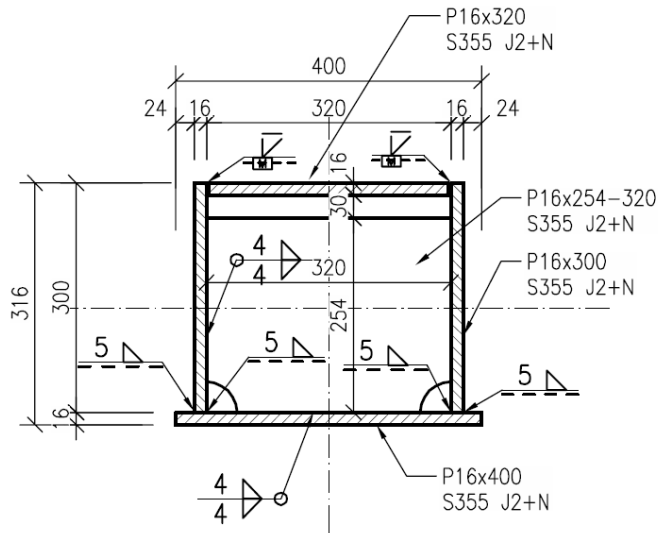


FIG. 4.7 CROSS-SECTION U1, U2.

[1]

## U3 - U5

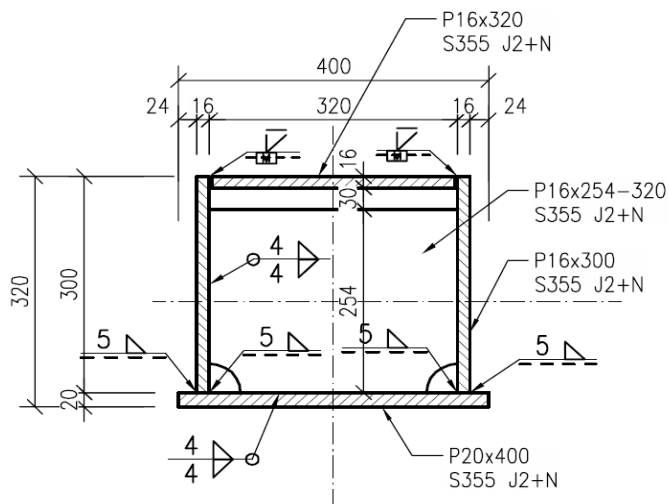


FIG. 4.9 CROSS-SECTION U3-U5.

[1]

## D1

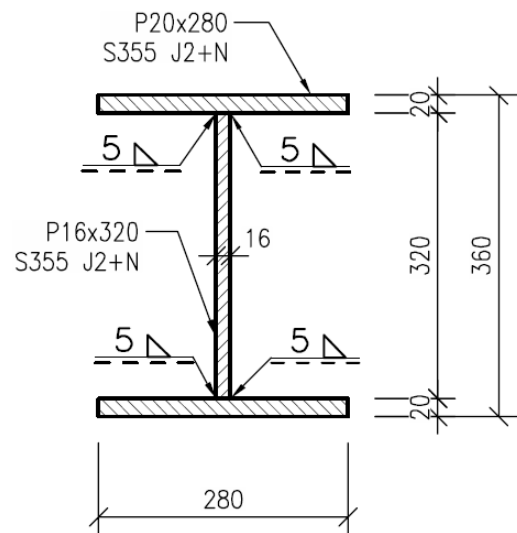


FIG. 4.10 CROSS-SECTION D1.

[1]

## D2

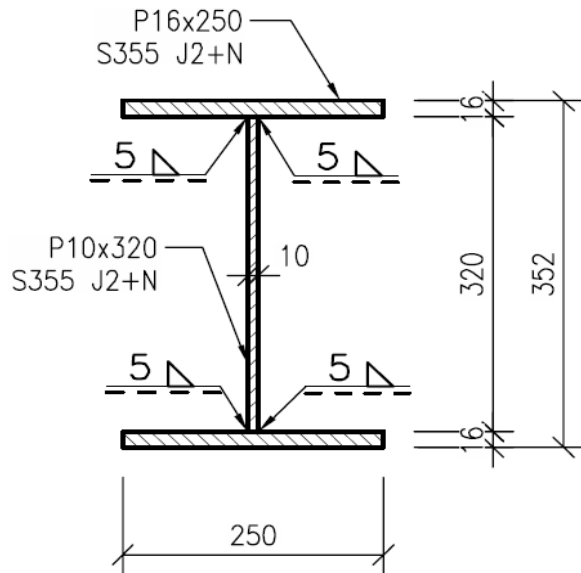


FIG. 4. 12 40 CROSS-SECTION D2.  
[1]

## D3

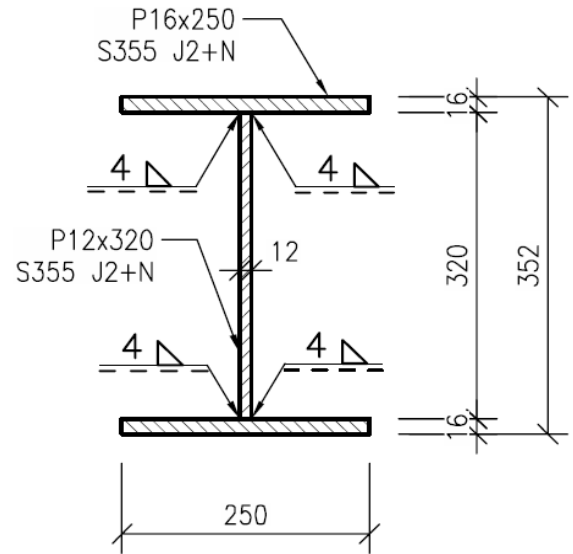


FIG. 4. 11 CROSS-SECTION D3.  
[1]

## D4

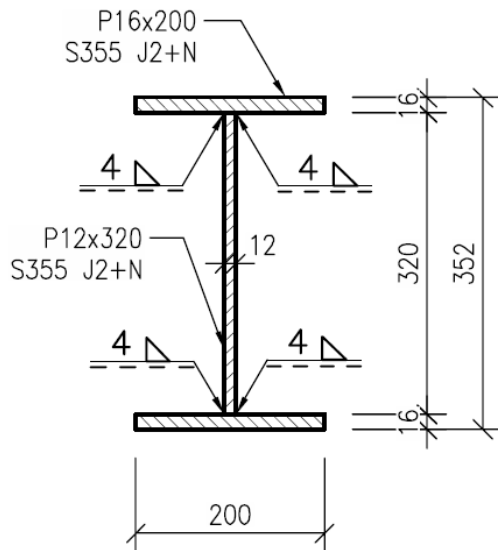


FIG. 4. 13 CROSS-SECTION D4.  
[1]

## D5

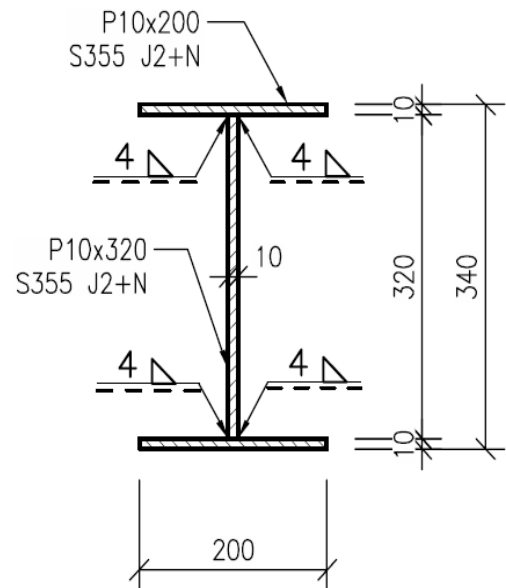


FIG. 4.14 CROSS-SECTION D5.  
[1]

## T1

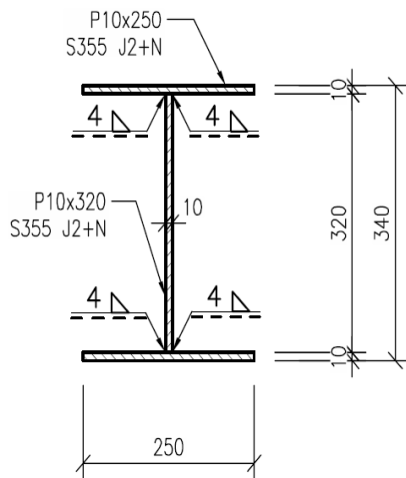


FIG. 4. 15 CROSS-SECTION T1.  
[1]

## T2, T3

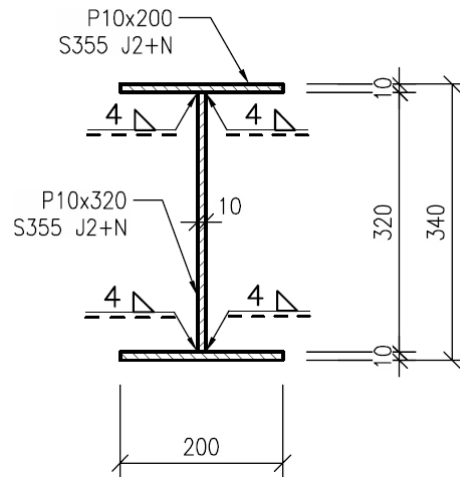


FIG. 4. 16 CROSS-SECTION T2, T3.  
[1]

## T4, T5

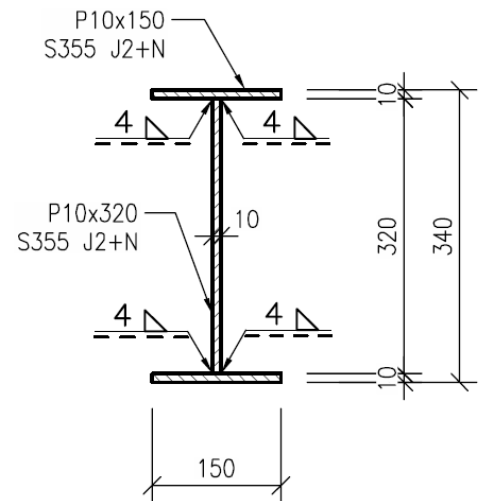


FIG. 4. 17 CROSS-SECTION T4, T5.  
[1]

## S0

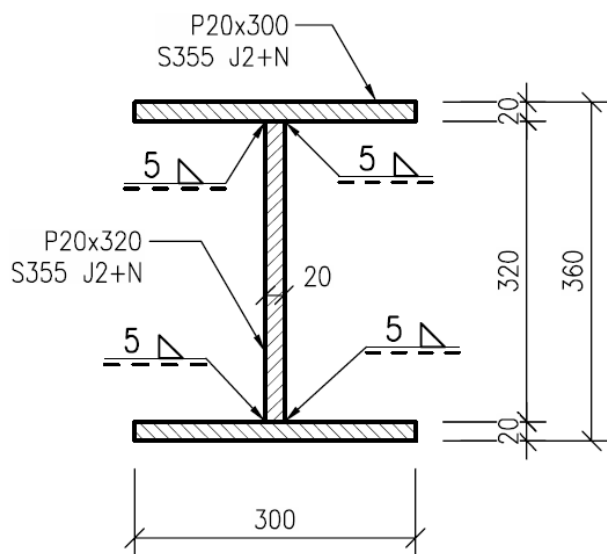


FIG. 4. 18 CROSS-SECTION S0. [1]

## S

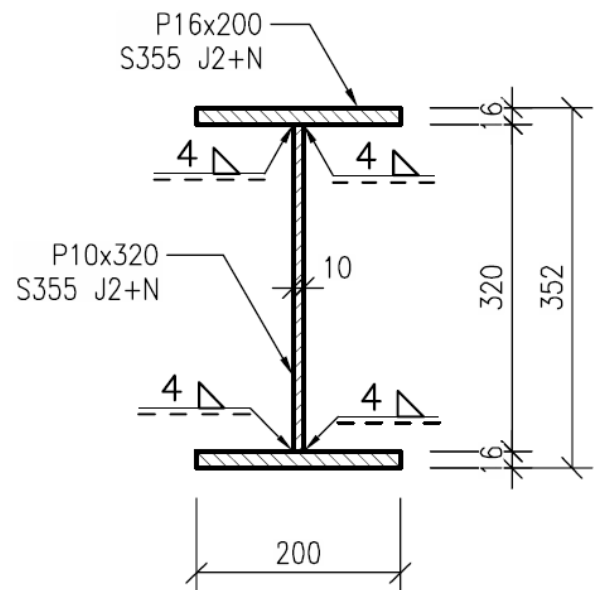


FIG. 4. 19 CROSS-SECTION S. [1]



#### 4.1.5 Coloring the bridge for better orientation of cross-sections

We decided to add color effects to the bridge for more illustration and to make it easier to find wanted cross-sections. There are in total 15 different colors that can be found in the tab. 4.1.

**TAB. 4.1 COLOR AND NUMBERS OF CROSS-SECTIONS**

| Cross-sections Name | Number of bar              | Cross-section area in $mm^2$ | colors corresponding to bar |
|---------------------|----------------------------|------------------------------|-----------------------------|
| O1,O2               | 11,12,19,20                | 22000                        | Red                         |
| O3                  | 13,18                      | 26000                        | Cyan                        |
| O4,O5               | 14,15,16,17                | 29000                        | Blue                        |
| U1,U2               | 1,2,9,10                   | 211200                       | Orange                      |
| U3,U4,U5            | 3,4,5,6,7,8                | 22720                        | Yellow                      |
| D1                  | 23,24,67,70                | 16320                        | Purple                      |
| D2                  | 28,29,62,65                | 11200                        | Brown                       |
| D3                  | 33,34,57,60                | 11840                        | Grey                        |
| D4                  | 38,39,52,55                | 10240                        | Dark Green                  |
| D5                  | 43,44,47,50                | 7200                         | Pink                        |
| T1                  | 22,25,68,69                | 8200                         | Dark Blue                   |
| T2,T3               | 27,30,32,35,63,64,58,59    | 7200                         | Gold                        |
| T4,T5               | 37,40,42,45,53,54,48,49    | 6200                         | Black                       |
| S                   | 26,31,36,41,46,51,56,61,66 | 9600                         | Yellow                      |
| SO                  | 21,71                      | 18400                        | Orange                      |

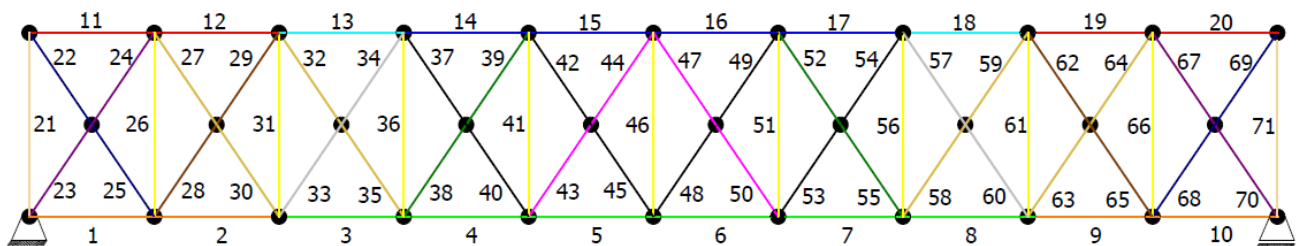


**FIG. 4. 20 FINDING THE POSITION OF CROSS-SECTION BY COLORS.**

## 4.2 Static analysis

We make static analysis of any truss system to distinguish if the system is statically internally or externally determinate or indeterminate. Basically, by doing the analysis, we can find out how many equations we have and how many unknown parameters we have, so if the number of equations is the same as the number of unknown parameters, so the system is statically determinate, otherwise, if the number of equations doesn't equal the number of unknown parameters then the system is statically indeterminate, so for our case, it will be explained better in the next step.

### 4.2.1 External static analysis

Well, we have to consider our system of the truss (bridge) as one whole rigid body then apply a free body diagram which means just draw the reaction forces from the supports, in our case we have in the bottom left pin support and in the bottom right roller support. We are free to choose the direction of the forces. We can check if the direction of the force was chosen right if the magnitude was positive if not so it should be in the opposite direction. The designation of the forces was done to be similar as in Maple software to avoid confusion otherwise, the big letters should also be an index of the force, and they are as in fig. 4.21.

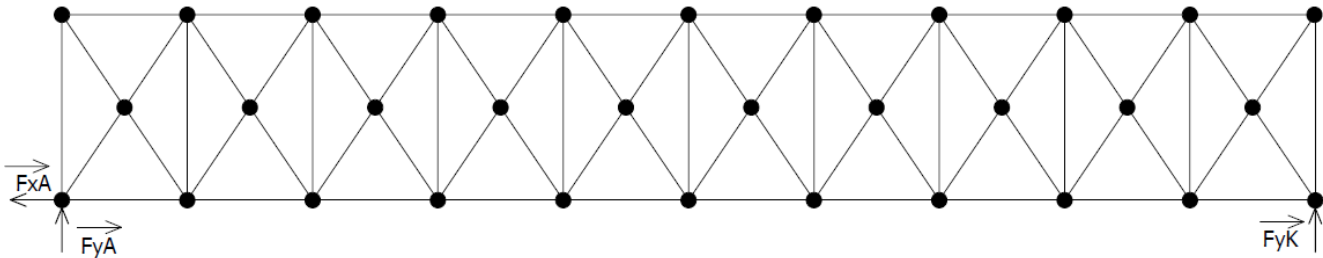


FIG. 4.21 RELACED SUPPORTS.

- So as we can observe from fig. 4.21 we have three unknown forces  $NP = \{F_{xA}, F_{yA}, F_{yK}\}$
- In our case, we have the 2D system, so we have three static equilibrium equations from the formula below we can get.

$$S_{ex} = \mu_{ex} - v_{ex}$$

$$\mu_{ex} = 3$$

$$v_{ex} = 3$$

$$s_{ex} = 0$$

- As we can observe from the formula, we got  $s_{ex} = 0$ , which means that our bridge is an external static determinant.

### 4.2.2 Internal static analysis

When it comes to internal static analysis it is a bit different from external static analysis case, as we know that we are solving our bridge based on a truss theory which means that we have to consider our system of the truss (Bridge) as so many bars connected with others with nodes.

- In the system, we have 71 bars and 32 nodes, using the following formula we get.
  - $P = 71$
  - $K = 32$
  - $P = (2 \times k - 3) \Rightarrow 71 = (2 \times 32 - 3)$
  - $71 \neq 61$
  - For the system to be statically determinate, both sides of equality have to be the same.
  - The system is, therefore,  $10 \times$  internally statically indeterminate, therefore  $S_{in} = 0$ .
- This means that our system is statically indeterminate basically, we have 10 more unknowns, as we know from our knowledge from algebra, to solve a system of equations, the number of the equation has to be the same as the number of unknown parameters.
  - So, to decipher this problem, we have to use Castigliano's theorem to find out these ten unknown parameters to make both sides equal.

### 4.3 Bridge's self-weight load

In this case, we took into consideration self-weight loading because it plays a massive role in the calculations of bridge's deformation, normal forces, and nominal stresses, the loading must be applied only to the nodes, to make this happen, all bars had been split into half their length after the split passes each node in the structure take half of the bar then multiply it by gravitational acceleration and the density, well by doing that we got the weight of the bridge certainly, we also added the weight of the bridge deck, the following example of the calculation of the forces acting on the nodes had been included for better orientation and explanation, and it is as follows.

- Let us take as an example node (A) to avoid mistakes in the equation because it is quite long, the masses of the bars had been calculated individually the calculation was as follows.
- $m = \rho \times V \Rightarrow m = \rho \times X \times S$ , where  $\rho = 7850 \text{ [kg/m}^3\text{]} \dots$  density  
 $X = \text{length of the bar [m]}$   
 $S = \text{cross-section of the bar [mm}^2\text{]}$   
 $g = 9.81 \text{ [m/s}^2\text{]} \dots$ gravitational acceleration.

$$F_g = \frac{1}{2} \times g = (m_1 + m_{21} + m_{23} + m_{so} + m_{TrL} + m_{Lz1r})$$

- As we can observe, the index of the letter m indicates the numbering of the bar and the parameter  $m_{so}$   $m_{TrL}$   $m_{Lz1r}$  are the parameter of the bridge's deck.

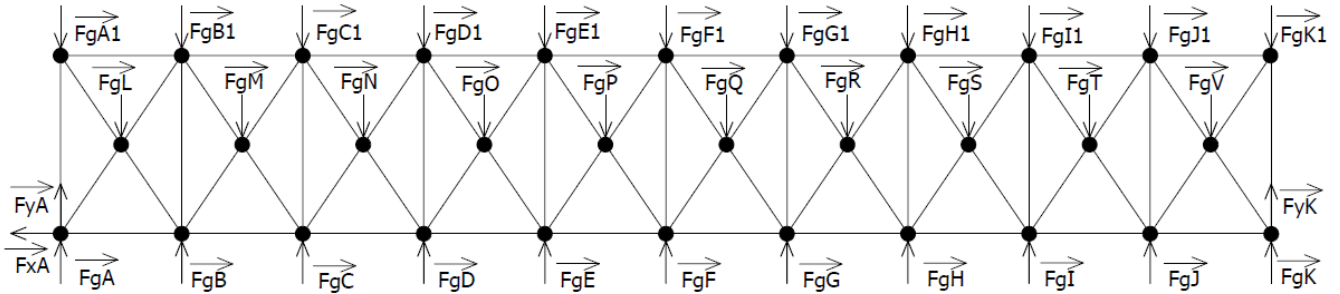


FIG. 4.22 GRAVITATIONAL FORCE FROM BRIDGE'S SELF-WEIGHT.

TAB. 4.2 GRAVITATIONAL LOADING ACTING ON NODES.

| Gravitational Forces [N] |       |      |       |     |       |
|--------------------------|-------|------|-------|-----|-------|
| FgA                      | 12715 | FgA1 | 10485 | FgL | 10870 |
| FgB                      | 14705 | FgB1 | 14815 | FgM | 8157  |
| FgC                      | 14850 | FgC1 | 14317 | FgN | 8441  |
| FgD                      | 14589 | FgD1 | 15353 | FgO | 7288  |
| FgE                      | 13545 | FgE1 | 15477 | FgP | 5940  |
| FgF                      | 13324 | FgF1 | 15025 | FgQ | 5940  |
| FgG                      | 13545 | FgG1 | 15477 | FgR | 7288  |
| FgH                      | 14589 | FgH1 | 15353 | FgS | 8441  |
| FgI                      | 14850 | FgI1 | 14317 | FgT | 8157  |
| FgJ                      | 14705 | FgJ1 | 14815 | FgV | 10870 |
| FgK                      | 12715 | FgK1 | 10485 |     |       |

#### 4.3.1 Free body diagram

We had also done a free body diagram for the construction, which means that each node is released, then we got a static equilibrium equation per each node, as in fig.4.23.

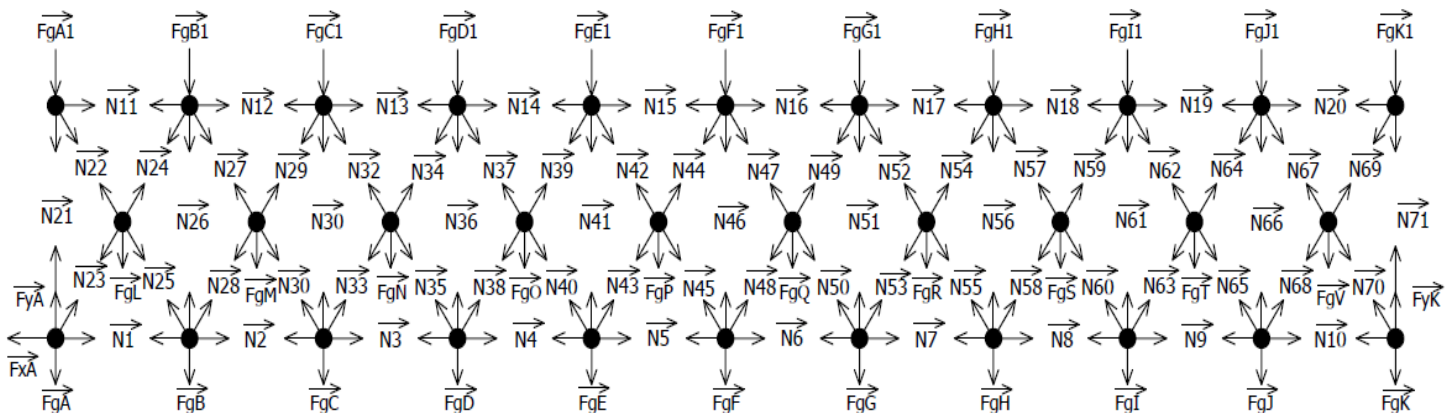


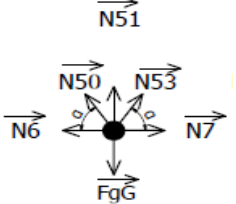
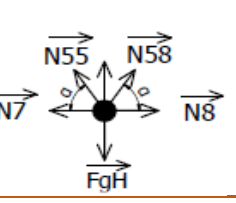
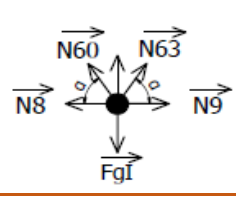
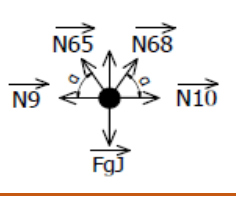
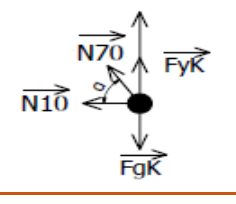
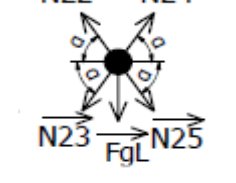
FIG. 4.23 FREE BODY DIAGRAM.

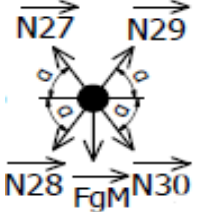
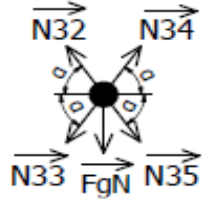
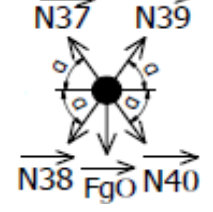
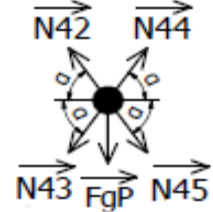
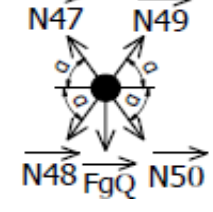
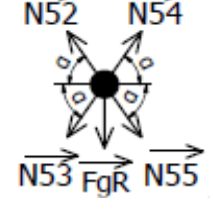
After releasing the nodes, we got 64 static equilibrium equations,  $\sum F_x = 0$  and  $\sum F_y = 0$ , for each node, we got an equation for X and Y, the equation for the moment can not be applied because it equals zero.

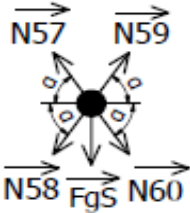
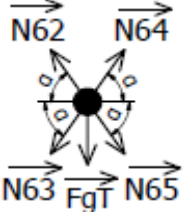
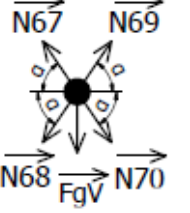
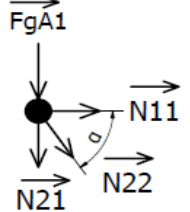
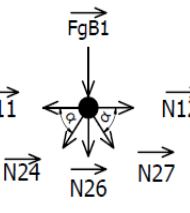
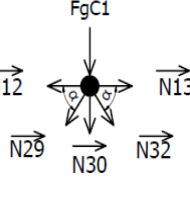
#### 4.3.2 Static equilibrium equations

**TAB. 4.3 RELEASED NODES.**

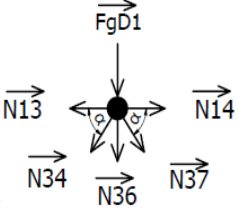
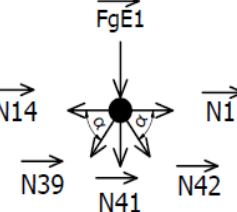
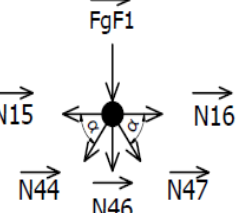
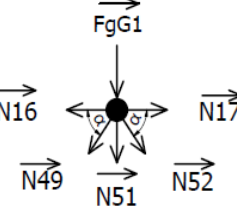
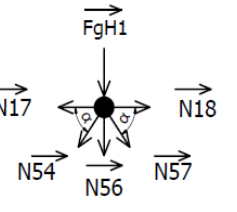
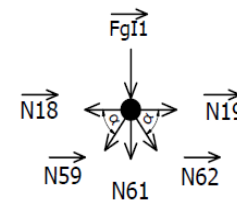
| Figures   | Released Node | Equations   |
|---|---------------|---|
| <b>FIG. 4. 24</b><br><b>RELEASED NODE</b><br><b>A</b> |               | $f1 := N01 + N23 * \cos(\alpha) - Fxa = 0$ $f2 := N21 + N23 * \sin(\alpha) - Fga + Fya = 0$                                       |
| <b>FIG. 4. 25</b><br><b>RELEASED NODE</b><br><b>B</b> |               | $f3 := N02 - N01 + N28 * \cos(\alpha) - N25 * \cos(\alpha) = 0$ $f4 := N26 + N28 * \sin(\alpha) + N25 * \sin(\alpha) - FgB = 0$   |
| <b>FIG. 4. 26</b><br><b>RELEASED NODE</b><br><b>C</b> |               | $f5 := N03 - N02 + N33 * \cos(\alpha) - N30 * \cos(\alpha) = 0$ $f6 := N31 + N33 * \sin(\alpha) + N30 * \sin(\alpha) - FgC = 0$   |
| <b>FIG. 4. 27</b><br><b>RELEASED NODE</b><br><b>D</b> |               | $f7 := N04 - N03 + N38 * \cos(\alpha) - N35 * \cos(\alpha) = 0$ $f8 := N36 + N38 * \sin(\alpha) + N35 * \sin(\alpha) - FgD = 0$   |
| <b>FIG. 4. 28</b><br><b>RELEASED NODE</b><br><b>E</b> |               | $f9 := N05 - N04 + N43 * \cos(\alpha) - N40 * \cos(\alpha) = 0$ $f10 := N41 + N43 * \sin(\alpha) + N40 * \sin(\alpha) - FgE = 0$  |
| <b>FIG. 4. 29</b><br><b>RELEASED NODE</b><br><b>F</b> |               | $f11 := N06 - N05 + N48 * \cos(\alpha) - N45 * \cos(\alpha) = 0$ $f12 := N46 + N48 * \sin(\alpha) + N45 * \sin(\alpha) - FgF = 0$ |

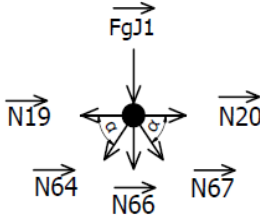
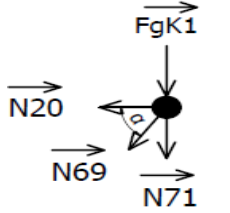
|   |   |  |
|---|---|--|
| <p><b>FIG. 4.30</b><br/><b>RELEASED NODE</b><br/><b>G</b></p> |    | $f_{13} := N_{07} - N_{06} + N_{53} * \cos(\alpha) - N_{50} * \cos(\alpha) = 0$ $f_{14} := N_{51} + N_{53} * \sin(\alpha) + N_{50} * \sin(\alpha) - F_{gG} = 0$  |
| <p><b>FIG. 4.31</b><br/><b>RELEASED NODE</b><br/><b>H</b></p> |    | $f_{15} := N_{08} - N_{07} + N_{58} * \cos(\alpha) - N_{55} * \cos(\alpha) = 0$ $f_{16} := N_{56} + N_{58} * \sin(\alpha) + N_{55} * \sin(\alpha) - F_{gH} = 0$  |
| <p><b>FIG. 4.32</b><br/><b>RELEASED NODE</b><br/><b>I</b></p> |    | $f_{17} := N_{09} - N_{08} + N_{63} * \cos(\alpha) - N_{60} * \cos(\alpha) = 0$ $f_{18} := N_{61} + N_{63} * \sin(\alpha) + N_{60} * \sin(\alpha) - F_{gI} = 0$  |
| <p><b>FIG. 4.33</b><br/><b>RELEASED NODE</b><br/><b>J</b></p> |  | $f_{19} := N_{10} - N_{09} + N_{68} * \cos(\alpha) - N_{65} * \cos(\alpha) = 0$ $f_{20} := N_{66} + N_{68} * \sin(\alpha) + N_{65} * \sin(\alpha) - F_{gJ} = 0$  |
| <p><b>FIG. 4.34</b><br/><b>RELEASED NODE</b><br/><b>K</b></p> |  | $f_{21} := -N_{10} - N_{70} * \cos(\alpha) = 0$ $f_{22} := N_{71} + N_{70} * \sin(\alpha) - F_{gK} + F_{yK} = 0$   |
| <p><b>FIG. 4.35</b><br/><b>RELEASED NODE</b><br/><b>L</b></p> |  | $f_{23} := N_{24} * \cos(\alpha) + N_{25} * \cos(\alpha) - N_{22} * \cos(\alpha) - N_{23} * \cos(\alpha) = 0$ $f_{24} := N_{24} * \sin(\alpha) + N_{22} * \sin(\alpha) - N_{23} * \sin(\alpha) - N_{25} * \sin(\alpha) - F_{gL} = 0$ |

|   |   |  |
|---|---|--|
| <p><b>FIG. 4.36</b><br/><b>RELEASED NODE</b><br/><b>M</b></p> |    | $f_{25} := N_{29} * \cos(\alpha) + N_{30} * \cos(\alpha) - N_{27} * \cos(\alpha) - N_{28} * \cos(\alpha) = 0$ $f_{26} := N_{29} * \sin(\alpha) + N_{27} * \sin(\alpha) - N_{28} * \sin(\alpha) - N_{30} * \sin(\alpha) - F_{gM} = 0$ |
| <p><b>FIG. 4.37</b><br/><b>RELEASED NODE</b><br/><b>N</b></p> |    | $f_{27} := N_{34} * \cos(\alpha) + N_{35} * \cos(\alpha) - N_{32} * \cos(\alpha) - N_{33} * \cos(\alpha) = 0$ $f_{28} := N_{34} * \sin(\alpha) + N_{32} * \sin(\alpha) - N_{33} * \sin(\alpha) - N_{35} * \sin(\alpha) - F_{gN} = 0$ |
| <p><b>FIG. 4.38</b><br/><b>RELEASED NODE</b><br/><b>O</b></p> |    | $f_{29} := N_{39} * \cos(\alpha) + N_{40} * \cos(\alpha) - N_{37} * \cos(\alpha) - N_{38} * \cos(\alpha) = 0$ $f_{30} := N_{39} * \sin(\alpha) + N_{37} * \sin(\alpha) - N_{38} * \sin(\alpha) - N_{40} * \sin(\alpha) - F_{gO} = 0$ |
| <p><b>FIG. 4.39</b><br/><b>RELEASED NODE</b><br/><b>P</b></p> |  | $f_{31} := N_{44} * \cos(\alpha) + N_{45} * \cos(\alpha) - N_{42} * \cos(\alpha) - N_{43} * \cos(\alpha) = 0$ $f_{32} := N_{44} * \sin(\alpha) + N_{42} * \sin(\alpha) - N_{43} * \sin(\alpha) - N_{45} * \sin(\alpha) - F_{gP} = 0$ |
| <p><b>FIG. 4.40</b><br/><b>RELEASED NODE</b><br/><b>Q</b></p> |  | $f_{33} := N_{49} * \cos(\alpha) + N_{50} * \cos(\alpha) - N_{47} * \cos(\alpha) - N_{48} * \cos(\alpha) = 0$ $f_{34} := N_{49} * \sin(\alpha) + N_{47} * \sin(\alpha) - N_{48} * \sin(\alpha) - N_{50} * \sin(\alpha) - F_{gQ} = 0$ |
| <p><b>FIG. 4.41</b><br/><b>RELEASED NODE</b><br/><b>R</b></p> |  | $f_{35} := N_{54} * \cos(\alpha) + N_{55} * \cos(\alpha) - N_{52} * \cos(\alpha) - N_{53} * \cos(\alpha) = 0$ $f_{36} := N_{54} * \sin(\alpha) + N_{52} * \sin(\alpha) - N_{53} * \sin(\alpha) - N_{55} * \sin(\alpha) - F_{gR} = 0$ |

|  |   |  |
|--|---|--|
| <p><b>FIG. 4.42</b><br/><b>RELEASED NODE</b><br/><b>S</b></p>  |    | $f_{37} := N_{59} * \cos(\alpha) + N_{60} * \cos(\alpha) - N_{57} * \cos(\alpha) - N_{58} * \cos(\alpha) = 0$ $f_{38} := N_{59} * \sin(\alpha) + N_{57} * \sin(\alpha) - N_{58} * \sin(\alpha) - N_{60} * \sin(\alpha) - F_{gS} = 0$ |
| <p><b>FIG. 4.43</b><br/><b>RELEASED NODE</b><br/><b>T</b></p>  |    | $f_{39} := N_{64} * \cos(\alpha) + N_{65} * \cos(\alpha) - N_{62} * \cos(\alpha) - N_{63} * \cos(\alpha) = 0$ $f_{40} := N_{64} * \sin(\alpha) + N_{62} * \sin(\alpha) - N_{63} * \sin(\alpha) - N_{65} * \sin(\alpha) - F_{gT} = 0$ |
| <p><b>FIG. 4.44</b><br/><b>RELEASED NODE</b><br/><b>V</b></p>  |   | $f_{41} := N_{69} * \cos(\alpha) + N_{70} * \cos(\alpha) - N_{67} * \cos(\alpha) - N_{68} * \cos(\alpha) = 0$ $f_{42} := N_{69} * \sin(\alpha) + N_{67} * \sin(\alpha) - N_{68} * \sin(\alpha) - N_{70} * \sin(\alpha) - F_{gV} = 0$ |
| <p><b>FIG. 4.45</b><br/><b>RELEASED NODE</b><br/><b>A1</b></p> |  | $f_{43} := N_{11} + N_{22} * \cos(\alpha) = 0$ $f_{44} := -N_{21} - N_{22} * \sin(\alpha) - F_{gA1} = 0$   |
| <p><b>FIG. 4.46</b><br/><b>RELEASED NODE</b><br/><b>B1</b></p> |  | $f_{45} := N_{12} - N_{11} + N_{27} * \cos(\alpha) - N_{24} * \cos(\alpha) = 0$ $f_{46} := -N_{26} - N_{27} * \sin(\alpha) - N_{24} * \sin(\alpha) - F_{gB1} = 0$  |
| <p><b>FIG. 4.47</b><br/><b>RELEASED NODE</b><br/><b>C1</b></p> |  | $f_{47} := N_{13} - N_{12} + N_{32} * \cos(\alpha) - N_{29} * \cos(\alpha) = 0$ $f_{48} := -N_{31} - N_{29} * \sin(\alpha) - N_{32} * \sin(\alpha) - F_{gC1} = 0$  |



|  |   |   |
|--|---|---|
| <p><b>FIG. 4.48</b><br/><b>RELEASED NODE</b><br/><b>D1</b></p> |    | $f_{49} := N_{14} - N_{13} + N_{37} * \cos(\alpha) - N_{34} * \cos(\alpha)$ $= 0$ $f_{50} := -N_{36} - N_{34} * \sin(\alpha) - N_{37} * \sin(\alpha) - F_{gD1}$ $= 0$ |
| <p><b>FIG. 4.49</b><br/><b>RELEASED NODE</b><br/><b>E1</b></p> |    | $f_{51} := N_{15} - N_{14} + N_{42} * \cos(\alpha) - N_{39} * \cos(\alpha)$ $= 0$ $f_{52} := -N_{41} - N_{39} * \sin(\alpha) - N_{42} * \sin(\alpha) - F_{gE1}$ $= 0$ |
| <p><b>FIG. 4.50</b><br/><b>RELEASED NODE</b><br/><b>F1</b></p> |   | $f_{53} := N_{16} - N_{15} + N_{47} * \cos(\alpha) - N_{44} * \cos(\alpha)$ $= 0$ $f_{54} := -N_{46} - N_{44} * \sin(\alpha) - N_{47} * \sin(\alpha) - F_{gF1}$ $= 0$ |
| <p><b>FIG. 4.51</b><br/><b>RELEASED NODE</b><br/><b>G1</b></p> |  | $f_{55} := N_{17} - N_{16} + N_{52} * \cos(\alpha) - N_{49} * \cos(\alpha)$ $= 0$ $f_{56} := -N_{51} - N_{49} * \sin(\alpha) - N_{52} * \sin(\alpha) - F_{gG1}$ $= 0$ |
| <p><b>FIG. 4.52</b><br/><b>RELEASED NODE</b><br/><b>H1</b></p> |  | $f_{57} := N_{18} - N_{17} + N_{57} * \cos(\alpha) - N_{54} * \cos(\alpha)$ $= 0$ $f_{58} := -N_{56} - N_{54} * \sin(\alpha) - N_{57} * \sin(\alpha) - F_{gH1}$ $= 0$ |
| <p><b>FIG. 4.53</b><br/><b>RELEASED NODE</b><br/><b>I1</b></p> |  | $f_{59} := N_{19} - N_{18} + N_{62} * \cos(\alpha) - N_{59} * \cos(\alpha)$ $= 0$ $f_{60} := -N_{61} - N_{59} * \sin(\alpha) - N_{62} * \sin(\alpha) - F_{gI1}$ $= 0$ |

|  |   |   |
|--|---|---|
| <p><b>FIG. 4.54</b><br/><b>RELEASED NODE</b><br/><b>J1</b></p> |  | $f_{61} := N_{20} - N_{19} + N_{67} * \cos(\alpha) - N_{64} * \cos(\alpha) = 0$ $f_{62} := -N_{66} - N_{64} * \sin(\alpha) - N_{67} * \sin(\alpha) - F_{gJ1} = 0$ |
| <p><b>FIG. 4.55</b><br/><b>RELEASED NODE</b><br/><b>K1</b></p> |  | $f_{63} := -N_{20} - N_{69} * \cos(\alpha) = 0$ $f_{64} := -N_{71} - N_{69} * \sin(\alpha) - F_{gK1} = 0$   |

#### 4.3.2 Solving the system of equations

After applying the free body diagram, we got static equilibrium equations where their number was 64 equation since we got in our internal static analysis in chapter 4.2.2 ten times statically indeterminate, so to solve this system, we had to use Castigliano's theorem to get 10 more equations.

- We made a partial free body diagram more in fig.4.56, we randomly chose 10 bars to apply the partial free body diagram on them, and the bars are ( N22, N27, N32, N37, N42, N47, N52, N57, N62, N67 ).
- Castigliano's theorem will be as follows.

$$\sum_{i=1}^{71} \int_0^{L_i} \frac{N_i}{E * S_i} * \frac{dN_i}{dN_j} * dx_i = 0$$

Where :

N... is the normal force

E... is Young's modulus of elasticity in tension

S... is a Cross-section area of the bar

Nj...the index j changes according to the index of normal forces, which had been partially released.

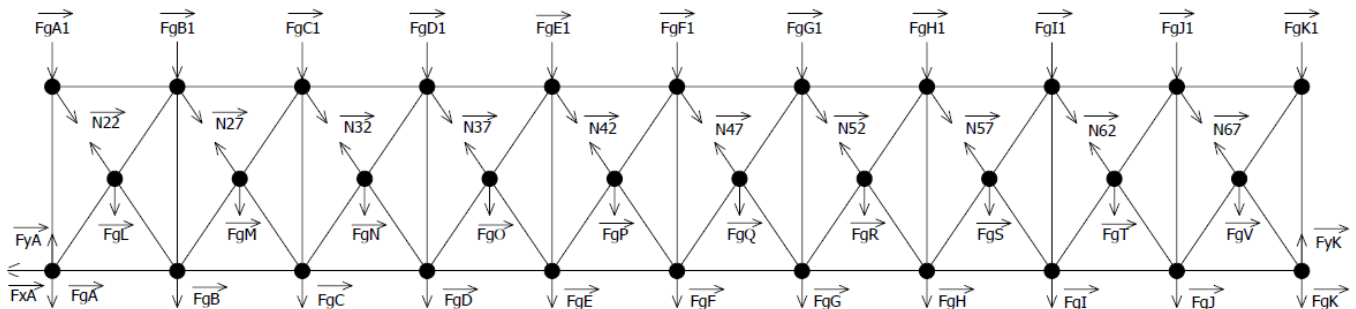


**FIG. 4. 56 PARTIAL FREE BODY  
DIAGRAM.**

The solving process was done by a software called Maple, so at the beginning, after ordering the equation from eq. 1 to eq. 64 we used command `solve({equations},{unknown parameters})`, basically what this command did was making equations as a function of the partial released normal force (N22, N27, N32, etc.) more in the chapter 4.3.2, fig. 4.57 is the solved equation to clarify more, the yellow underlines are the 10 normal forces we gained from the partial free body diagram, that we made the equations as a function of them.

$$\begin{aligned}
& \{F_{xa} = 0., F_{ya} = 1.957297190 \cdot 10^5, F_{yk} = 1.957297190 \cdot 10^5, N01 = -0.7191619645 \cdot N22 + 1.785673797 \cdot 10^5, N02 = -0.7191619645 \cdot N27 + 3.097043349 \cdot 10^5, N03 \\
& = -0.7191619645 \cdot N32 + 4.036130350 \cdot 10^5, N04 = -0.7191619645 \cdot N37 + 4.576467277 \cdot 10^5, N05 = -0.7191619645 \cdot N42 + 4.746943643 \cdot 10^5, N06 = -0.7191619645 \cdot N47 \\
& + 4.569492687 \cdot 10^5, N07 = -0.7191619645 \cdot N52 + 4.030165232 \cdot 10^5, N08 = -0.7191619645 \cdot N57 + 3.098511684 \cdot 10^5, N09 = -0.7191619645 \cdot N62 + 1.771632848 \cdot 10^5, \\
& N10 = -0.7191619645 \cdot N67 + 5625.558503, N11 = -0.7191619645 \cdot N22, N12 = -0.7191619645 \cdot N27 - 1.729418212 \cdot 10^5, N13 = -0.7191619645 \cdot N32 - 3.054828713 \cdot 10^5, \\
& N14 = -0.7191619645 \cdot N37 - 3.992447379 \cdot 10^5, N15 = -0.7191619645 \cdot N42 - 4.538749425 \cdot 10^5, N16 = -0.7191619645 \cdot N47 - 4.716200380 \cdot 10^5, N17 = \\
& -0.7191619645 \cdot N52 - 4.538749425 \cdot 10^5, N18 = -0.7191619645 \cdot N57 - 3.992447379 \cdot 10^5, N19 = -0.7191619645 \cdot N62 - 3.054828713 \cdot 10^5, N20 = -1.729418212 \cdot 10^5 \\
& - 0.7191619645 \cdot N67, N21 = -0.6948424777 \cdot N22 - 10485.34394, N23 = N22 - 2.482992546 \cdot 10^5, N24 = N22 - 2.404768742 \cdot 10^5, N25 = N22 - 7822.380466, N26 = \\
& -0.6948424777 \cdot N22 + 1.522784738 \cdot 10^5 - 0.6948424777 \cdot N27, N28 = N27 - 1.901692809 \cdot 10^5, N29 = N27 - 1.842993047 \cdot 10^5, N30 = N27 - 5869.976191, N31 = \\
& -0.6948424777 \cdot N27 + 1.137412266 \cdot 10^5 - 0.6948424777 \cdot N32, N33 = N32 - 1.364507143 \cdot 10^5, N34 = N32 - 1.303765651 \cdot 10^5, N35 = N32 - 6074.149230, N36 = \\
& -0.6948424777 \cdot N32 + 75237.34487 - 0.6948424777 \cdot N37, N38 = N37 - 81208.39632, N39 = N37 - 75963.70120, N40 = N37 - 5244.695115, N41 = \\
& -0.6948424777 \cdot N37 + 37305.44330 - 0.6948424777 \cdot N42, N43 = N42 - 28949.55908, N44 = N42 - 24674.68583, N45 = N42 - 4274.873254, N46 = \\
& -0.6948424777 \cdot N42 + 2119.860988 - 0.6948424777 \cdot N47, N48 = N47 + 20399.81257, N49 = N47 + 24674.68583, N50 = N47 - 4274.873254, N51 = \\
& -0.6948424777 \cdot N47 - 32622.38290 - 0.6948424777 \cdot N52, N53 = N52 + 70719.00609, N54 = N52 + 75963.70120, N55 = N52 - 5244.695115, N56 = \\
& -0.6948424777 \cdot N52 - 68136.63699 - 0.6948424777 \cdot N57, N58 = N57 + 1.243024158 \cdot 10^5, N59 = N57 + 1.303765651 \cdot 10^5, N60 = N57 - 6074.149230, N61 = \\
& -0.6948424777 \cdot N57 - 1.049089345 \cdot 10^5 - 0.6948424777 \cdot N62, N63 = N62 + 1.784293285 \cdot 10^5, N64 = N62 + 1.842993047 \cdot 10^5, N65 = N62 - 5869.976191, N66 = \\
& -0.6948424777 \cdot N62 - 1.428740588 \cdot 10^5 - 0.6948424777 \cdot N67, N68 = 2.326544937 \cdot 10^5 + N67, N69 = 2.404768742 \cdot 10^5 + N67, N70 = N67 - 7822.380466, N71 = \\
& -1.775788910 \cdot 10^5 - 0.6948424777 \cdot N67\}
\end{aligned}$$

**FIG. 4.57 EQUATION AS A FUNCTION OF PARTIAL .RELEASED FORCE.**

After getting the equations as functions of partial released, normal forces were expressed derivation individually according to the normal force N22 using the following command.

```

for i from 1 to 71 do dN22[i] := diff(N[i], N22) end do:
eval(dN22);

```

After expressing the derivatives, it was already possible to compile the deformation condition by using the following command.

$$f65 := \text{sum} \left( \left( \frac{N[j] \cdot L[j]}{E \cdot S[j]} \cdot dN22[j] \right), j = 1 .. 71 \right) = 0 :$$

As the same previous two steps were deformation conditions expressed for the rest of the partially released normal forces, we obtained 10 more equations. All system was solved using the following command.

```

solve( {f1, f2, f3, f4, f5, f6, f7, f8, f9, f10, f11, f12, f13, f14, f15, f16,
f17, f18, f19, f20, f21, f22, f23, f24, f25, f26, f27, f28, f29, f30, f31,
f32, f33, f34, f35, f36, f37, f38, f39, f40, f41, f42, f43, f44, f45, f46,
f47, f48, f49, f50, f51, f52, f53, f54, f55, f56, f57, f58, f59, f60, f61,
f62, f63, f64, f65, f66, f67, f68, f69, f70, f71, f72, f73, f74}, {Fya,
Fxa, Fyk, N01, N02, N03, N04, N05, N06, N07, N08, N09, N10,
N11, N12, N13, N14, N15, N16, N17, N18, N19, N20, N21, N22,
N23, N24, N25, N26, N27, N28, N29, N30, N31, N32, N33, N34,
N35, N36, N37, N38, N39, N40, N41, N42, N43, N44, N45, N46,
N47, N48, N49, N50, N51, N52, N53, N54, N55, N56, N57, N58,
N59, N60, N61, N62, N63, N64, N65, N66, N67, N68, N69, N70,
N71} ) :

```

**FIG. 4. 58 EQUATIONS AND NORMAL FORCES IN MAPLE SOFTWARE.**

The output of this system of equations were the normal forces and reaction forces from supports.

- $F_{ya} = 1.957297190 * 10^5$  [N]
- $F_{xa} = 0$  [N]
- $F_{yk} = 1.957297190 * 10^5$  [N]

After we got the normal forces, we could calculate the nominal stresses and deflections, So the calculations are as follows.

- To calculate nominal stress, we just had to divide the normal force by cross-section. Again because there are 71 bars which mean 71 nominal stresses, we used Maple software. Let's take bar number 21 as an example, as we can see in fig. 4.59.
- It is very important to keep in mind that the negative value of Nominal Stress means that the bar is under compression, and the positive value of Nominal Stress means that the bar is under tension.

$$\text{sigma\_nom}[21] := \frac{N[21]}{SSO} :$$

**FIG. 4. 59 FINDING THE NOMINAL STRESS IN MAPLE SOFTWARE.**

The most loaded bars of the whole system in terms of Normal Forces. More in Tap. 4.4.

- N5, N6, is symmetrical and has a value of **461056** N, the load is compressive, and they are in the bottom part of the bridge.
- N15, N16, is also symmetrical and having a value of **-467513** N, the load is tensile, and they are in the top part of the bridge.
- Also, the most loaded bars in terms of Nominal Stress. More in Tap. 4.4.
  - N5, N6, is symmetrical and has a value of **20.2930** MPa, and they are in the bottom part of the bridge.
  - N15, N16, is also symmetrical and having a value of **-16.1211** MPa, and they are in the top part of the bridge.

So, the most loaded part of the bridge was in the middle then decreasing to the edges as per our expectations. When it comes to the nominal stress, it also depends on the cross-section, so if we change the cross-section, then the most loaded bars in terms of Nominal Stress definitely will change. We chose the most loaded bars in terms of tensile and compressive load more in the tab. 4.4 the rest results of the bars can be found in attachment number 9.

**TAB. 4.4 NORMAL FORCE AND NOMINAL STRESS IN BARS WITH BRIDGE SELF-WEIGHT.**

| Bar | Normal Force [N] | Nominal Stress [MPa] |
|-----|------------------|----------------------|
| N5  | 461056           | 20.2930              |
| N6  | 461056           | 20.2930              |
| N15 | -467513          | -16.1211             |
| N16 | -467513          | -16.1211             |

- To calculate deflections, we used Castigliano's theorem. As is evident from bridge geometry, the most significant displacement (deflection) can be expected on the joints farthest from the supports, according to that, we chose 10 forces along with the bridge from node A1 to node K1 to observe a gradual change in (deflection).
- Then we deferentially derived all the normal forces according to the 10 forced that had been chosen, as we can see in fig. 4.59-2.

**for  $i$  from 1 to 71 do  $dal[i] := diff(N[i], FgA1)$  end do:**

**FIG.4.59-2 DIFFERENTIAL DERIVE ACCORDING TO A1 IN MAPLE SOFT WARE.**

After the deferential derivative, we integrated it according to the formula below, and index P changes from A1 to K1.

$$up = \sum_{i=1}^{71} \int_0^{L_i} \frac{N_i}{E * S_i} * \frac{dN_i}{dFp} * dx_i$$

- The formula in the software Maple will look like in fig. 4.60.
- The displacements of the individual joints in the vertical direction are given in the Tab. 4.5.

$$ua1 := sum\left(\left(\frac{N[j] \cdot L[j]}{E \cdot S[j]} \cdot dal[j]\right), j = 1 .. 71\right);$$

**FIG. 4.60 FINDING THE DISPLACEMENT IN MAPLE SOFTWARE.**

**TAB. 4. 5 DISPLACEMENT OF NODES.**

| Upper Nodes | Displacement [mm] | Bottom Nodes | Displacement [mm] |
|-------------|-------------------|--------------|-------------------|
| A1          | 0.0750            | A            | 0                 |
| B1          | 2.9692            | B            | 3.0290            |
| C1          | 5.6497            | C            | 5.6715            |
| D1          | 7.6636            | D            | 7.6734            |
| E1          | 8.9511            | E            | 8.9442            |
| F1          | 9.4012            | F            | 9.3872            |
| G1          | 8.9511            | G            | 8.9442            |
| H1          | 7.6636            | H            | 7.6734            |
| I1          | 5.6497            | I            | 5.6715            |
| J1          | 2.9692            | J            | 3.0290            |
| K1          | 0.0750            | K            | 0                 |

The Deflection of the bridge reaches the highest value at the top of the Bridge, particularly at joint F1, which equals 9.4012 mm, then gradually decreases until the edges, Also at the bottom part of the Bridge, The Deflection reaches the highest value at joint F which equals 9.3872 mm, then gradually decreases until the edges, but when it comes to joint A and K they equal to zero because they are connected with the supports.

#### 4.3.3 Checking the limit state of elasticity

Limit state of elasticity has been checked for the most stressed bars in the Bridge, so to check the limit state of elasticity, we took the highest value of Nominal Stress, which was at joint N5 or N6 it doesn't matter because they are symmetry and it equals 20.2929 MPa, in case if the value was negative we just take the absolute value of it, then we used the following formula.

$$K_K = \frac{R_e}{\sigma_{nom}} = \frac{210}{20.29} = 10.34$$

#### 4.4 Load acting on the Bridge from Train plus self-load of Bridge

This section will be the closest to the real-life situations because we took into consideration the weight of the passing Train on the Bridge, of course, we did not neglect the weight of the Bridge itself as well as the most Intensive situation occurs when a train passes on the bridge like deformation and buckling, through the Bridge passes both passenger and freight transport it is combined. The factor of safety according to the limit state of elasticity was checked using the same method as in chapter 4.3.3.

##### 4.4.1 Train specifications

The train that passes through the Bridge is Regio Nova ČD class B2, in our case, we considered that two wagons and two locomotives will pass through the Bridge at once to obtain the maximum weight on the bridge, so every wagon and locomotive weights 18t which means in total we have 72t, the calculations are the same for wagons and locomotives.

Because the wheels are the only contact with the Bridge, so our calculations were with the wheels, of course, we did not neglect the weight of the whole construction of the wagon and locomotive. In one locomotive or wagon, we have 8 wheels. Since we are dealing with the 2D problem, we took symmetry into considerations, thanks to symmetry, we dealt with just 4 wheels for each wagon and locomotive, in fig. 4.16, we can see the distribution of the forces and the whole length of the wagon or locomotive.

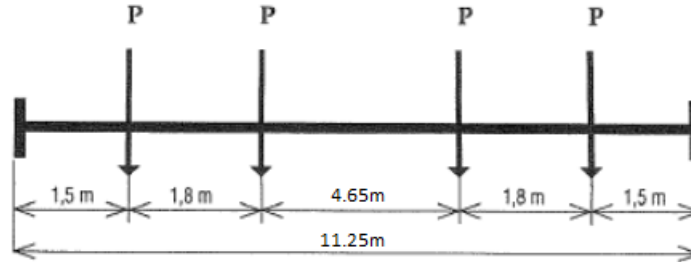


FIG. 4.61 TRAIN WEIGHT DISTRIBUTION.

- To calculate the magnitude of the force exerted by one wheel of the train on the deck, we used the following formula.

$$F_T = \frac{m_T \cdot g}{2 \cdot 4} = \frac{18 \cdot 10^3 \cdot 9.81}{2 \cdot 4} = 22072.5 \text{ N}$$

When the train passed over the bridge, 4 phases of passage were selected, in these phases were analyzed the impact of the train on the bridge and changing of deflection and nominal stresses along the whole bridge, the forces from the train was applied to the nodes, but there were cases when the force was not acting directly on the node this situation was solved that the force was split between the two nodes that the force was acting between them, for example, if the force is acting in the middle of the bar between node A and node B then the force was split into half, so node A takes half of the force and node B also takes the half, of course, all forces of the train had been add to the resultant forces of the bridge self-weight.

#### 4.4.2 Phase 1

In this phase, the train passes the first quarter of the bridge and reaches to node D, the forces generated from the train weight are not acting on any of the nodes, so they were recalculated to act on the nodes more in fig. 4.62. we can see the forces acting on the nodes after the recalculation.

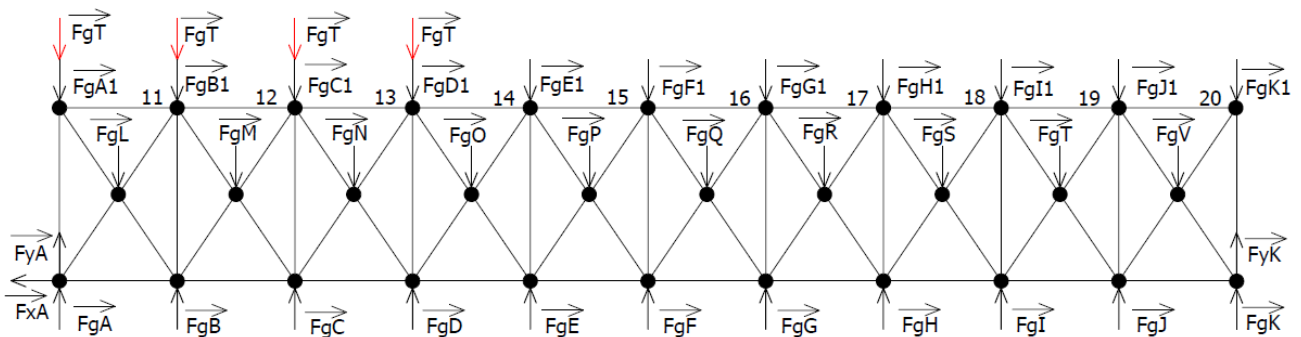


FIG. 4.62 PHASE 1 FORCE DISTRIBUTION.

The forces acting on the nodes remain the same as in the tab. 4.2 in chapter 4.3, except those acting on the following nodes (A1, B1, C1, D1), to those nodes were added forces created by the self-weight bridge and the forces created from the weight of the passing train. The rest of the results of displacement, normal forces, and nominal stresses can be found in attachment number 10.

**TAB. 4.6 DISPLACEMENT IN NODES, GRAVITATIONAL FORCES, AND REACTION FORCES.**

| Node | Displacement [mm] | Node | Displacement [mm] | Gravitational Forces [N] |        |
|------|-------------------|------|-------------------|--------------------------|--------|
| uA1  | 0.1085            | uA   | 0                 | FgA1                     | 22868  |
| uB1  | 3.6678            | uB   | 3.7270            | FgB1                     | 46564  |
| uC1  | 6.8832            | uC   | 6.8845            | FgC 1                    | 46066  |
| uD1  | 9.1611            | uD   | 9.1584            | FgD1                     | 27736  |
| uE1  | 10.5193           | uE   | 10.5077           | Reaction Force [N]       |        |
| uF1  | 10.9014           | uF   | 10.8853           | Fya                      | 270753 |
| uG1  | 10.2728           | uG   | 10.2668           | Fyk                      | 208969 |
| uH1  | 8.7285            | uH   | 8.7411            |                          |        |
| uI1  | 6.3981            | uI   | 6.4228            |                          |        |
| uJ1  | 3.3506            | uJ   | 3.4154            |                          |        |
| uK1  | 0.0800            | uK   | 0                 |                          |        |

**TAB. 4.7 NORMAL FORCES AND NOMINAL STRESSES IN THE BARS, TRAIN PHASE 1.**

| Bar | Norma Force [N] | Nominal Stress [MPa] | Factor of safety |
|-----|-----------------|----------------------|------------------|
| N5  | 535514          | 23.5702              | 8.9              |
| N6  | 522576          | 23.0007              | 9.1              |
| N15 | -543786         | -18.7513             | 11.2             |
| N16 | -529320         | -18.2524             | 11.5             |

#### 4.4.3 Phase 2

In this phase, the train passes 7 nodes, and it reaches to node G1, the forces generated from the train weight are not acting on any of the nodes also, so they were recalculated to act on the nodes in fig. 4.63, we can see the forces acting on the nodes after the recalculation.

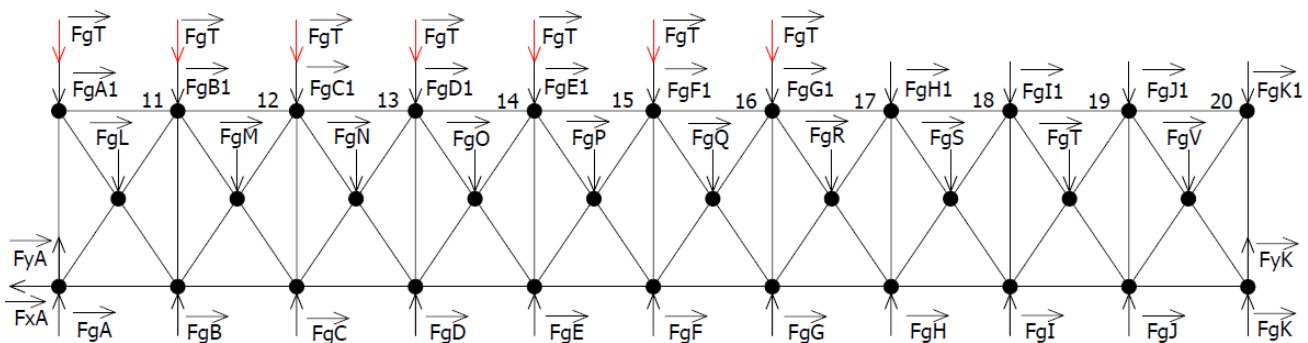


**FIG. 4.63 PHASE 2 FORCE DISTRIBUTION.**



The forces acting on the nodes also remain the same as in the tab. 4.2 in chapter 4.3 except those acting on the following nodes (A1, B1, C1, D1, E1, F1, G1), those nodes were added forces created by the self-weight bridge, and the forces created from the weight of the passing train. The rest of the displacement results, normal forces, and nominal stresses can be found in attachment N. 11.

**TAB. 4.8 DISPLACEMENT IN NODES, GRAVITATIONAL FORCES, AND REACTION FORCES.**

| Node | Displacement [mm] | Node | Displacement [mm] | Gravitational Forces [N] |        |
|------|-------------------|------|-------------------|--------------------------|--------|
| uA1  | 0.1481            | uA   | 0                 | FgA1                     | 22868  |
| uB1  | 4.9584            | uB   | 4.7822            | FgB1                     | 27197  |
| uC1  | 9.4238            | uC   | 8.9174            | FgC 1                    | 46066  |
| uD1  | 12.7345           | uD   | 11.9846           | FgD1                     | 40119  |
| uE1  | 14.7917           | uE   | 13.8566           | FgE1                     | 47226  |
| uF1  | 15.4433           | uF   | 14.3693           | FgF1                     | 46774  |
| uG1  | 14.5614           | uG   | 13.4696           | FgG1                     | 27860  |
| uH1  | 12.2972           | uH   | 11.3747           | Reaction Force [N]       |        |
| uI1  | 8.9444            | uI   | 8.2964            | Fya                      | 319298 |
| uJ1  | 4.6556            | uJ   | 4.3843            | Fyk                      | 248687 |
| uK1  | 0.1020            | uK   | 0                 |                          |        |

**TAB. 4. 9 NORMAL FORCES AND NOMINAL STRESSES IN THE BARS, TRAIN PHASE 2.**

| Bar | Norma Force [N] | Nominal Stress [MPa] | Factor of safety |
|-----|-----------------|----------------------|------------------|
| N5  | 726891          | 31.9934              | 6.5              |
| N6  | 702060          | 30.9005              | 6.7              |
| N15 | -733297         | -25.2861             | 8.3              |
| N16 | -706998         | -24.3792             | 8.6              |

#### 4.4.4 Phase 3

In this phase, the train passes 8 nodes it reaches to node H1, the forces generated from the train weight are not acting on any of the nodes also, so they were recalculated to act on the nodes in fig. 4.65, we can see the forces acting on the nodes after the recalculation.

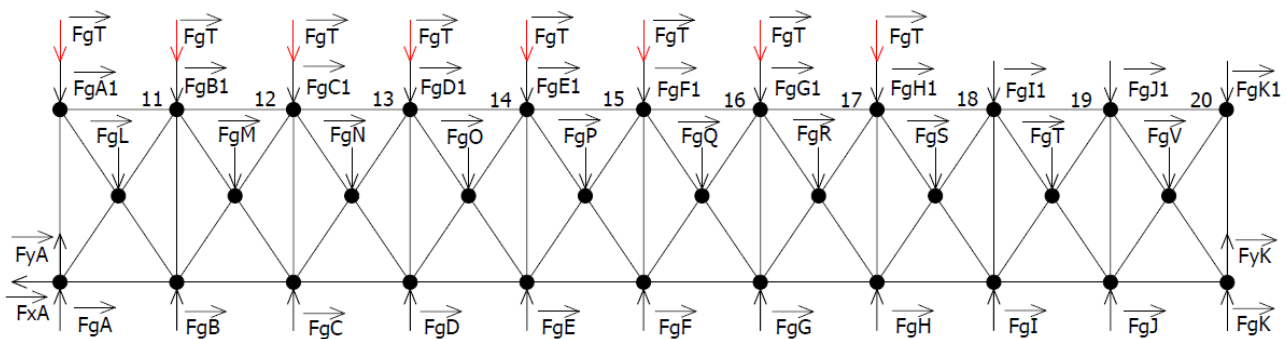


**FIG. 4.64 PHASE 3 FORCE DISTRIBUTION.**

The forces acting on the nodes remain the same as in the tab. 4.2 in chap. 4.3, except those acting on the following nodes (A1, B1, C1, D1, E1, F1, G1, H1), those nodes were added forces created by the self-weight bridge and the forces created from the weight of the passing train. The rest of the displacement results, normal forces, and nominal stresses can be found in attachment N. 12.

**TAB. 4.10 DISPLACEMENT IN NODES, GRAVITATIONAL FORCES, AND REACTION FORCES.**

| Node | Displacement [mm] | Node | Displacement [mm] | Gravitational Forces [N] |        |
|------|-------------------|------|-------------------|--------------------------|--------|
| uA1  | 0.1481            | uA   | 0                 | FgA1                     | 22868  |
| uB1  | 4.9584            | uB   | 5.0464            | FgB1                     | 27198  |
| uC1  | 9.4238            | uC   | 9.4396            | FgC 1                    | 46067  |
| uD1  | 12.7345           | uD   | 12.7286           | FgD1                     | 40119  |
| uE1  | 14.7917           | uE   | 14.7634           | FgE1                     | 47226  |
| uF1  | 15.4433           | uF   | 15.3984           | FgF1                     | 46774  |
| uG1  | 14.5614           | uG   | 14.5331           | FgG1                     | 27860  |
| uH1  | 12.2972           | uH   | 12.3128           | FgH1                     | 27737  |
| uI1  | 8.9444            | uI   | 8.9827            | Reaction Force [N]       |        |
| uJ1  | 4.6556            | uJ   | 4.7423            | Fya                      | 344539 |
| uK1  | 0.1020            | uK   | 0                 | Fyk                      | 267578 |

**TAB. 4. 11 NORMAL FORCES AND NOMINAL STRESSES IN THE BARS, TRAIN PHASE 3.**

| Bar | Norma Force [N] | Nominal Stress [MPa] | Factor of safety |
|-----|-----------------|----------------------|------------------|
| N5  | 771976          | 33.9779              | 6.1              |
| N6  | 760686          | 33.4809              | 6.2              |
| N15 | -779072         | -26.8646             | 7.8              |
| N16 | -765848         | -26.4086             | 7.9              |

#### 4.4.5 Phase 4

In this phase, the train passes 11 nodes it reaches to node K1, the forces generated from the train weight are not acting on any of the nodes also, so they were recalculated to act on the nodes in fig. 4.65, we can see the forces acting on the nodes after the recalculation.

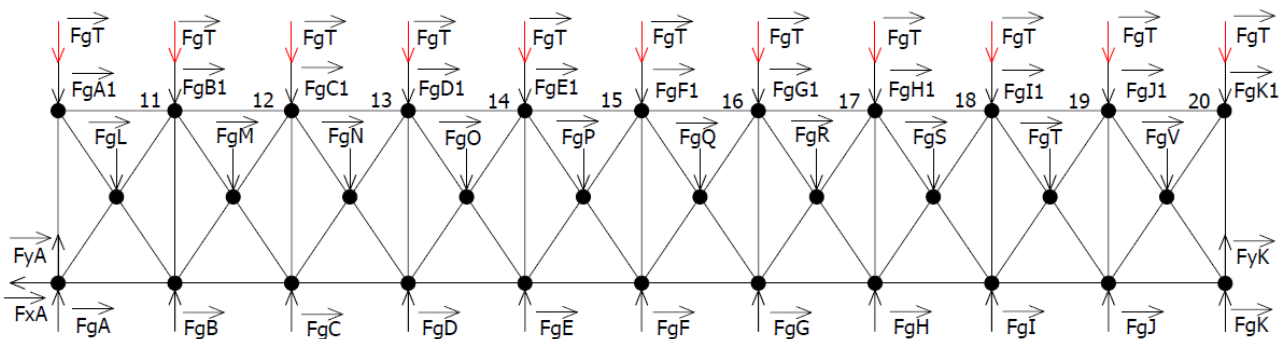


**FIG. 4.65 PHASE 4 FORCE DISTRIBUTION.**

The forces acting on the nodes remain the same as in the tab. 4.2 in chapter 4.3, except those acting on the following nodes (A1, B1, C1, D1, E1, F1, G1, H1, I1, J1, K1), those nodes were added forces created by the self-weight bridge and the forces created from the weight of the passing train. The rest of the displacement results, normal forces, and nominal stresses can be found in attachment N. 13.

**TAB. 4.12 DISPLACEMENT IN NODES, GRAVITATIONAL FORCES.**

| Node | Displacement [mm] | Node | Displacement [mm] | Gravitational Forces [N] |       |
|------|-------------------|------|-------------------|--------------------------|-------|
| uA1  | 0.1530            | uA   | 0                 | FgA1                     | 42234 |
| uB1  | 5.3397            | uB   | 5.4326            | FgB1                     | 39580 |
| uC1  | 10.1722           | uC   | 10.1908           | FgC 1                    | 46067 |
| uD1  | 13.7993           | uD   | 13.7962           | FgD1                     | 47103 |
| uE1  | 16.1132           | uE   | 16.0859           | FgE1                     | 40243 |
| uF1  | 16.9434           | uF   | 16.8964           | FgF1                     | 46774 |
| uG1  | 16.1295           | uG   | 16.0965           | FgG1                     | 47226 |
| uH1  | 13.7946           | uH   | 13.7979           | FgH1                     | 40119 |
| uI1  | 10.1779           | uI   | 10.1956           | FgI1                     | 46067 |
| uJ1  | 5.3542            | uJ   | 5.4402            | FgJ1                     | 46564 |
| uK1  | 0.1355            | uK   | 0                 | FgK1                     | 22868 |

**TAB. 4.13 REACTION FORCES.**

| Reaction Force [N] |        |
|--------------------|--------|
| Fya                | 357778 |
| Fyk                | 342602 |

**TAB. 4.14 NORMAL FORCES AND NOMINAL STRESSES IN THE BARS TRAIN PHASE 4.**

| Bar | Norma Force [N] | Nominal Stress [MPa] | Factor of safety |
|-----|-----------------|----------------------|------------------|
| N5  | 833496          | 36.6856              | 5.72             |
| N6  | 835144          | 36.7581              | 5.71             |
| N15 | -840879         | -28.9958             | 7.24             |
| N16 | -842122         | -29.0387             | 7.23             |

#### 4.4.6 Conclusion of the four phases

As we can see in Figures (4.62, 4.63, 4.64, 4.65) that the locomotives and wagons pass gradually on the top of the bridge from the beginning, which is the left part of the bridge, to the end, which is the right part of the bridge so for the calculations, we had to split the process of passing it into four phases to analyze the different positions of the train weight on the bridge however according to that we predicted that the Normal forces, Nominal stresses, and displacement would increase gradually in each Phase which should be correct because in every phase we are increasing the weight on the bridge by adding into the nodes recalculated forces created by wagons and locomotives weight.

The most loaded phase should be the fourth because, in the fourth phase, we have two locomotives, one wagon, and a half wagon, on the bridge, which makes it the heavier phase for more in fig. 4.65, according to our expectation, the fourth phase will be the most dangerous one when it comes to the buckling limit state due to the high values of compression forces.

As we can see in all phases, the common things are that the most loaded bar when it comes to nominal stress and normal force in tension is bar N5 except in phase four is bar N6, and the most loaded bar in compression is bar N15 again except in phase four it is bar N16, and the highest numbers of nominal stress, normal force, and deflection we can find in the fourth phase.

All phases are similar in the most deflected node, which is node F1 then node F with a tiny difference, in phase 2 and phase 3 the deflection in node F is totally the same the reason behind that is that phase 2 and phase 3 did not get significant changes in loads, so the difference was mainly in the bottom part of the bridge.

We could also notice in tables (4.6, 4.8, 4.10, 4.12) that there is a zero deflection in all phases at node A and K, and it should be zero because at node A we have pin support mounted to it, and at node K, we have roller support also mounted to it.

The safety against the limit state of elasticity was calculated for each phase to make sure that the construction is safe after increasing a heavy load in every phase, so we took the highest absolute value of nominal stress into our calculations, so we got the factor of safety in phase 1  $K_k = 8.9$  and decreasing to  $K_k = 5.7$  in phase 4, which means that the load gets heavier most likely although the factor of safety is low it's still in the safe zone that the bridge wouldn't collapse or exceed the limit state of elasticity.

## 4.5 Statically Determinate assignment

In this section, we made a simpler model of the bridge because one of the goals of the bachelor thesis is to change the degree of static indeterminacy so that we changed it to a statically determinate task, which means that 20 bars and 10 nodes from the middle part of the bridge have been removed because we changed the topology. It was evident that our static indeterminant bridge is 10 times statically indeterminate and it was more than enough to reduce it just by 10 bars and keep the nodes to achieve the static determinacy but in our more straightforward model we reduced the bars by 20 times the reason why we did this significant change is that we wanted the bridge to look like in a real-life construction, not an imaginary bridge, however, after reducing the bars we had to take out the nodes in the middle of the bridge as well the removed nodes were ( L, M, N, O, P, Q, R, S, T, V ), Finally, after the reduction process, we ended with a static determinate structure having 41 bars and 11 nodes are effected by simple tension and compression, the dimensions of the whole bridge remain the same does not change the total length is  $4140 \times 10$  which means 41400 mm, and the height is 4000 mm, the supports also stay the same which means two supports on the left pin support which allows just rotation on Z-axis (perpendicular) and the right is supported by roller support means that the part of the bridge can move horizontally and rotate around the Z-axis (perpendicular).

### 4.5.1 The main descriptions of the bridge

The bridge was described as simple as possible to make it easy in calculations and orientations, using an alphabet system and numbering, it is as follows.

### 4.5.2 The main dimensions

The main dimensions describe the full length of the part of the bridge, which is 41400 mm, the height, which is 4000 mm, the length of one block, which is 4140 mm, the length of inner bars which is 5757mm, and the angle between the bars which is  $44.01^\circ$ .

### 4.5.6 The naming of nodes and numbering of bars

This part of the bridge contains 41 bars separated by nodes, so they were numbered from 1 to 41, starting from the bottom left to the top of the bridge. This part of the bridge contains 11 nodes, so they were named alphabetically, starting from bottom left by letter A to the bottom right by letter K, the upper part of the bridge was copied from the bottom but with adding 1 like this (A1).

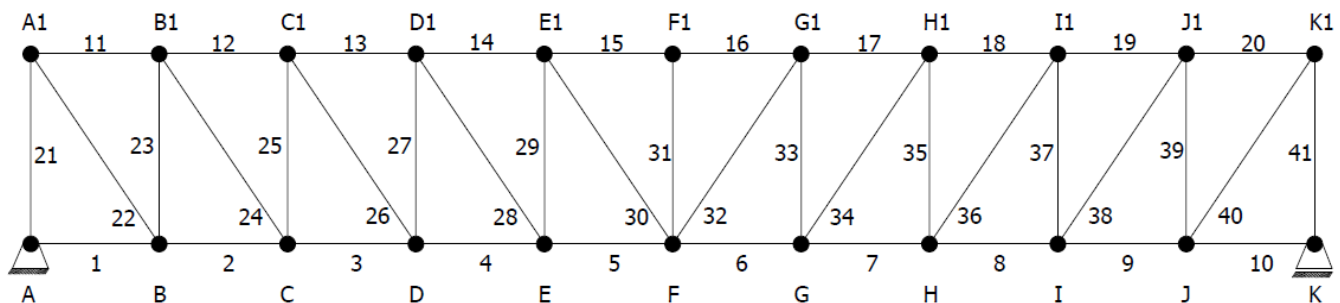


FIG. 4.66 NUMBERING THE BARS AND NAMING THE NODES.

#### 4.5.7 Cross-sections

For the construction of the bridge were used 10 different types of cross-sections. They are the same as in the statically indeterminate structure. They can be found in chapter 4.1.5.

**TAB. 4. 15 COLOR AND NUMBERS OF CROSS-SECTIONS.**

| Cross-sections Name | Number of bar              | Cross-section area in $mm^2$ | colours corresponding to bar |
|---------------------|----------------------------|------------------------------|------------------------------|
| O1,O2               | 11,12,19,20                | 22000                        | Red                          |
| O3                  | 13,18                      | 26000                        | Yellow                       |
| O4,O5               | 14,15,16,17                | 29000                        | Green                        |
| U1,U2               | 1,2,9,10                   | 211200                       | Blue                         |
| U3,U4,U5            | 3,4,5,6,7,8                | 22720                        | Magenta                      |
| T1                  | 22,40                      | 8200                         | Grey                         |
| T2,T3               | 24,26,36,38                | 7200                         | Grey                         |
| T4,T5               | 28,30,32,34                | 6200                         | Grey                         |
| S                   | 23,25,27,29,31,33,35,37,39 | 9600                         | Orange                       |
| SO                  | 21,41                      | 18400                        | Dark Green                   |

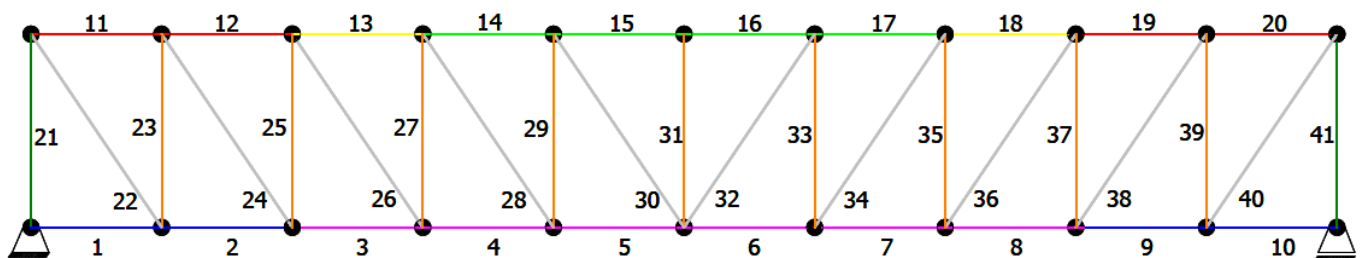


**FIG. 4.67 FINDING THE POSITION OF CROSS-SECTION BY COLORS.**

#### 4.6 Static analysis

We make static analysis of any truss system to distinguish if the system is statically internally or externally determined or not determined, basically, by doing the analysis, we can find out how many equations we have and how many unknowns parameters we have, so if the number of equations is the same as the number of unknowns parameters, so the system is statically determined, otherwise if the number of equations not equal to the number of unknown parameters then the system is statically undetermined, so for our case will be explained better in the next step.

#### 4.6.1 External static analysis

Well, we have to consider our system of the truss (bridge) as on whole rigid body then released the supports which means just draw the reaction forces for supports, in our case we have in the bottom left pin support and in the bottom right roller support, and we are free to choose the direction of the forces however they are same as in chapter 4.2.1 fig. 4.21, in this easier model, nothing has been changed according to the supports they are the same as in the real-life model.

- So, as we can observe from fig. 4.21 in chapter 4.2.1, we have three unknown forces we gained them from releasing the supports  $NP = \{F_{xA}, F_{yA}, F_{yK}\}$
- In our case, we have the 2D system, so we have three static equilibrium equations from the formula below we can get.

$$S_{ex} = \mu_{ex} - v_{ex}$$

$$\mu_{ex} = 3$$

$$v_{ex} = 3$$

$$S_{ex} = 0$$

- As we can observe from the formula, we got  $S_{ex} = 0$ , which means that our bridge is an external static determinant.

#### 4.6.2 Internal static analysis

When it comes to internal static analysis is a bit different from external static analysis case, as we know that we are solving our bridge based on a truss theory which means that we have to consider our system of the truss (Bridge) as so many bars connected with others with nodes.

- In the system, we have 41 bars and 22 nodes, using the following formula we get.
- $P = 41$ .... Where P is number of bars
- $K = 22$ .... Where K is number of Nodes
- $P = (2 \times k - 3) \Rightarrow 41 = (2 \times 22 - 3)$
- $41 = 41$
- For the system to be statically determinate, both sides of equality have to be the same.
- As we can see from the formula that both sides are equals which means we have got 41 equations and 41 unknowns, this is the definition of a static determinate structure.

#### 4.7 Bridge's self-weight load

In this chapter, we calculated the forces created from the bridge's weight, the steps of calculation and the used equations are the same as in the static indeterminate task, detailed information were mentioned in chapter 4.3, the only changes are in the results the cannot be same according to our changes in the structure of the bridge.

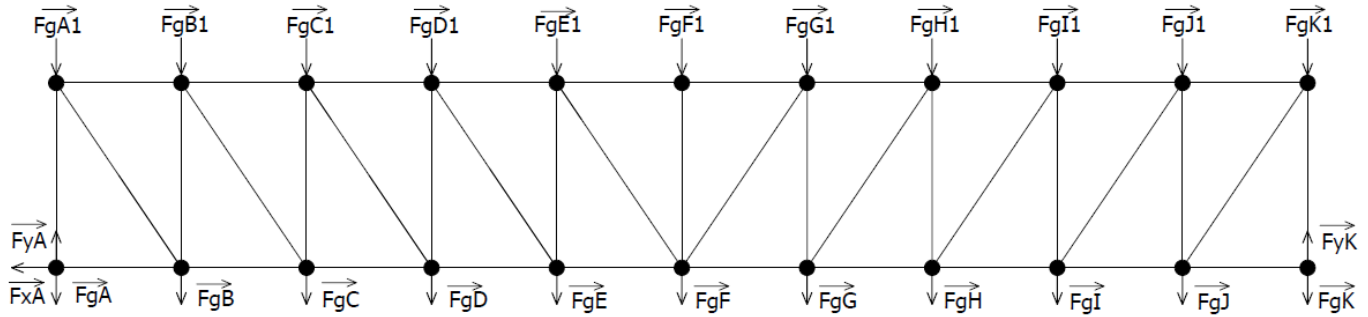


FIG. 4.68 GRAVITATIONAL FORCES FROM BRIDGE'S SELF-WEIGHT.

TAB. 4.16 GRAVITATIONAL LOADING ACTING ON NODES.

| Gravitational Forces [N] |       |      |       |
|--------------------------|-------|------|-------|
| FgA                      | 9097  | FgA1 | 10485 |
| FgB                      | 12222 | FgB1 | 11197 |
| FgC                      | 12226 | FgC1 | 11835 |
| FgD                      | 12319 | FgD1 | 12729 |
| FgE                      | 11949 | FgE1 | 13207 |
| FgF                      | 13324 | FgF1 | 11833 |
| FgG                      | 11949 | FgG1 | 13207 |
| FgH                      | 12319 | FgH1 | 12729 |
| FgI                      | 12226 | FgI1 | 11835 |
| FgJ                      | 12222 | FgJ1 | 11197 |
| FgK                      | 9097  | FgK1 | 10485 |

#### 4.7.1 Free body diagram.

It has been drawn a free body diagram for all construction, which means that each node is released, then we got a static equilibrium equation per each node in the X and the Y direction, and the moment is zero. The releasing process will be the same as in chapter 4.3.2, and only it will be in a different configuration; the nodes will be fewer. The released nodes and their equations can be found in attachment N. 58.

#### 4.7.2 Solving the system of equations

After applying the free body diagram, we got static equilibrium equations where their number was 44 equation, from our internal static analysis in chapter 4.6.2, we found that the number of unknown parameters equals to the number of the equations thanks to that, we did not have to do any special modifications if the Maple software unlike in statically indeterminate task chapter 4.1.

```
solve( {f1, f2, f3, f4, f5, f6, f7, f8, f9, f10, f11, f12, f13, f14, f15, f16,
f17, f18, f19, f20, f21, f22, f23, f24, f25, f26, f27, f28, f29, f30, f31,
f32, f33, f34, f35, f36, f37, f38, f39, f40, f41, f42, f43, f44}, {Fya,
Fxa, Fyk, N01, N02, N03, N04, N05, N06, N07, N08, N09, N10,
N11, N12, N13, N14, N15, N16, N17, N18, N19, N20, N21, N22,
N23, N24, N25, N26, N27, N28, N29, N30, N31, N32, N33, N34,
N35, N36, N37, N38, N39, N40, N41} )
```

FIG. 4.69 EQUATIONS AND NORMAL FORCES IN MAPLE SOFTWARE.



The solving process was done by a software called Maple, so at the beginning, after ordering the equation from eq. 1 to eq. 44 we used command `solve({equations},{unknown parameters})`, basically what this command did was finding the values of the normal forces and reactions forces, the reaction forces from supports.

- $F_{ya} = 1.298496887 \cdot 10^5$  [N]
- $F_{xa} = 0$  [N]
- $F_{yk} = 1.298496887 \cdot 10^5$  [N]

We can see that the reaction forces in this task have a smaller magnitude than the reaction forces in a static determinate task because the load on the bars is less since we decreased the bars in the construction by 20.

After we got the normal forces, we could calculate the nominal stresses and deflections, So the calculations are as follows.

- To calculate nominal stress, we just had to divide the normal force by cross-section, again because 41 bars mean 41 nominal stresses, we used Maple software. Let's take bar number 21 as an example, as we can see in fig. 4.70
- It is essential to keep in mind that the negative value of Nominal Stress means that the bar is under compression, and the positive value of Nominal Stress means that the bar is under tension.

$$\text{sigma\_nom}[21] := \frac{N[21]}{SSO} :$$

FIG. 4.70 FINDING THE NOMINAL STRESS IN MAPLE SOFTWARE.

The most loaded bars of the whole system in terms of Normal Forces are

- N5, N6, is symmetrical and has a value of 308050 N, and they are in the bottom part of the bridge.
- N15, N16, is also symmetrical and having a value of -321069 N, and they are in the top part of the bridge.

Also, the most loaded bars in terms of Nominal Stress

- N22, N40, is symmetrical and has a value of 19.3527 MPa, and they are in the bottom part of the bridge.

So, the most loaded part of the bridge in terms of normal stress was in the middle then decreasing to the edges as per our expectations, when it comes to the nominal stress, it highly depends on the cross-section, that's the reason why bars N22, N40 are the most loaded, and bars N1, and N10 has zero values because they do not transmit any force. The rest results of the bars can be found in attachment N. 36.

**TAB. 4.17 NORMAL FORCES AND NOMINAL STRESSES IN THE BARS BRIDGE SELF-WEIGHT.**

| Bar | Norma Force [N] | Nominal Stress [MPa] | Bar | Norma Force [N] | Nominal Stress [MPa] |
|-----|-----------------|----------------------|-----|-----------------|----------------------|
| N5  | 308050          | 13.5586              | N22 | 158692          | 19.3527              |
| N6  | 308050          | 13.5586              | N40 | 158692          | 19.3527              |
| N15 | -321070         | -11.0714             | N1  | 0               | 0                    |
| N16 | -321070         | -11.0714             | N10 | 0               | 0                    |

- To calculate deflections, we used Castigliano's theorem. As is evident from bridge geometry, the most significant displacement (deflection) can be expected. On the joints farthest from the supports, according to that, we chose 10 forces along with the bridge from node A1 to node K1 to observe a gradual change in (deflection).
- Then we deferentially derived all the normal forces according to the 10 forced that had been chosen, as you can see in fig. 4.71.

**for  $i$  from 1 to 41 do  $da1[i] := diff(N[i], FgA1)$  end do:**

**FIG. 4.71 DIFFERENTIAL DERIVE ACCORDING TO A1 IN MAPLE SOFT**

After the deferential derivative, we integrated according to formula bellow

$$u_R = \sum_{i=1}^{41} \int_0^{L_i} \frac{N_i}{E \cdot S_i} * \frac{dN_i}{dF_p} * dx_i$$

- The formula in the software Maple will look like in fig. 4.72.
- The displacements of the individual joints in the vertical direction are given in the tab. 4.18.

$$ua1 := sum\left(\left(\frac{N[j] \cdot L[j]}{E \cdot S[j]} \cdot da1[j]\right), j = 1 .. 41\right);$$

**FIG. 4.72 FINDING THE DISPLACEMENT IN MAPLE SOFT WARE.**

**TAB. 4.18 DISPLACEMENT OF NODES.**

| Node | Displacement [mm] | Node | Displacement [mm] |
|------|-------------------|------|-------------------|
| uA1  | 0.1250            | uA   | 0                 |
| uB1  | 2.8435            | uB   | 2.6490            |
| uC1  | 5.2209            | uC   | 5.0728            |
| uD1  | 6.9882            | uD   | 6.8880            |
| uE1  | 8.1042            | uE   | 8.0530            |
| uF1  | 8.4688            | uF   | 8.4453            |
| uG1  | 8.1042            | uG   | 8.0530            |
| uH1  | 6.9882            | uH   | 6.8880            |
| uI1  | 5.2209            | uI   | 5.0728            |
| uJ1  | 2.8435            | uJ   | 2.6490            |
| uK1  | 0.1250            | uK   | 0                 |

The Deflection of the bridge reaches the highest value at the top of the Bridge, particularly at joint F1, which equals 8.4688 mm, then gradually decreases until the edges, also at the bottom part of the Bridge, The Deflection reaches the highest value at joint F which equals 8.4453 mm, then gradually decreases until the edges, but when it comes to joint A and K they equal to zero because they are connected with the supports. After all, there cannot be allowed any displacement.

#### 4.7.3 Checking the limit state of elasticity

The limit state of elasticity has been checked for the most stressed bars in the Bridge, so to check the limit state of elasticity, we took the highest value of Nominal Stress, which was at joint N5 or N6 doesn't matter because they are symmetry. It equals 19.3527 MPa, in case if the value was negative, we just take the absolute value of it, then we used the following formula.

$$K_K = \frac{R_e}{\sigma_{nom}} = \frac{210}{19.35} = 10.85$$

#### 4.8 Load acting on the Bridge from Train plus self-load of Bridge

This section will be the closest to the real-life situations because we took into consideration the weight of the passing Train on the Bridge, of course, we did not neglect the weight of the Bridge itself as well as the most dangerous situation occurs when a Train passes on the Bridge like Deformation and Buckling, through the Bridge passes both passenger and freight transport it is combined.

##### 4.8.1 Train specifications

The train that passes through the Bridge is the same as in a statically indeterminate case Regio Nova ČD class B2, the consideration still the same, which is that two wagons and two locomotives will pass through the Bridge at once to obtain the maximum weight on the bridge. Hence, every wagon and locomotive weights still the same 18 t, which gives us a total of 72 t, the calculations are the same for wagons and locomotives.

Because the wheels are the only contact with the Bridge, so our calculations were with the wheels. Of course, we did not neglect the weight of the whole construction of the wagon and locomotive. In one locomotive or wagon, we have 8 wheels since we are dealing with the 2D problem as well we took the symmetry of the bridge into considerations, thanks to symmetry, we dealt with just four wheels for each wagon and locomotive in fig. 4.61 chapter 4.4.1, we can see the distribution of the forces and the whole length of wagon or locomotive.

- For the calculation of the force exerted by one wheel of the train on the bridge rails, the same formula as in the static indeterminate task was applied more in chapter 4.4.1.

When the train passed over the bridge, 4 phases of passage were selected, in these phases were analyzed the impact of the train on the bridge and changing of deflection and nominal Stresses along the whole Bridge, the forces from the train was applied to the nodes, but there were cases when the force was not acting directly on the node this situation was solved that the force was split between the two nodes that the force was acting between them, for example, if the force is acting in the middle the bar between node A and node B then the force was split into half, so node A takes half of the force and node B also takes the half, of course, all forces of the train had been add to the resultant forces of the bridge self-weight. According to the limit state of elasticity, the factor of safety was checked using the absolute value of the higher magnitude Nominal stress.

#### 4.8.2 Phase 1

In this phase, the train passes the first quarter of the bridge and reaches to the node D, the forces generated from the train weight are not acting on any of the nodes so they were recalculated to act on the nodes more in fig.4.73, we can see the forces acting on the nodes after the recalculation.

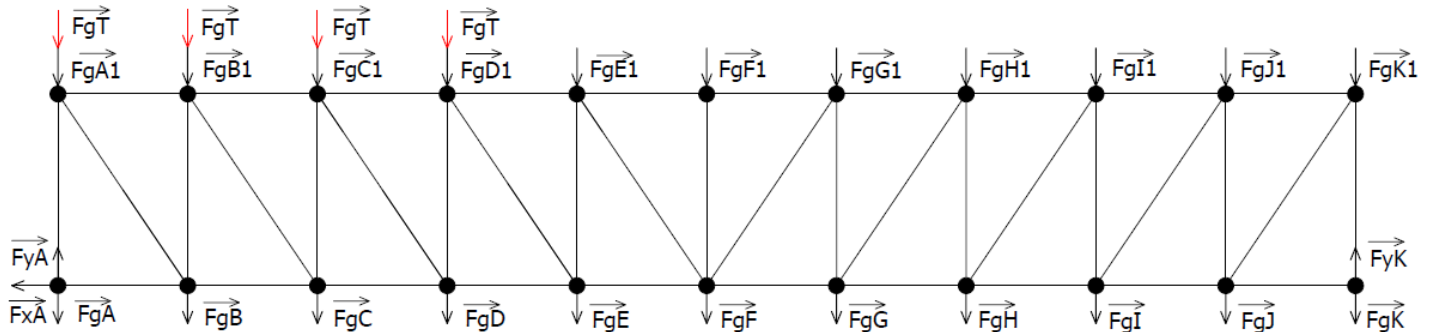


FIG. 4.73 PHASE 1 FORCE DISTRIBUTION.

The forces acting on the nodes remain the same as in the tab. 4.16, except those acting on the following nodes (A1, B1, C1, D1), to those nodes were added forces created by the self-weight bridge and the forces created from the weight of the passing train. The rest results of normal forces and nominal stresses can be found in attachment N. 37.

TAB. 4. 19 DISPLACEMENT IN NODES, GRAVITATIONAL FORCES, AND REACTION FORCES.

| Node | Displacement [mm] | Node | Displacement [mm] | Gravitational Forces [N] |             |
|------|-------------------|------|-------------------|--------------------------|-------------|
| uA1  | 0.2026            | uA   | 0                 | FgA1                     | 22868       |
| uB1  | 4.0397            | uB   | 3.7208            | FgB1                     | 42946       |
| uC1  | 7.1596            | uC   | 6.9502            | FgC 1                    | 43584       |
| uD1  | 9.1792            | uD   | 9.0808            | FgD1                     | 25111.92298 |
| uE1  | 10.2473           | uE   | 10.2224           | Reaction Force [N]       |             |
| uF1  | 10.4584           | uF   | 10.4349           | Fya                      | 204873      |
| uG1  | 9.8439            | uG   | 9.7665            | Fyk                      | 143089      |
| uH1  | 8.3639            | uH   | 8.2375            |                          |             |
| uI1  | 6.1804            | uI   | 6.0061            |                          |             |
| uJ1  | 3.3368            | uJ   | 3.1160            |                          |             |
| uK1  | 0.1387            | uK   | 0                 |                          |             |

TAB. 4. 20 NORMAL FORCES AND NOMINAL STRESSES IN THE BARS TRAIN PHASE 1.

| Bar | Norma Force [N] | Nominal Stress [MPa] | Bar | Norma Force [N] | Nominal Stress [MPa] |
|-----|-----------------|----------------------|-----|-----------------|----------------------|
| N5  | 390268          | 17.1773              | N1  | 0               | 0                    |
| N6  | 362862          | 15.9710              | N10 | 0               | 0                    |
| N14 | -390268         | -13.4575             | N22 | 248844          | 30.3469              |
| N15 | -389584         | -13.4339             | N23 | -160685         | -16.7380             |

#### 4.8.3 Phase 2

In this phase, the train passes 7 nodes, and it reaches node G1. The forces generated from the train weight are not acting on any of the nodes also, so they were recalculated to act on the nodes more in fig. 4.74, we can see the forces acting on the nodes after the recalculation.

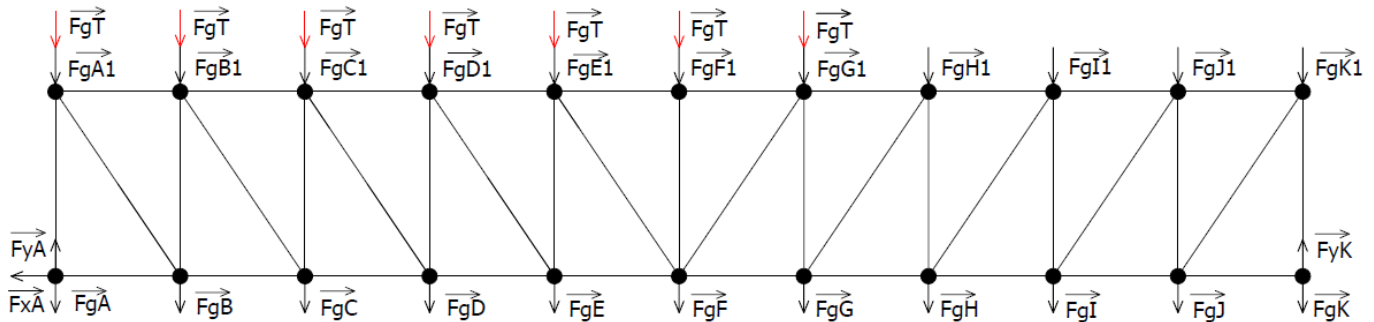


FIG. 4.74 PHASE 2 FORCE DISTRIBUTION.

The forces acting on the nodes remain the same as in the tab. 4.16, except for those acting on the following nodes (A1, B1, C1, D1, E1, F1, G1), those nodes were added forces created by the self-weight bridge and the forces created from the weight of the passing train. The rest results of normal forces and nominal stresses can be found in the attachment. N. 38.

TAB. 4. 21 DISPLACEMENT IN NODES, GRAVITATIONAL FORCES, AND REACTION FORCES.

| Node | Displacement [mm] | Node | Displacement [mm] | Gravitational Forces [N] |        |
|------|-------------------|------|-------------------|--------------------------|--------|
| uA1  | 0.2529            | uA   | 0                 | FgA1                     | 22868  |
| uB1  | 5.4529            | uB   | 5.0378            | FgB1                     | 42946  |
| uC1  | 9.8874            | uC   | 9.5817            | FgC 1                    | 43584  |
| uD1  | 13.0382           | uD   | 12.8434           | FgD1                     | 37494  |
| uE1  | 14.9074           | uE   | 14.8108           | FgE1                     | 44956  |
| uF1  | 15.3189           | uF   | 15.2324           | FgF1                     | 43582  |
| uG1  | 14.2168           | uG   | 14.0605           | FgG1                     | 25590  |
| uH1  | 11.8566           | uH   | 11.6514           | Reaction Force [N]       |        |
| uI1  | 8.6358            | uI   | 8.3827            | Fya                      | 253418 |
| uJ1  | 4.6048            | uJ   | 4.3052            | Fyk                      | 182807 |
| uK1  | 0.1798            | uK   | 0                 |                          |        |

TAB. 4. 22 NORMAL FORCES AND NOMINAL STRESSES IN THE BARS, TRAIN PHASE 2.

| Bar | Norma Force [N] | Nominal Stress [MPa] | Bar | Norma Force [N] | Nominal Stress [MPa] |
|-----|-----------------|----------------------|-----|-----------------|----------------------|
| N5  | 578428          | 25.4589              | N1  | 0               | 0                    |
| N6  | 527297          | 23.2085              | N10 | 0               | 0                    |
| N15 | -582311         | -20.0797             | N22 | 318709          | 38.8669              |
| N16 | -582311         | -20.0797             | N23 | -209229         | -21.7947             |

#### 4.8.4 Phase 3

In this phase, the train passes 8 nodes, and it reaches node H1, the forces generated from the train weight are not acting on any of the nodes also, so they were recalculated to act on the nodes in fig. 4.75, we can see the forces acting on the nodes after the recalculation.

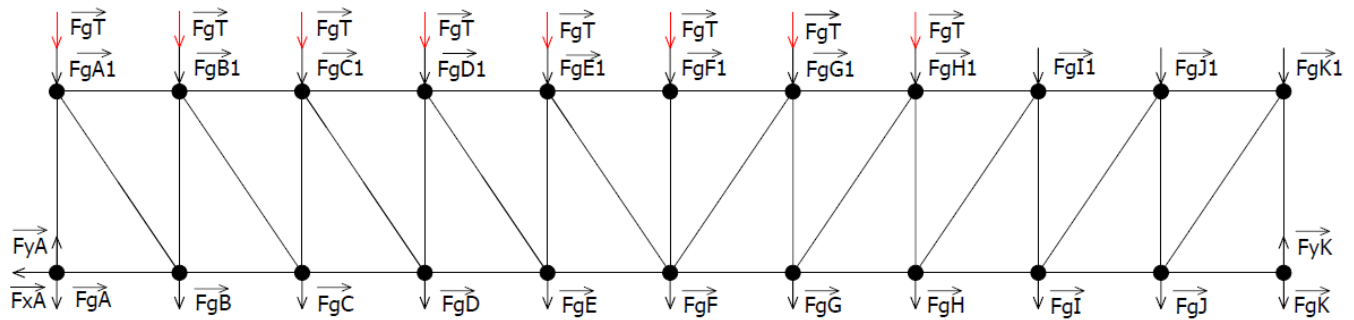


FIG. 4.75 PHASE 3 FORCE DISTRIBUTION.

The forces acting on the nodes remain the same as in the tab. 4.16, except for those acting on the following nodes (A1, B1, C1, D1, E1, F1, G1, H1), those nodes were added forces created by the self-weight bridge, and the forces created from the weight of the passing train. The rest results of normal forces and nominal stresses can be found in attachment N. 39.

TAB. 4. 23 DISPLACEMENT IN NODES, GRAVITATIONAL FORCES, AND REACTION FORCES.

| Node | Displacement [mm] | Node | Displacement [mm] | Gravitational Forces [N] |        |
|------|-------------------|------|-------------------|--------------------------|--------|
| uA1  | 0.2790            | uA   | 0                 | FgA1                     | 42234  |
| uB1  | 5.7720            | uB   | 5.3452            | FgB1                     | 35963  |
| uC1  | 10.5625           | uC   | 10.2313           | FgC1                     | 43584  |
| uD1  | 14.0339           | uD   | 13.8136           | FgD1                     | 44478  |
| uE1  | 16.1072           | uE   | 15.9989           | FgE1                     | 37973  |
| uF1  | 16.7130           | uF   | 16.6265           | FgF1                     | 43582  |
| uG1  | 15.7319           | uG   | 15.5628           | FgG1                     | 44957  |
| uH1  | 13.1978           | uH   | 12.9551           | FgH1                     | 25112  |
| uI1  | 9.5904            | uI   | 9.2997            | Reaction Force [N]       |        |
| uJ1  | 5.1013            | uJ   | 4.7643            | Fya                      | 278659 |
| uK1  | 0.1994            | uK   | 0                 | Fyk                      | 201698 |

TAB. 4. 24 NORMAL FORCES AND NOMINAL STRESSES IN THE BARS, TRAIN PHASE 3.

| Bar | Normal Force [N] | Nominal Stress [MPa] | Bar | Normal Force [N] | Nominal Stress [MPa] |
|-----|------------------|----------------------|-----|------------------|----------------------|
| N5  | 617204           | 27.1656              | N1  | 0                | 0                    |
| N6  | 592689           | 26.0867              | N10 | 0                | 0                    |
| N15 | -634396          | -21.8757             | N22 | 327163           | 39.8979              |
| N16 | -634396          | -21.8757             | N23 | -215104          | -22.4067             |

#### 4.8.5 Phase 4

In this phase, the train passes 11 nodes, and it reaches node K1, the forces generated from the train weight are not acting on any of the nodes also, so they were recalculated to act on the nodes in fig. 4.76, we can see the forces acting on the nodes after the recalculation. The rest results of normal forces and nominal stresses can be found in attachment N. 40.

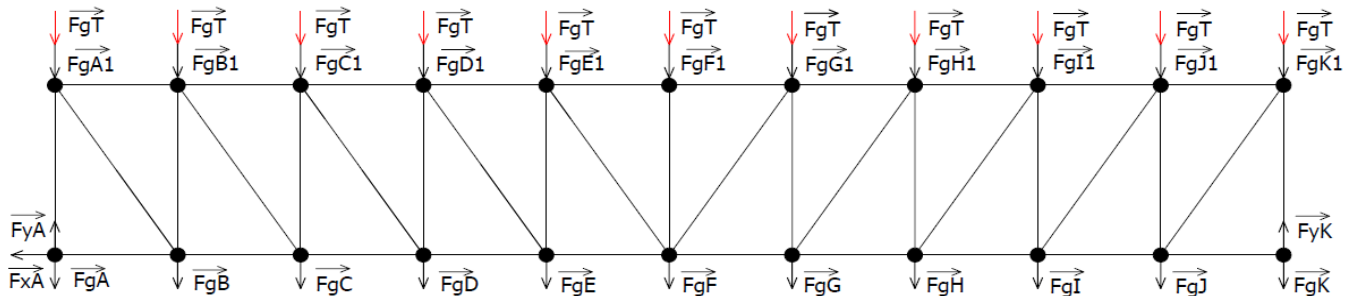


FIG. 4.76 PHASE 4 FORCE DISTRIBUTION.

The forces acting on the nodes remain the same as in the tab. 4.16, except those acting on the following nodes (A1, B1, C1, D1, E1, F1, G1, H1, I1, J1, K1), those nodes were added forces created by the self-weight bridge and the forces created from the weight of the passing train.

TAB. 4. 25 DISPLACEMENT IN NODES, GRAVITATIONAL FORCES.

| Node | Displacement [mm] | Node | Displacement [mm] | Gravitational Forces [N] |       |
|------|-------------------|------|-------------------|--------------------------|-------|
| uA1  | 0.2927            | uA   | 0                 | FgA1                     | 42234 |
| uB1  | 6.2652            | uB   | 5.8121            | FgB1                     | 35962 |
| uC1  | 11.5219           | uC   | 11.1645           | FgC 1                    | 43584 |
| uD1  | 15.4096           | uD   | 15.1631           | FgD1                     | 44478 |
| uE1  | 17.8469           | uE   | 17.7123           | FgE1                     | 37972 |
| uF1  | 18.7025           | uF   | 18.6161           | FgF1                     | 43582 |
| uG1  | 17.8749           | uG   | 17.7321           | FgG1                     | 44956 |
| uH1  | 15.3888           | uH   | 15.1478           | FgH1                     | 37494 |
| uI1  | 11.5290           | uI   | 11.1770           | FgI1                     | 43584 |
| uJ1  | 6.29744           | uJ   | 5.8360            | FgJ1                     | 42946 |
| uK1  | 0.27704           | uK   | 0                 | FgK1                     | 22868 |

TAB. 4. 26 REACTION FORCES.

| Reaction Force [N] |        |
|--------------------|--------|
| Fya                | 291898 |
| Fyk                | 276722 |

TAB. 4. 27 NORMAL FORCES AND NOMINAL STRESSES IN THE BARS, TRAIN PHASE 4

| Bar | Norma Force [N] | Nominal Stress [MPa] | Bar | Norma Force [N] | Nominal Stress [MPa] |
|-----|-----------------|----------------------|-----|-----------------|----------------------|
| N5  | 672016          | 29.5781              | N1  | 0               | 0                    |
| N6  | 674907          | 29.7054              | N10 | 0               | 0                    |
| N15 | -702910         | -24.2383             | N22 | 346217          | 42.2216              |
| N16 | -702910         | -24.2383             | N24 | 276870          | 38.4541              |

## 4.9 Conclusion of the four phases

As we can see in Figures (4.73, 4.74, 4.75, 4.76) that the locomotives and wagons pass gradually on the top of the bridge from the beginning, which is the left part of the bridge, to the end, which is the right part of the bridge so for the calculations, we had split the process of passing it into four phases to analyze the different position of the train weight on the bridge however according to that we predicted that the Normal forces, Nominal stresses, and displacement would increase gradually in each Phase which should be correct because in every phase we are increasing the weight on the bridge by adding into the nodes recalculated forces created by wagons and locomotives weight.

The most loaded phase should be the fourth because, in the fourth phase, we have two locomotives, one wagon, and a half wagon, on the bridge, which makes it the heavier phase for more in fig. 4.76, according to our expectation, the fourth bridge will be the most dangerous one when it comes to the buckling limit state due to the high values of compression forces.

### ❖ Phase1

In this phase from tables 4.19, and 4.20 we got.

- The most nominal stress in tension applied at bar number N22 of value 30.3469 MPa, and the maximum stress in compression applied at bar N23 of value a -16.738 MPa, the maximum absolute Nominal stress is the same at bar N22 of value at 30.346 MPa.
- The maximum tension force is applied at the bar number N5 of value at 390268 N, and the maximum compression force is applied at the bar number N14 of value at -390268 N, the maximum absolute force is the same at bar N5 and N14 of value at 390268 N.
- The maximum deflection applied is at node F1 in the middle-upper part of the bridge at a value of 10.4584 mm and node F in the middle-bottom part of the bridge at a value of 10.4349 mm.
- Checking the factor of safety according to the limit state of elasticity using the absolute value of the Nominal stress.

$$K_K = \frac{R_e}{\sigma_{nom}} = \frac{210}{30.34} = 6.92$$

### ❖ Phase2

In this phase from tables 4.21, and 4.22 we got.

- The most nominal stress in tension applied at bar number N22 of value 38.8669 MPa, and the maximum stress in compression applied at bar N23 of value at -21.79478723 MPa, the maximum absolute Nominal stress is the same at bar N22 of value at 38.8669 MPa.
- The maximum tension force is applied at the bar number N5 of value at 578428 N, and the maximum compression force is applied at the bar number N15 and N16 of value at -582311 N, the maximum absolute force is the same at bar N15 and N16 of value at 582311 N.



- The maximum deflection applied is at node F1 in the middle-upper part of the bridge at a value of 15.3189 mm and node F in the middle-bottom part of the bridge at a value of 15.2324 mm.
- Checking the factor of safety according to the limit state of elasticity using the absolute value of the Nominal stress.

$$K_K = \frac{R_e}{\sigma_{nom}} = \frac{210}{38.86} = 5.40$$

### ❖ Phase3

In this phase from tables 4.23, and 4.24 we got

- The most nominal stress in tension applied at bar number N22 of value 39.8979 MPa, and the maximum stress in compression applied at bar N23 of value at -22.4067 MPa, the maximum absolute Nominal stress is the same at bar N22 of value at 39.8979 MPa.
- The maximum tension force is applied at the bar number N5 of value at 617204 N, and the maximum compression force is applied at the bar number N15 of value at -634396 N, the maximum absolute force is the same at bar N15 and N16 of value at 634396 N.
- The maximum deflection applied is at node F1 in the middle-upper part of the bridge at a value of 16.7130 mm] and node F in the middle-bottom part of the bridge at a value of 16.6265 mm.
- Checking the factor of safety according to the limit state of elasticity using the absolute value of the Nominal stress.

$$K_K = \frac{R_e}{\sigma_{nom}} = \frac{210}{39.89} = 5.26$$

### ❖ Phase4

In this phase from tables 4.25, 4.26, and 4.27, we got.

- The most nominal stress in tension applied at bar number N22 of value 42.2216 MPa, and the maximum stress in compression applied at bar N16 of value at -24.2383 MPa, the maximum absolute Nominal stress is the same at bar N22 of value at 42.2216 MPa.
- The maximum tension force is applied at the bar number N6 of value at 674907 N, and the maximum compression force is applied at the bar number N15 and N16 of value at -702910 N, the maximum absolute force is the same at bar N15 and N16 of value at 702910 N.
- The maximum deflection applied is at node F1 in the middle-upper part of the bridge at a value of 18.7025 mm and node F in the middle-bottom part of the bridge at a value of 18.6161 mm.

- Checking the factor of safety according to limit state of elasticity using the absolute value of the Nominal stress

$$K_K = \frac{R_e}{\sigma_{nom}} = \frac{210}{42.22} = 4.97$$

As we can see in all phases, the common things are that the most loaded bar when it comes to nominal stress and normal force, in tension is bar N5 and the most loaded bar in compression is bar N15 again except in phase four is bar N16, and the highest numbers of nominal stress, normal force, and deflection we can find in the fourth phase.

All phases are similar in the most deflected node, which is node F1, after it tightly node F with a very small difference.

We could also notice that there is a zero deflection in all phases at node A and K, and it should be zero because at node A we have pin support mounted to it, and at node K, we have roller support also mounted to it.

The safety against the limit state of elasticity was calculated for each phase to make sure that the construction is safe after increasing a heavy load in every phase, so we took the highest absolute value of nominal stress into our calculations so we got the factor of safety in phase 1  $K_k = 6.92$  and decreasing to  $K_k = 4.97$  in phase 4, which means that the loads get heavier most likely, the construction will fail against the elasticity limit state and collapse.

#### 4.10 Checking the buckling stability limit state of the bridge.

One of the most dangerous situations that can occur when a bar is under high compressive loading is occurring a buckling, and if the bar is under high compression, it can lead to buckling. Therefore, the limit state of buckling can only be achieved under a high-stress pressure so that the deformation of the bar changes from compression to bending.

In order for the buckling limit state to occur before the limit state of elasticity, it must meet the condition that the slenderness of the checked bar is higher than the critical slenderness.

According to the type of placement of individual bars in our bridge structure, the coefficient  $\alpha$  was chosen for placement between two rotational supports, therefore  $\alpha = \pi$ . So, the slenderness is therefore determined as follows.

$$\lambda_{Kr} = \pi \cdot \sqrt{\frac{E}{R_e}} = \pi \cdot \sqrt{\frac{210 \cdot 10^3}{210}} = 99.34$$

So, to check the limit state of buckling, we compared the result of critical slenderness with the slenderness of the individual bars which were determined for bars loaded with compression according to the following relationship.

$$\lambda = \frac{l}{\sqrt{\frac{I_{min}}{s}}}$$

##### 4.10.1 Self-weight load

Because the variant self-load has the fewest loads when it compares to the others, so we decided to move it into attachments holding number 1.

#### 4.10.2 Load acting on the Bridge from Train plus self-load of Bridge

In this chapter, we will check the limit state of buckling for both structures (statically determinate and statically indeterminate) under the bridge's self-weight. We will also consider the weight of passing locomotives and wagons. The critical force must apply the determination of safety that decides if a bar is safe against buckling limit state since the highest slenderness of the bars is at the value of 84.79 more in tab. 1, in attachment 1, and both structures have the same properties, and it is enough to determine only one critical force. However, we calculated it using the following formula.

$$F_{kr} = \frac{\alpha^2 \cdot E \cdot J_{min}}{l^2} = 2766943 \text{ [N]}$$

##### a) Safety for a static indeterminate structure

Form tab. 1, in attachment 1, bars (36,41,46,51) has the highest value of slenderness, and the bar number (46) has the most elevated normal force under compression at -23662 N in-phase(4), the negative sign means that the bar is under compression; however, we took the absolute value, and to find the factor of safety, we divided the critical force by the normal force acting on the bar as follows.

$$K_v = \frac{F_{kr}}{F} = 117$$

Thus, the safety of the train-load structure dropped to almost a third of the original value, which was calculated for a statically indeterminate structure, where the system was loaded only by its own weight. Nevertheless, security is high enough.

##### b) Safety for a static determinate structure

Form tab.1, bars (23,25,27,29,31,33,35,37,39) has the highest value of slenderness and the bar number (23) has the highest nominal stress under compression at -283839 N in-phase (4). to find the factor of safety, we divided the critical force by the normal force as follows.

$$K_v = \frac{F_{kr}}{F} = 9.7$$

If we compare the resulting safety with the safety that came out under the load only by the self-weight of the bridge, we observe a deterioration again. Here, too, it is assumed that with greater stress on the bridge structure, the buckling failure will occur earlier than the elasticity failure.

## 5 Numerical Calculations using finite element method

In this section, we used the finite element method to solve or structures. The software that has been used was Ansys workbench, it is necessary to mention that the solution is only approximate and is always a slight tolerance of error, but Usually, the accuracy of the solution is sufficient for our analyzing application. In our steps of the solution, it is possible to use a bar or link-type element bar bodies. However, a Link element transmits only axial loads, and only displacement parameters can be calculated with it, but in Bar element can be used for other calculations also such as torsion, bending, shear. This section shows the results obtained using the simulation software ANSYS, which will serve as a check of the accuracy of analytical calculations.

## 5.1 Statically indeterminate structure 2D

We created a model in software Ansys that has the exact geometrical dimensions of the bridge as in chapter 4.1.2, fig. 4.2, and the cross-sections are the same also as in chapter 4.1.5, figures (4.6-4.18). In this chapter, the 2D comparison will be applied for the self-weight bridge and a passing train in phase 4 plus the bridge's self-weight. However, in this thesis will be written just the statically indeterminate case, and the statically determinate case will be attached in attachment holding number 8.

### 5.1.1 Self-weight bridge analyzing displacement and normal forces

In this section, we built a model with self-bridge's loading effect, and it led to the displacement and created normal forces.

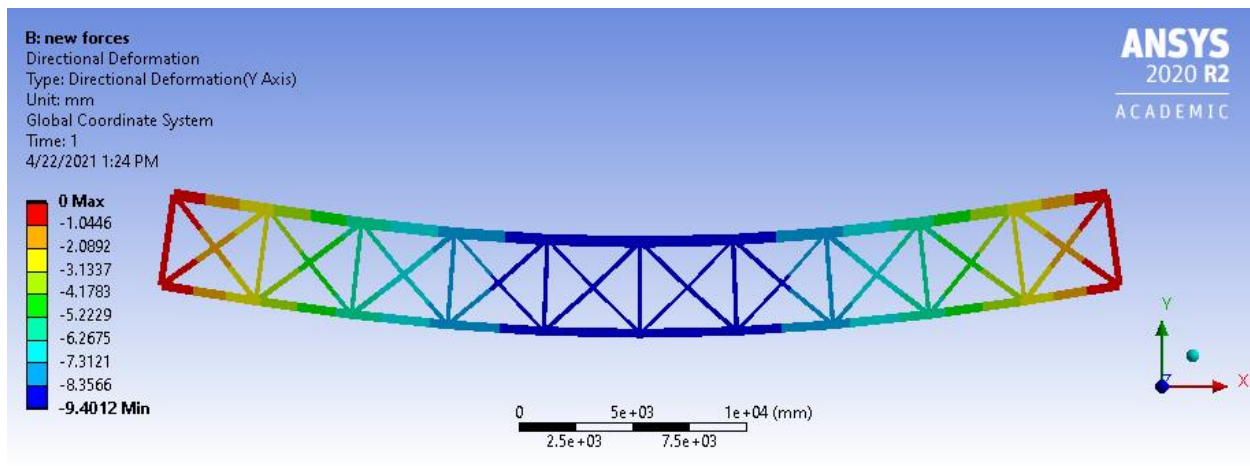


**FIG. 5.1 DEFLECTION OF THE BRIDGE IN Y AXIS [MM]. SELF-WEIGHT.**

As we can see in fig. 5.1 the minimum displacements are in the edges with red color that is because the nodes are close to the supports, but as we can see, the displacement is gradually increasing to the middle, where gets the highest values in blue color. However, the maximum displacement is in node F, which is reasonable because node F is the furthest node from the supports, and it is under tension force.

Fig. 5.2 graphically shows the effect of nominal stresses on individual bars of the bridge structure.

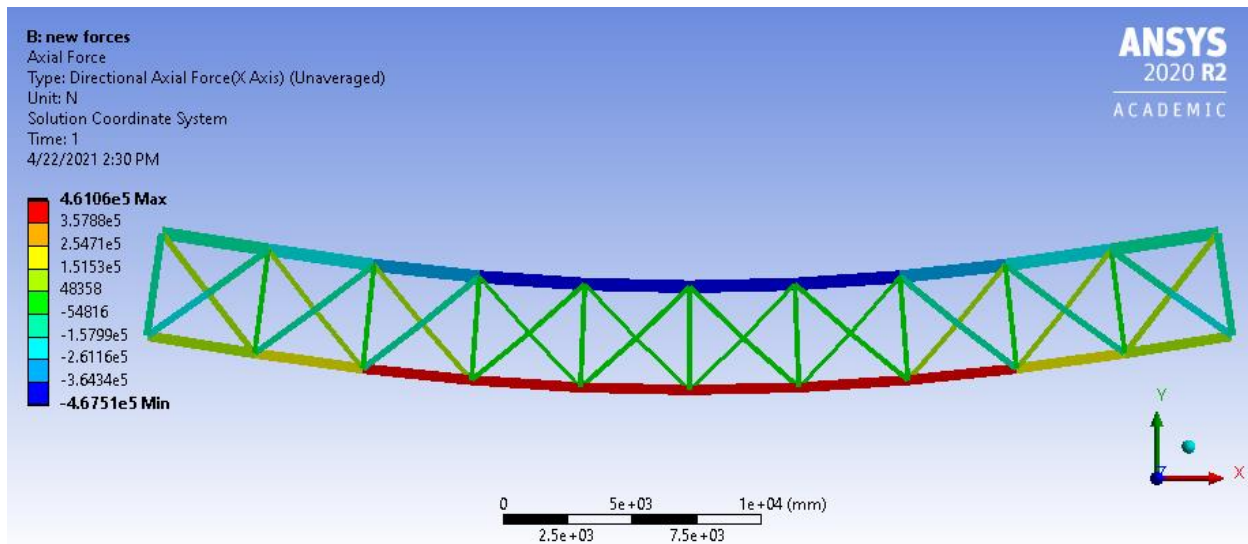


**FIG. 5.2 AXIAL FORCES ACTION ON THE BARS IN [N]. SELF-WEIGHT.**

As we can see in fig. 5.2, we got the maximum values at the middle bottom of the bridge with red color and the minimum values at the middle top of the bridge with blue color, well the sign does not matter. It indicates if the bar is under compressive or tension force, which means that we got the highest compression forces at the top of the bridge and the highest tension at the bottom of the bridge.

### 5.1.2 Comparison between Numerical and Analytical results

In tab. 5.1, we had compared the numerical and the analytical results to check the accuracy of the analytical calculation. We compared displacements in the nodes and normal forces in the bars. However, because the number of bars is 71 and the number of nodes is 32, we decided to choose just 10 of each for our comparison. as we can see, the results coincide with great accuracy. The rest of the results can be found in the attachment holding numbers 19, and 20.

**TAB. 5. 1 COMPARISON OF NORMAL FORCE AND DISPLACEMENT NUMERICAL AND ANALYTICAL.**

|      | Analytical         | Numerical          |                 |       | Analytical           | Numerical            |                 |
|------|--------------------|--------------------|-----------------|-------|----------------------|----------------------|-----------------|
| Bars | Norma<br>Force [N] | Norma<br>Force [N] | Accuracy<br>[%] | Nodes | Displacement<br>[mm] | Displacement<br>[mm] | Accuracy<br>[%] |
| N3   | 359446.12          | 359450.00          | 0.00108         | uA1   | 0.0750694            | -0.075069            | 0.00054         |
| N4   | 429031.60          | 429030.00          | 0.00037         | uB1   | 2.96923898           | -2.9696              | 0.012           |
| N5   | 461056.00          | 461060.00          | 0.00087         | uC1   | 5.64977065           | -5.6497              | 0.0013          |
| N6   | 461056.00          | 461060.00          | 0.00087         | uD1   | 7.66365248           | -7.6636              | 0.00068         |
| N7   | 429031.60          | 429030.00          | 0.00037         | uE1   | 8.95119433           | -8.9511              | 0.0011          |
| N8   | 359446.12          | 359450.00          | 0.00108         | uF1   | 9.40127928           | -9.4012              | 0.00084         |
| N15  | -467513.30         | -467510.00         | 0.00071         | uG1   | 8.95119433           | -8.9511              | 0.0011          |
| N16  | -467513.30         | -467510.00         | 0.00071         | uH1   | 7.66365248           | -7.6636              | 0.00068         |
| N21  | -72517.04          | -72517.00          | 0.00006         | uI1   | 5.64977065           | -5.6497              | 0.0013          |
| N46  | -7089.44           | -7089.70           | 0.00363         | uJ1   | 2.96923898           | -2.9696              | 0.012           |
| N42  | 18964.24           | 18964.00           | 0.00128         | uK1   | 0.0750694            | -0.075069            | 0.00054         |

### 5.1.3 Train's-weight phase 4 analyzing displacement and normal forces

In this model's analyzing we decided to study the heavies or the most loaded phase of all 4 phases, which is the fourth phase, so we applied the same analysis, which are displacement and normal forces.

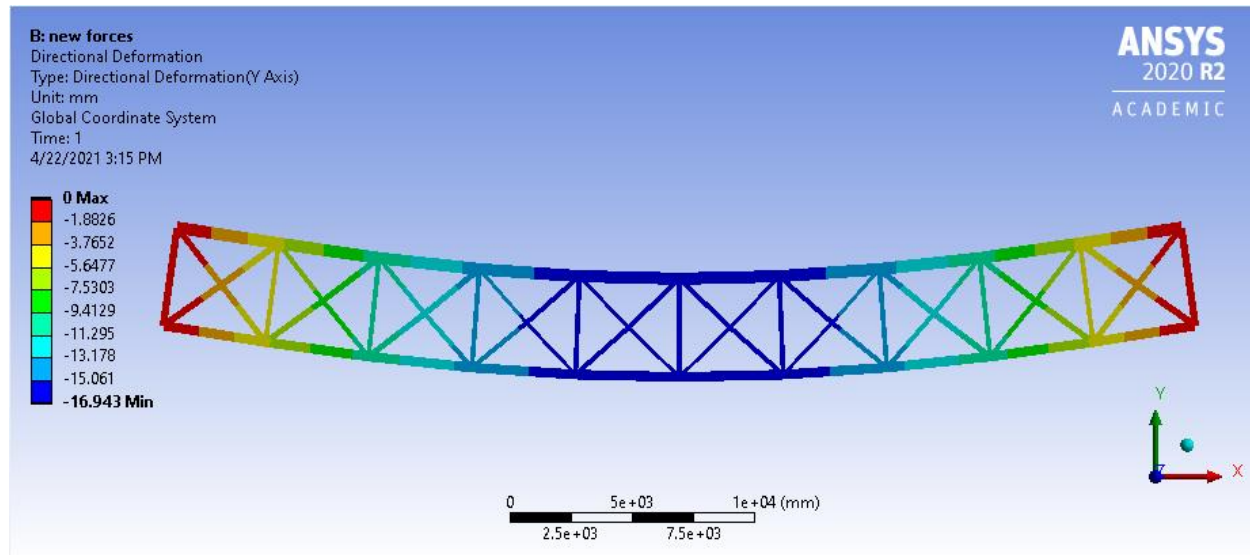


Fig. 5.3 Deflection of the Bridge in Y axis [mm]. passing train.

As we can see in fig. 5.4, the maximum and minimum values have almost the same spot as in the case when the bridge is just self-loaded more in chapter 5.1.1, and the only change was in the magnitude of the displacements, which is the highest displacement value at node F in the middle bottom of the bridge.

fig. 5.4 graphically shows the effect of nominal stresses on individual bars of the bridge structure while the locomotives and wagons pass on the bridge that means the heavies loading on the bridge is being applied.

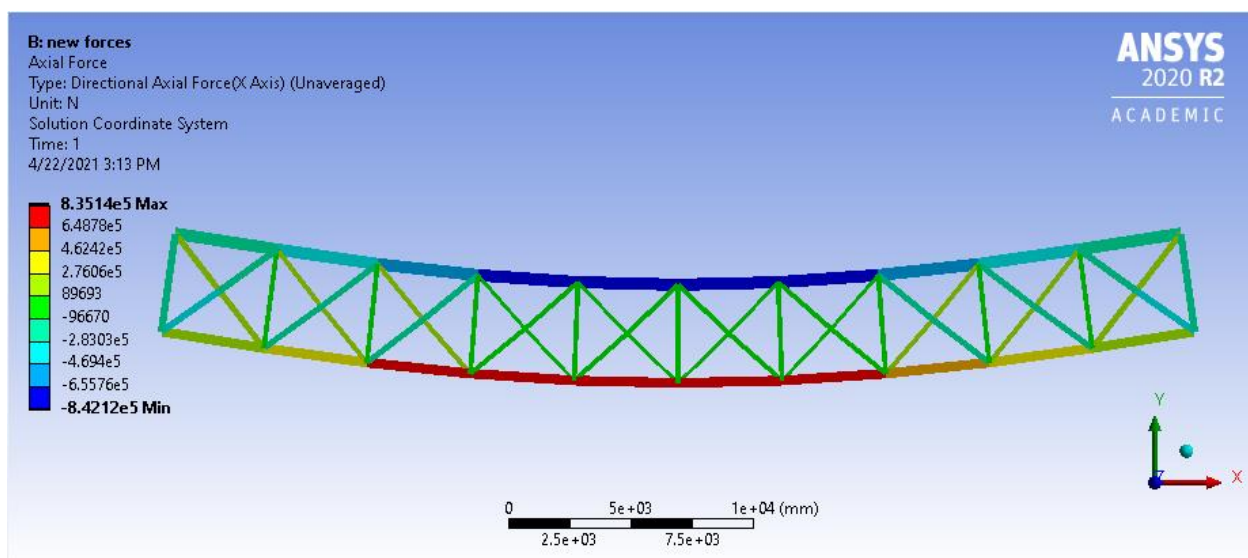


FIG. 5.4 AXIAL FORCES ACTION ON THE BARS IN [N] . PASSING TRAIN.



As we can see in fig. 5.4, the maximum and minimum values have almost the same spot as in the case when the bridge is just self-loaded more in chapter 5.1.1, and the only changes were in the magnitude of the normal forces.

#### 5.1.4 Comparison between Numerical and Analytical results

In tab. 5.2, we had compared the numerical and the analytical results to check the accuracy of the analytical calculation. We compared displacements in the nodes and normal forces in the bars. As we can see, the results coincide with great precision.

**TAB. 5. 2 COMPARISON NORMAL FORCE AND DISPLACEMENT NUMERICALLY AND ANALYTICALLY.**

|      | Analytical         | Numerical          |                 |      | Analytical           | Numerical            |                 |
|------|--------------------|--------------------|-----------------|------|----------------------|----------------------|-----------------|
| Bars | Norma<br>Force [N] | Norma<br>Force [N] | Accuracy<br>[%] | Node | Displacement<br>[mm] | Displacement<br>[mm] | Accuracy<br>[%] |
| N3   | 648756.76          | 648760.00          | 0.00050         | uA1  | 0.15304301           | -0.153040            | 0.0020          |
| N4   | 773933.76          | 773930.00          | 0.00049         | uB1  | 5.33972416           | -5.339700            | 0.00045         |
| N5   | 833496.63          | 833500.00          | 0.00040         | uC1  | 10.1721678           | -10.172000           | 0.0016          |
| N6   | 835144.95          | 835140.00          | 0.00059         | uD1  | 13.7993374           | -13.799000           | 0.0024          |
| N7   | 775084.08          | 775080.00          | 0.00053         | uE1  | 16.1132241           | -16.133000           | 0.12            |
| N8   | 648049.47          | 648050.00          | 0.00008         | uF1  | 16.9433727           | -16.943000           | 0.0022          |
| N15  | -840879.1          | -840880.00         | 0.00011         | uG1  | 16.1295396           | -16.129000           | 0.0033          |
| N16  | -842122            | -842120.00         | 0.00024         | uH1  | 13.7945701           | -13.794000           | 0.0041          |
| N21  | -147839.5          | -147840.00         | 0.00031         | uI1  | 10.1778725           | -10.178000           | 0.0013          |
| N42  | 32035.655          | 32036.00           | 0.0011          | uJ1  | 5.35424629           | -5.354200            | 0.00086         |
| N46  | -23662.01          | -23662.00          | 0.000040        | uK1  | 0.13545456           | -0.135450            | 0.0034          |

## 5.2 Statically indeterminate structure 3D

Since the 2D structures were always the simplification of the real-life situation, we made a 3D structure to match real-life construction. We created two parallel faces in the z-axis connected with a deck which looks as in fig. 5.5. From the sides, they are connected with rods which look as in fig. 5.9. The upper section is connected by straight bars, which look like fig. 5.6, with 3000 mm width into z-axis, the cross-section remains the same as in 2D structure more in chapter 4.1.5, the only differences are at the sided of the bridge, which has a cross-section TRr, TRl more in fig.5.11, and at the bottom section of the bridge which is the deck has S1, S2, S3, S4, S5 cross-sections more in fig. 5.7, 5.8, 5.10.

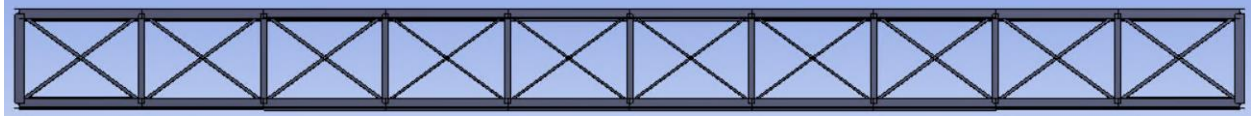


FIG. 5. 5 DECK IN THE BOTTOM PART.

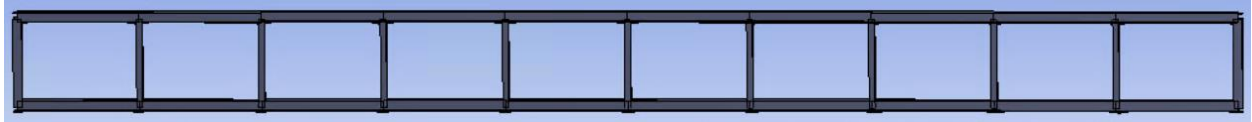


FIG. 5.6 UPPER PART CONNECTION.

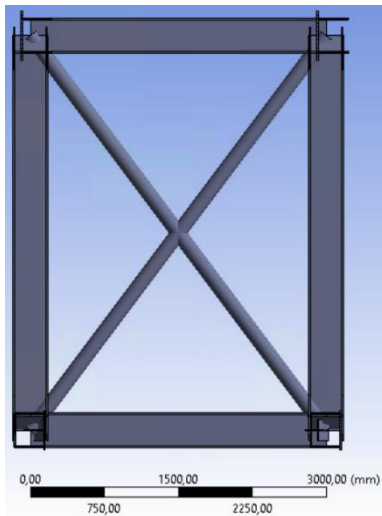


FIG. 5.9 RODE  
CONNECTION FOR THE  
SIDES OF THE BRIDGE.

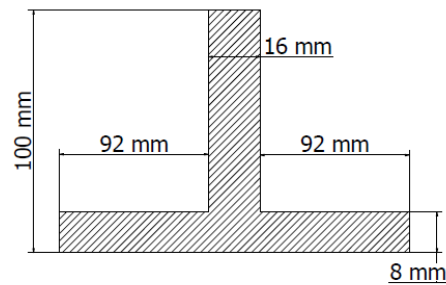


FIG. 5. 7 CROSS-SECTION  
S2, S3.

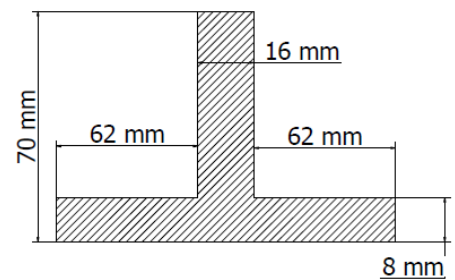


FIG. 5. 8 CROSS-SECTION  
S4, S5.

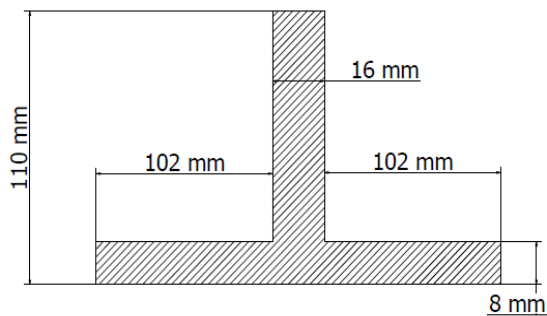


FIG. 5. 10 CROSS-  
SECTION S1.

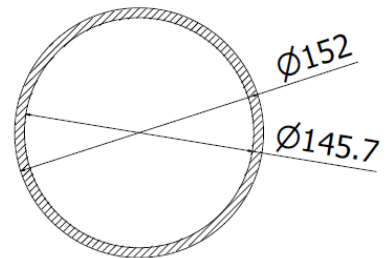


FIG. 5. 11 CROSS-SECTION  
TRR, TRL.



### 5.2.1 Load acting on the Bridge from passing Train in phase 4 plus self-load of Bridge analyzing displacement and normal forces

In this section, we analyzed the static indeterminate structure and chose the condition when the train passes in the fourth phase, which is the heaviest condition. Bellow, we can see in fig. 5.12, the deflection of the whole construction in the Y-axis and the normal forces in fig. 5.13. The results are in the tab. 5.3.

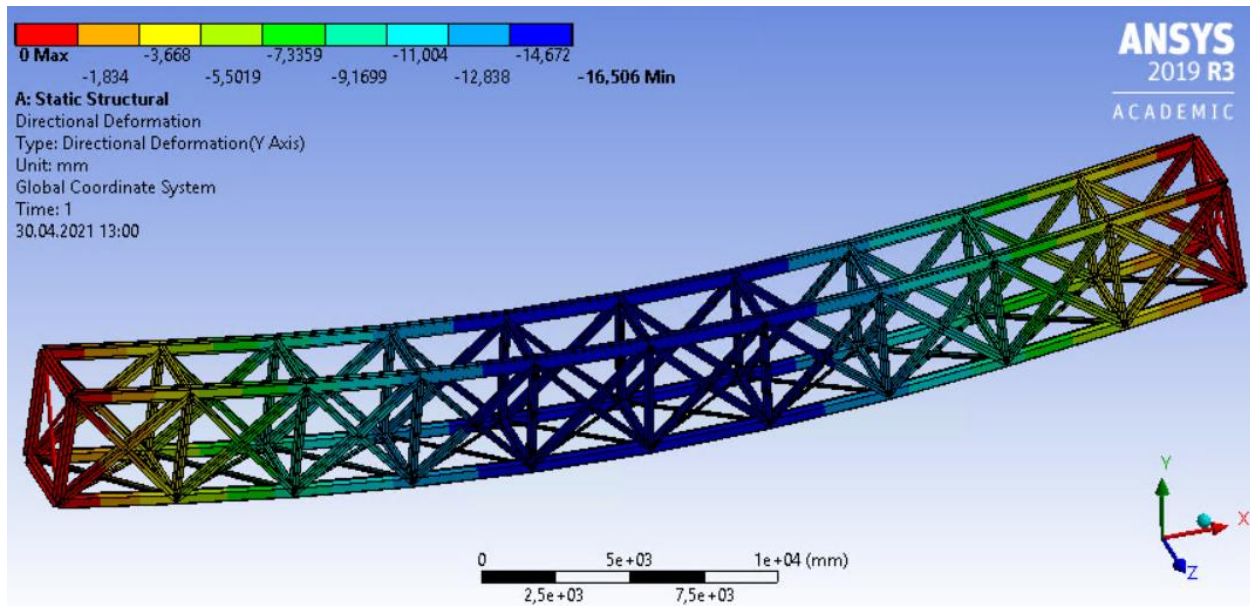


FIG. 5.12 DEFLECTION OF THE BRIDGE IN Y AXIS [MM] PASSING TRAIN.

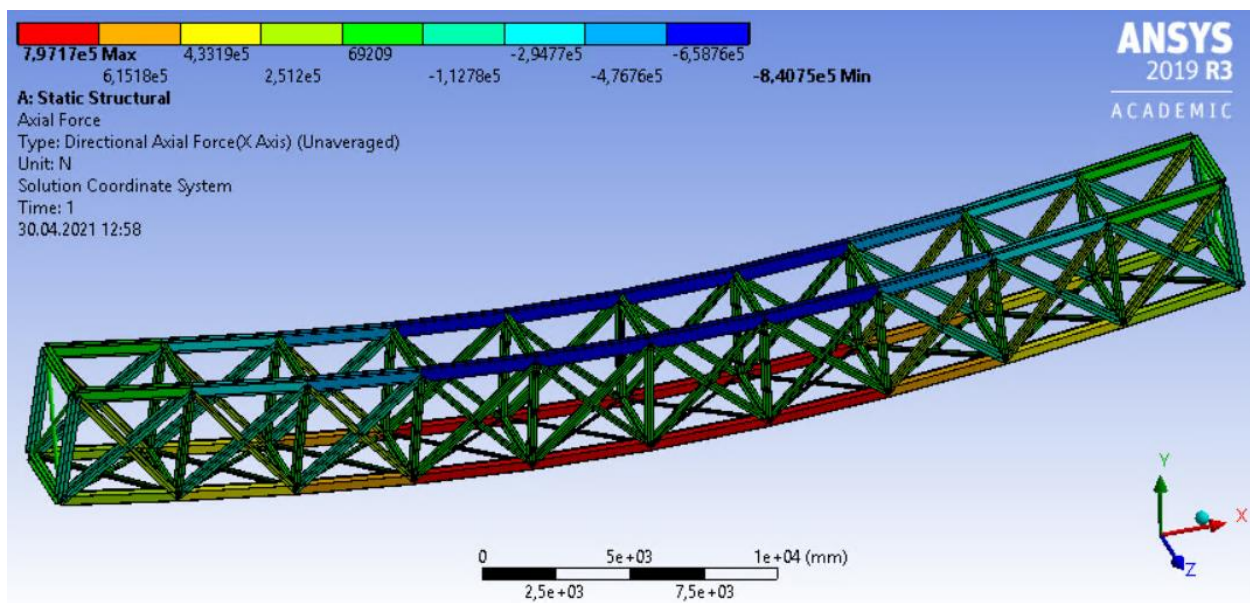


FIG. 5.13 AXIAL FORCES ACTION ON THE BARS IN [N] . PASSING TRAIN.

### 5.2.2 Comparison between 3D and 2D structure Numerically

The resulting normal forces and deflections are, therefore, similar in both variants. There is a big difference between the bars that are near the bridge deck; that is because increasing the stiffness when the model was changed caused a decrease in the normal forces of the bars at the bridge deck.

**TAB. 5. 3 COMPARISON NORMAL FORCE, DISPLACEMENT NUMERICALLY 2D WITH D3.**

|      | 3D              | 2D              |              |       | 3D                | 2D                |              |
|------|-----------------|-----------------|--------------|-------|-------------------|-------------------|--------------|
| Bars | Norma Force [N] | Norma Force [N] | Accuracy [%] | Nodes | Displacement [mm] | Displacement [mm] | Accuracy [%] |
| N3   | 607080          | 648760          | 6.42         | uA1   | -0.14658          | -0.15304          | 4.22         |
| N4   | 738820          | 773930          | 4.54         | uB1   | -5.1888           | -5.3397           | 2.83         |
| N5   | 795600          | 833500          | 4.55         | uC1   | -9.896            | -10.172           | 2.71         |
| N6   | 797170          | 835140          | 4.55         | uD1   | -13.433           | -13.799           | 2.65         |
| N7   | 739920          | 775080          | 4.54         | uE1   | -15.694           | -16.133           | 2.72         |
| N8   | 606410          | 648050          | 6.43         | uF1   | -16.506           | -16.943           | 2.58         |
| N15  | -839510         | -840880         | 0.16         | uG1   | -15.71            | -16.129           | 2.60         |
| N16  | -840750         | -842120         | 0.16         | uH1   | -13.429           | -13.794           | 2.65         |
| N21  | -141600         | -147840         | 4.22         | uI1   | -9.9016           | -10.178           | 2.72         |
| N42  | 30128           | 32036           | 5.96         | uJ1   | -5.2032           | -5.3542           | 2.82         |
| N46  | -21008          | -23662          | 11.22        | uK1   | -0.12963          | -0.13545          | 4.30         |

### 5.2.3 Model modification

As we know, the 2D model is a simplification of the real-life model 3D, so of course, that the 3D model will be stiffer than the 2D model because it has for more the deck which is connected to the bottom section of the bridge, therefore we tried to make the results more accurate. However, one of the solutions was by increasing the cross-section area of the 2D model at the bottom part of the bridge; therefore, cross-section U1, U2 was increased from  $21120 \text{ mm}^2$  to  $23712 \text{ mm}^2$  and cross-section U3, U4 was also increased from  $22720 \text{ mm}^2$  to  $23794 \text{ mm}^2$ . Thanks to these changes, we can now see a better accuracy rate in the tab. 5.4.

**TAB. 5. 4 COMPARISON NORMAL FORCE, DISPLACEMENT NUMERICALLY IN 2D WITH 3D, AFTER CHANGING CROSS-SECTION.**

|      | 3D              | 2D              |              |       | 3D                | 2D                |              |
|------|-----------------|-----------------|--------------|-------|-------------------|-------------------|--------------|
| Bars | Norma Force [N] | Norma Force [N] | Accuracy [%] | Nodes | Displacement [mm] | Displacement [mm] | Accuracy [%] |
| N3   | 607080          | 649840          | 6.58         | uA1   | -0.14658          | -0.15189          | 3.50         |
| N4   | 738820          | 775300          | 4.71         | uB1   | -5.1888           | -5.1848           | 0.08         |
| N5   | 795600          | 834810          | 4.70         | uC1   | -9.896            | -9.8995           | 0.04         |
| N6   | 797170          | 836460          | 4.70         | uD1   | -13.433           | -13.448           | 0.11         |
| N7   | 739920          | 776450          | 4.70         | uE1   | -15.694           | -15.71            | 0.10         |
| N8   | 606410          | 649130          | 6.58         | uF1   | -16.506           | -16.523           | 0.10         |
| N15  | -839510         | -839570         | 0.01         | uG1   | -15.71            | -15.726           | 0.10         |
| N16  | -840750         | -840810         | 0.01         | uH1   | -13.429           | -13.443           | 0.10         |
| N21  | -141600         | -146720         | 3.49         | uI1   | -9.9016           | -9.9048           | 0.03         |
| N42  | 30128           | 30214           | 0.28         | uJ1   | -5.2032           | -5.199            | 0.08         |
| N46  | -21008          | -21128          | 0.57         | uK1   | -0.12963          | -0.13429          | 3.47         |

## 6 Conclusion

The main goal of this bachelor thesis was to apply Stress-Strain analysis of the railway bridge in Zahrádky near Česká Lípa and apply different assumptions and simplifications.

The first section of this thesis was dedicated to searching and obtaining the input data and essential information which were obtained from Railway administration, state organizations Regional Headquarters Hradec Králové through **Ing. Pavel Novák**. Thus, the theory was developed, which was necessary to know for the solution of individual parts of the bachelor's thesis. Therefore, the theory was taken from sources that contained information mainly in statics and Strength of Material. Based on our knowledge from that fields, we were able to simplify the bridge's structure into a two-dimensional model.

The second section was the analytical calculation in two-dimension, which was assisted by the Maple program. To perform an analytical analysis, we needed to create a virtual model of a bar system, and since the bridge, in reality, has, in addition, a deck, Therefore, it was included in the calculation, which should correspond and come as close as possible to the actual solution of the real bridge. Moreover, the load factors such as wind load and the effect of dynamic forces when the train passes over the bridge were neglected because it would exceed the goals of this bachelor thesis, On the other hand, the load from the bridge itself and the load from a passing train set were took into consideration in our analysis. However, the analytical calculation was divided into two sections, the first one is a statically indeterminate structure, and the second one is a statically determinate structure, furthermore in each section was considered the bridges self-weight and a passing train as the loading's factors.

In the statically indeterminate structure with  $S = 10$ , under a self-bridge's load effect. The results show that the maximum values of the normal forces can be found in the middle part of the bridge, at the upper and the bottom horizontal bars, while the upper section is under compressive load, the bottom section is under a tensile load, the outcome was large deflection in the middle of the bridge specifically in node F1, and the value of the displacement of a given node in the vertical direction is 9.4012 mm. The highest nominal stress acts in the bottom part of the bridge, specifically on the bars N5, N6 it is a tensile load with a value of 20.29 MPa since it is the highest value it was used to check the safety with respect to the limit state of elasticity. Therefore, the safety factor is 10.34.

Then we analyzed statically indeterminate structure under passing wagons, and locomotives load effect. Since they pass gradually from the beginning of the bridge to the end, we had to split the analysis to fits the reality. Therefore, the calculation was divided into four phases.

In the first phase, the train set passes on the first four nodes from node A1 to node D1, and There is a significant increase in nominal stresses in the bars and deflection in the nodes. The maximum tensile stress acts on bar N5 at the value of 23.57 MPa, and maximum compressive stress acts on bar N15 at the value of -18.75 MPa. The maximum deflection of node F1 increased 10.9013 mm. however, the safety factor  $k_k = 8.9$  represents a sufficiently large reserve.

In the second phase, the train set reaches node G1. Again, there is an increase in nominal stresses in the bars and deflection in the nodes. The maximum tensile stress acts on bar N5 at the value of 31.99 MPa, and maximum compressive stress acts on bar N15 at the value of -25.28 MPa. The maximum deflection of node F1 increased to 15.4432 mm. we can observe a decrease in the safety factor where we got a value at  $k_k = 6.5$ .

In the third phase, the train set reaches node H1, which mean it is only one node ahead, therefore we did not observe a noticeable increase in nominal stresses and deflection. The maximum tensile stress acts on bar N5 at the value of 33.97 MPa, and maximum compressive stress acts on bar N15 at the value of -26.86 MPa. The maximum deflection of node F1 remained totally the same value, 15.4432 mm. we can observe a slight decrease in the safety factor where we got a value at  $k_k = 6.1$ .

In the fourth phase, the train set is on the whole bridge from node A1 to node K1. There is a significant increase in nominal stresses in the bars and deflection in the nodes when we compare with the self-load only. The maximum tensile stress acts on bar N6 at the value of 36.75 MPa, and maximum compressive stress acts on bar N16 at the value of -29.03 MPa. The maximum deflection of node F1 increased to 16.943 mm. we can observe a decrease in the safety factor where we got a value at  $k_k = 5.7$ . we can also observe a significant increase in reaction forces in the supports from  $F_{ya} = 195729$  N,  $F_{yk} = 195729$  in self bridges load to  $F_{ya} = 357778$  N,  $F_{yk} = 342602$  N in the fourth phase of the passing train set.

In the statically determinate structure, we made changes to the construction to achieve the static determinacy. Therefore, we reduced the number of bars by 20 and the number of nodes by 10. Firstly, we considered the bridge's self-load. When we analyzed the normal forces and the nominal stresses, the highest values in terms of normal forces were as expected, they were the same as in the static indeterminate structure, which means in the middle of the bridge. The upper horizontal section is under compressive load, and the bottom section is under a tensile load. But the highest nominal stress was at bar N22 at the value of 19.35 MPa since it is the highest value, it was used to check the safety with respect to the limit state of elasticity. Therefore, the safety factor is 10.85. We got the highest deflection in the vertical direction in node F1 at the value of 8.4688 mm.

Then we analyzed the statically determinate structure under passing wagons and locomotives load effect. We applied the same process, which was used in the static indeterminate structure, which means we had four phases of a passing train set.

In the first phase, the train set passes on the first four nodes from node A1 to node D1, and There is a significant increase in nominal stresses in the bars and deflection in the nodes. The maximum tensile stress acts on bar N22 at the value of 30.34 MPa, and maximum compressive stress acts on bar N23 at the value of -16.73 MPa. The maximum deflection of node F1 increased 10.4584 mm. however, the safety factor is  $k_k = 6.9$ .

In the second phase, the train set reaches node G1. Again, there is an increase in nominal stresses in the bars and deflection in the nodes. The maximum tensile stress acts on bar N22 at the value of 38.86 MPa, and maximum compressive stress acts on bar N23 at the value of -21.79 MPa. The maximum deflection of node F1 increased to 15.3189 mm. we can observe a decrease in the safety factor where we got a value at  $k_k = 5.4$ .

In the third phase, the train set reaches node H1, which mean it is only one node ahead, therefore we did not observe a noticeable increase in nominal stresses and deflection. The maximum tensile stress acts on bar N22 at the value of 39.89 MPa, and maximum compressive stress acts on bar N23 at the value of -22.40 MPa. The maximum deflection of node F1 remained totally the same value, 16.7130 mm. we can observe a slight decrease in the safety factor where we got a value at  $k_k = 5.2$ .

In the fourth phase, the train set is on the whole bridge from node A1 to node K1. There is a significant increase in nominal stresses in the bars and deflection in the nodes when we compare with the self-load only. The maximum tensile stress acts on bar N22 at the value of 42.22 MPa, and maximum compressive stress acts on bar N39 at the value of -24.22 MPa. The maximum deflection of node F1 increased to 18.7025 mm. we can observe a decrease in the safety factor where we got a value at  $k_k = 4.9$ . we can also observe a significant increase in reaction forces in the supports from  $F_{ya} = 129849$  N,  $F_{yk} = 129849$  in self bridges load to  $F_{ya} = 291898$  N,  $F_{yk} = 276722$  N in the fourth phase of the passing train set.

Next, we checked the buckling stability limit state for a chosen models in both structures, statically indeterminate and statically determinate. We decided to choose a self-bridge's load because it is the lightest model and the second one a model with a passing train set in the fourth phase. After all, it is the heaviest model, and we could compare between them. For a statically indeterminate structure, the safety is very high in the self-bridge's load, and its value is 390. However, if the train set is crossing the bridge, safety drops to almost a third of the value under self-weight, its value becomes 117. but it is still higher than the safety to the limit state of elasticity. For statically determinate structure, the safety is 28 in the self-bridge's load, this safety decreases, even more, when the trainset passes across the bridge to the value of 12.

All models that were used in the analytical analysis were modeled and analyzed numerically using the finite element method with Ansys software helps. The output values of stress and strain were consistent. The identical results confirm the correctness of the construction of the analytical, computational model. Normal forces, nominal stresses, and deformation were compared. Our last mission in this thesis was to create a three-dimensional model of the original structure, which is statically indeterminate. This model was compared with the two-dimensional model, the results were not with that high accuracy. The reason is that when we designed the 2D model, we included the mass of the deck, but we could not include the rigidity of the deck, so we came with a solution which was increasing the cross-section area of the bottom part of the bridge for more of increasing steps in chapter 5.2.3, so after the change, we applied to the model the accuracy increased to a Reasonable number.

In conclusion, from individual results, when it comes to maximum displacement, the statically indeterminate structure has a slightly smaller value. And the factor of safety against the limit state of elasticity the statically indeterminate has higher values, but the differences are not too significant. And when it comes to buckling limit state, the statically indeterminate structure gets very high values in comparison with the statically determinate structure for sure. Therefore, the statically determinate construction is a more suitable construction for real-life use.

## List of resources

- [1] Ing. Zdeněk Iakmayer. E.1.4.19 - OK – Příhrada dolní pásy a ztužení [pdf]. [approx. 2013]. the document was provided by Ing. Pavel Novák.
- [2] JANÍČEK, Přemysl, Emanuel ONDRÁČEK, Jan VRBKA and Jiří BURŠA. Mechanika těles: pružnost a pevnost I. 3., přeprac. vyd., 1. Brno: CERM, 2004. ISBN 802142592X.
- [3] MATIJAK. Viadukt Karba 2015. In: *Wikipedie* [online]. 4. dubna 2015 [cit. 2021-5-12]. Available from: [https://cs.wikipedia.org/wiki/Most\\_v\\_Zahr%C3%A1dk%C3%A1ch](https://cs.wikipedia.org/wiki/Most_v_Zahr%C3%A1dk%C3%A1ch)
- [4] HÁK, Lukáš. Železniční most: Zahrádky u české lípy. In: *Mapio* [online]. [approx. 2011] [cit. 2021-5-12]. Available from: <https://mapio.net/pic/p-88871897/>
- [5] Libor Novotný. Železniční most, Zahrádky u České Lípy [Fotka]. Google maps: [online]. dub 2021 [cit. 2021-5-12]. Available from: <https://www.google.com/maps/place/%C5%BD%e9%99%A2%C4%8Dn%C3%AD+most+v+Zahr%C3%A1dk%C3%A1ch/@50.3479039,14.6679561,574477m/data=!3m1!1e3!4m5!3m4!1s0x47096966a511c7d7:0x712d33991855b650!8m2!3d50.6401316!4d14.5151608>
- [6] Janatam. Železniční most, Zahrádky u České Lípy [online]. [cit. 2021-4-30]. Available from: <http://www.janatam.cz/antiprice2015.htm>
- [7] Prof. RNDr. Ing. VRBKA Jan, DrSc.: PRUŽNOST A PEVNOST I [pdf]. 2011. Brno: Ústav mechaniky těles, mechatroniky a biomechaniky Fakulta strojního inženýrství VUT v Brně.
- [8] BURŠA, Jiří, Jana HORNÍKOVÁ, Přemysl JANÍČEK and Pavel ŠANDERA. Pružnost a pevnost [online]. Brno: CERM, 2003 [cit. 2018-05-15]. ISBN 80-7204-268-8. Available from: <<http://beta.fme.vutbr.cz/cpp/>>
- [9] HORNÍKOVÁ, Jana. Pružnost a pevnost: Interaktivní učební text. Brno: CERM, 2003. ISBN 80-7204-268-8.
- [10] FLORIAN, Zdeněk, Emanuel ONDRÁČEK and Karel PŘIKRYL. Mechanika těles: statika. Vyd. 7., CERM 2. Brno: CERM, 2007. ISBN 9788021434400.
- [11] ABED-MERAIM, Farid. Schematic representation of bifurcation-type buckling versus limit-point buckling. In: *ResearchGate* [online]. [cit. 2021-4-30]. Available from: [https://www.researchgate.net/figure/Schematic-representation-of-bifurcation-type-buckling-versus-limit-point-buckling\\_fig1\\_264146110](https://www.researchgate.net/figure/Schematic-representation-of-bifurcation-type-buckling-versus-limit-point-buckling_fig1_264146110)
- [12] CALLISTER, W. D. a D. G. RETHWISCH. Stress-strain curve. In: REDWING, Ron. *MATSE 81 Materials in today's world: Lesson 4. Mechanical properties. Plastic deformation* [online]. [cit. 2021-4-30]. Available from: <https://www.e-education.psu.edu/matse81/node/2104>



## Figures list

|  |    |
|--|----|
| Fig. 1.1 Location of the bridge on the maps.[4].....   | 10 |
| Fig. 1.2 Location of the bridge on the maps.[3].....   | 10 |
| Fig. 1.3 Location of the bridge on the maps. [5].....  | 10 |
| Fig. 1.4 Location of the bridge on the maps. [5].....  | 10 |
| Fig. 1.5 Location of the bridge according to the Czech Republic on the maps.[5] .....                            | 11 |
| Fig. 2. 1 choosing one part of the bridge.[6].....   | 11 |
| Fig. 3 1 .....   | 12 |
| Fig. 3.2 centerline at a bent bar.....   | 12 |
| Fig. 3.3 Maintaining the smoothness of the centerline. ....  | 13 |
| Fig. 3.4 Tention in a bar.....   | 13 |
| Fig. 3.5 Flection in a bar. ....   | 13 |
| Fig. 3.6 Torsion in a bar.....   | 13 |
| Fig. 3.7 shear in a bar.....   | 14 |
| Fig. 3.8 simplification from a bar into centerline. ....   | 14 |
| Fig. 3.9 bar state of stress displayed on a mohr's circle.....   | 14 |
| Fig. 3.10 bar state of stress displayed On a unit cube.....  | 14 |
| Fig. 3.11 Stress tensor for bar in tension. ....   | 14 |
| Fig. 3.12 cross-sectional area.....  | 15 |
| Fig. 3.13 Arbitrary cross-section area. ....   | 15 |
| Fig. 3.15 loading in reality vs in model. ....   | 16 |
| Fig. 3.14 Load distribution according to the Venant principle. ....  | 16 |
| Fig. 3.16 Application of S.V. principle. [9].....  | 16 |
| Fig. 3.17 computational models.....  | 17 |
| Fig. 3.18 Deformation of an elementary element by simple tension. ....   | 19 |
| Fig. 3.19 elastic and plastic deformation.[12].....  | 21 |
| Fig. 3.20 Bifurcation point in buckling.[11] .....   | 22 |
| Fig. 3 21 Values of coefficients $\alpha$ deposits.....  | 22 |
| Fig. 3 22 Values of coefficients $\alpha$ deposits.....  | 22 |
| Fig. 3 23 Dependence of compressive stress $\sigma_{Kr}$ . on the slenderness $\lambda$ for a tough material.... | 23 |
| Fig. 4.1 Bridge in the real-life. [6].....   | 24 |
| Fig. 4.2 Bridg's dimensions.....   | 24 |
| Fig. 4.3 Numbering the bars. ....  | 25 |
| Fig. 4.4 Naming the Nodes. ....  | 25 |
| Fig. 4.6 Cross-section O1, O2. [1] .....   | 25 |
| Fig. 4.5 Cross-section O3.[1].....   | 25 |
| Fig. 4.7 Cross-section U1, U2. [1] .....   | 26 |
| Fig. 4.8 Cross-section O4, O5. [1] .....   | 26 |
| Fig. 4. 9 Cross-section U3-U5. [1].....  | 26 |
| Fig. 4. 10 Cross-section D1. [1].....  | 26 |

|  |    |
|--|----|
| Fig. 4. 11 Cross-section D3. [1] .....                           | 27 |
| Fig. 4. 12 40 Cross-section D2. [1] .....                        | 27 |
| Fig. 4. 13 Cross-section D4. [1] .....                           | 27 |
| Fig. 4.14 Cross-section D5. [1] .....                            | 27 |
| Fig. 4. 15 Cross-section T1. [1] .....                           | 28 |
| Fig. 4. 16 Cross-section T2, T3. [1] .....                       | 28 |
| Fig. 4. 17 Cross-section T4, T5. [1] .....                       | 28 |
| Fig. 4. 18 Cross-section So. [1] .....                           | 28 |
| Fig. 4. 19 Cross-section S. [1] .....                            | 28 |
| Fig. 4. 20 finding the position of cross-section by colors. .... | 29 |
| Fig. 4.21 relaced supports. ....                                 | 30 |
| Fig. 4.22 gravitational force from bridge's self-weight. ....    | 32 |
| Fig. 4.23 free body diagram. ....                                | 32 |
| Fig. 4. 24 Released Node A .....                                 | 33 |
| Fig. 4. 25 Released Node B .....                                 | 33 |
| Fig. 4. 26 Released Node C .....                                 | 33 |
| Fig. 4. 27 Released Node D .....                                 | 33 |
| Fig. 4. 28 Released Node E.....                                  | 33 |
| Fig. 4. 29 Released Node F.....                                  | 33 |
| Fig. 4.30 Released Node G .....                                  | 34 |
| Fig. 4.31 Released Node H .....                                  | 34 |
| Fig. 4.32 Released Node I.....                                   | 34 |
| Fig. 4.33 Released Node J.....                                   | 34 |
| Fig. 4.34 Released Node K .....                                  | 34 |
| Fig. 4.35 Released Node L.....                                   | 34 |
| Fig. 4.36 Released Node M.....                                   | 35 |
| Fig. 4.37 Released Node N .....                                  | 35 |
| Fig. 4.38 Released Node O .....                                  | 35 |
| Fig. 4.39 Released Node P.....                                   | 35 |
| Fig. 4.40 Released Node Q .....                                  | 35 |
| Fig. 4.41 Released Node R .....                                  | 35 |
| Fig. 4.42 Released Node S.....                                   | 36 |
| Fig. 4.43 Released Node T.....                                   | 36 |
| Fig. 4.44 Released Node V .....                                  | 36 |
| Fig. 4.45 Released Node A1 .....                                 | 36 |
| Fig. 4.46 Released Node B1 .....                                 | 36 |
| Fig. 4.47 Released Node C1 .....                                 | 36 |
| Fig. 4.48 Released Node D1 .....                                 | 37 |
| Fig. 4.49 Released Node E1.....                                  | 37 |
| Fig. 4.50 Released Node F1 .....                                 | 37 |
| Fig. 4.51 Released Node G1 .....                                 | 37 |
| Fig. 4.52 Released Node H1 .....                                 | 37 |
| Fig. 4.53 Released Node I1 .....                                 | 37 |
| Fig. 4.54 Released Node J1.....                                  | 38 |
| Fig. 4.55 Released Node K1 .....                                 | 38 |
| Fig. 4. 56 Partial free body diagram. ....                       | 38 |



|  |    |
|--|----|
| Fig. 4.57 equation as a function of partial .released force. ....      | 39 |
| Fig. 4. 58 equations and normal forces in Maple software. ....         | 40 |
| Fig. 4. 59 Finding the nominal stress in Maple software. ....          | 40 |
| Fig. 4.60 Finding the displacement in Maple software. ....             | 41 |
| Fig. 4.61 train weight distribution. ....                              | 43 |
| Fig. 4.62 phase 1 force distribution. ....                             | 43 |
| Fig. 4.63 phase 2 force distribution. ....                             | 44 |
| Fig. 4.64 phase 3 force distribution. ....                             | 45 |
| Fig. 4.65 phase 4 force distribution. ....                             | 46 |
| Fig. 4.66 numbering the bars and naming the nodes. ....                | 49 |
| Fig. 4.67 finding the position of cross-section by colors. ....        | 50 |
| Fig. 4.68 gravitational forces from bridge's self-weight. ....         | 52 |
| Fig. 4.69 Equations and normal forces in Maple software. ....          | 52 |
| Fig. 4.70 finding the nominal stress in Maple software. ....           | 53 |
| Fig. 4.71 differential derive according to A1 in Maple soft ware. .... | 54 |
| Fig. 4.72 finding the displacement in Maple soft ware. ....            | 54 |
| Fig. 4.73 phase 1 force distribution. ....                             | 56 |
| Fig. 4.74 phase 2 force distribution. ....                             | 57 |
| Fig. 4.75 phase 3 force distribution. ....                             | 58 |
| Fig. 4.76 phase 4 force distribution. ....                             | 59 |
|  |    |
| Fig. 5.1 Deflection of the Bridge in Y axis [mm]. Self-weight. ....    | 64 |
| Fig. 5.2 axial forces action on the bars in [N]. Self-weight. ....     | 65 |
| Fig. 5.3 Deflection of the Bridge in Y axis [mm]. passing train. ....  | 66 |
| Fig. 5.4 axial forces action on the bars in [N] . passing train. ....  | 66 |
| Fig. 5. 5 Deck in the bottom part. ....                                | 68 |
| Fig. 5.6 Upper part connection. ....                                   | 68 |
| Fig. 5. 7 Cross-section S2, S3. ....                                   | 68 |
| Fig. 5. 8 Cross-section S4, S5. ....                                   | 68 |
| Fig. 5.9 rode connection for the sides of the bridge. ....             | 68 |
| Fig. 5. 10 Cross-section S1. ....                                      | 68 |
| Fig. 5. 11 Cross-section TRr, Trl. ....                                | 68 |
| Fig. 5.12 Deflection of the Bridge in Y axis [mm] passing train. ....  | 69 |
| Fig. 5.13 axial forces action on the bars in [N] . passing train. .... | 69 |

## List of tables

|  |    |
|--|----|
| Tab. 4.1 Color and numbers of cross-sections.....  | 29 |
| Tab. 4.2 gravitational loading acting on nodes. ....   | 32 |
| Tab. 4.3 released nodes. ....  | 33 |
| Tab. 4.4 Normal force and nominal stress in bars with Bridge self-weight. ....                               | 41 |
| Tab. 4. 5 Displacement of Nodes.....   | 42 |
| Tab. 4.6 Displacement in nodes, Gravitational Forces, and reaction forces.....                               | 44 |
| Tab. 4.7 Normal forces and nominal stresses in the bars, Train phase 1.....                                  | 44 |
| Tab. 4.8 Displacement in nodes, Gravitational Forces, and reaction forces.....                               | 45 |
| Tab. 4. 9 Normal forces and nominal stresses in the bars, Train phase 2.....                                 | 45 |
| Tab. 4.10 Displacement in nodes, Gravitational Forces, and reaction forces.....                              | 46 |
| Tab. 4. 11 Normal forces and nominal stresses in the bars, Train phase 3.....                                | 46 |
| Tab. 4.12 Displacement in nodes, Gravitational Forces. ....  | 47 |
| Tab. 4.13 reaction forces.....   | 47 |
| Tab. 4.14 Normal forces and nominal stresses in the bars Train phase 4.....                                  | 47 |
| Tab. 4. 15 Color and numbers of cross-sections.....  | 50 |
| Tab. 4.16 gravitational loading acting on nodes. ....  | 52 |
| Tab. 4.17 Normal forces and nominal stresses in the bars Bridge self-weight.....                             | 54 |
| Tab. 4.18 Displacement of Nodes.....   | 54 |
| Tab. 4. 19 Displacement in nodes, Gravitational Forces, and reaction forces.....                             | 56 |
| Tab. 4. 20 Normal forces and nominal stresses in the bars Train phase 1.....                                 | 56 |
| Tab. 4. 21 Displacement in nodes, Gravitational Forces, and reaction forces.....                             | 57 |
| Tab. 4. 22 Normal forces and nominal stresses in the bars, Train phase 2.....                                | 57 |
| Tab. 4. 23 Displacement in nodes, Gravitational Forces, and reaction forces.....                             | 58 |
| Tab. 4. 24 Normal forces and nominal stresses in the bars, Train phase 3.....                                | 58 |
| Tab. 4. 25 Displacement in nodes, Gravitational Forces. ....   | 59 |
| Tab. 4. 26 reaction forces.....  | 59 |
| Tab. 4. 27 Normal forces and nominal stresses in the bars, Train phase 4.....                                | 59 |
| Tab. 5. 1 Comparison of normal force and displacement numerical and analytical.....                          | 65 |
| Tab. 5. 2 Comparison normal force and displacement numerically and analytically.....                         | 67 |
| Tab. 5. 3 Comparison normal force, displacement numerically 2D with D3. ....                                 | 70 |
| Tab. 5. 4 Comparison normal force, displacement numerically in 2D with 3D, after changing cross-section..... | 70 |

## List of used symbols

| Symbol     | Unit                 | Meaning  |
|------------|----------------------|--|
| $\sigma$   | [MPa]                | Normal Stress.                                       |
| E          | [MPa]                | Young's modulus of elasticity in tension.            |
| $\sigma_k$ | [MPa]                | yield strength.                                      |
| S          | [mm <sup>2</sup> ]   | Cross Section of the bars.                           |
| $J_y$      | [mm <sup>4</sup> ]   | Quadratic moment.                                    |
| l          | [mm]                 | Length.  |
| u          | [mm]                 | Deflection.  |
| F          | [N]                  | Force.   |
| $F_{kr}$   | [N]                  | Critical Force.                                      |
| $F_T$      | [N]                  | Force created from the Train.                        |
| W          | [J]                  | Stress Energy.                                       |
| $\Lambda$  | [Jm <sup>-3</sup> ]  | Specific energy of stress.                           |
| $\rho$     | [kg/m <sup>3</sup> ] | Density.   |
| g          | [m/s <sup>2</sup> ]  | Gravitational acceleration.                          |
| m          | kg                   | Mass.  |
| $\lambda$  | [-]                  | The slenderness of the Bar.                          |
| k          | [-]                  | The factor of Safety against elasticity limit state. |
| $k_v$      | [-]                  | The factor of safety against buckling limit state.   |
| $\gamma$   | [-]                  | Bar centerline, angular deformation.                 |
| $\psi$     | [-]                  | Cross Section.                                       |

## List of attachments

| Attachment Number | File Name                                     | Description  |
|-------------------|---|--|
| Attachment N.1    | Checking the buckling                         | Checking buckling limit state, self-weight load for static indeterminate and determinate structure |
| Attachment N.2    | E.1.4.18 - OK - Příčné řezy                   | Drawing documentation of the cross-sections used in construction                                   |
| Attachment N.3    | E.1.4.19 - OK - Mostovka                      | Drawing documentation of the Deck used in construction   |
| Attachment N.4    | E.1.4.24 Výkaz materiálu OK                   | documentation of material used in construction   |
| Attachment N.5    | E.1.4.19 - OK - Příhrada dolní pásy a ztužení | Drawing documentation of the cross-sections used in construction                                   |
| Attachment N.6    | E.1.4.17 - OK - Sestava                       | Drawing documentation of the whole construction of the Bridge                                      |

|                 |  |   |
|-----------------|--|---|
| Attachment N.7  | E.1.4.11 - NS - pūd                                  | Drawing documentation of the floor plan   |
| Attachment N.8  | Statically determinate structure 2D                  | Solving statically determinate structure 2D numerically self-weight and trains weight and comparing between analytical and numerical structures |
| Attachment N.9  | Statically Indeterminate\Normal forces self-weight_A | Normal forces and nominal stresses result with self-weight load for S=10. Analytically  |
| Attachment N.10 | Statically Indeterminate\train_faze_1_A              | Normal forces and nominal stresses result with train phase 1 load for S=10. Analytically  |
| Attachment N.11 | Statically Indeterminate\train_faze_2_A              | Normal forces and nominal stresses result with train phase 2 load for S=10. Analytically  |
| Attachment N.12 | Statically Indeterminate\train_faze_3_A              | Normal forces and nominal stresses result with train phase 3 load for S=10. Analytically  |
| Attachment N.13 | Statically Indeterminate\train_faze_4_A              | Normal forces and nominal stresses result with train phase 4 load for S=10. Analytically  |
| Attachment N.14 | Statically Indeterminate\Normal forces self-weight_N | Normal forces and nominal stresses result with self-weight load for S=10. Numerically   |
| Attachment N.15 | Statically Indeterminate\train_faze_1_N              | Normal forces and nominal stresses result with train phase 1 load for S=10. Numerically   |
| Attachment N.16 | Statically Indeterminate\train_faze_2_N              | Normal forces and nominal stresses result with train phase 2 load for S=10. Numerically   |
| Attachment N.17 | Statically Indeterminate\train_faze_3_N              | Normal forces and nominal stresses result with train phase 3 load for S=10. Numerically   |
| Attachment N.18 | Statically Indeterminate\train_faze_4_N              | Normal forces and nominal stresses result with train phase 4 load for S=10. Numerically   |
| Attachment N.19 | Statically Indeterminate\compair_Normal_Force_A_N_2D | Comparison of the normal forces between analytical and numerical 2D statically indeterminate  |
| Attachment N.20 | Statically Indeterminate\compair_Displacement_A_N_2D | Comparison of the Displacement between analytical and numerical 2D statically indeterminate   |
| Attachment N.21 | Statically Indeterminate\Ansys-version_2_self_weight | Calculations in Ansys Workbench   |
| Attachment N.22 | Statically Indeterminate\Train_Faze_1                | Calculations in Ansys Workbench   |
| Attachment N.23 | Statically Indeterminate\Train_Faze_2                | Calculations in Ansys Workbench   |
| Attachment N.24 | Statically Indeterminate\Train_Faze_3                | Calculations in Ansys Workbench   |
| Attachment N.25 | Statically Indeterminate\Train_Faze_4                | Calculations in Ansys Workbench   |
| Attachment N.26 | Statically Indeterminate\deformation_self-wight      | Calculation of statically indeterminate variant in Maple software   |

|                 |  |  |
|-----------------|--|--|
| Attachment N.27 | Statically Indeterminate\self-weight_normal_forces_nominal_stresses  | Calculation of statically indeterminate variant in Maple software                        |
| Attachment N.28 | Statically Indeterminate\Deformation_with_train_faze_1               | Calculation of statically indeterminate variant in Maple software                        |
| Attachment N.29 | Statically Indeterminate\train_faze_1_normal_forces_nominal_stresses | Calculation of statically indeterminate variant in Maple software                        |
| Attachment N.30 | Statically Indeterminate\Deformation_with_train_faze_2               | Calculation of statically indeterminate variant in Maple software                        |
| Attachment N.31 | Statically Indeterminate\Train_faze_2_normal_forces_nominal_stresses | Calculation of statically indeterminate variant in Maple software                        |
| Attachment N.32 | Statically Indeterminate\Deformation_with_train_faze_3               | Calculation of statically indeterminate variant in Maple software                        |
| Attachment N.33 | Statically Indeterminate\Train_faze_3_normal_forces_nominal_stresses | Calculation of statically indeterminate variant in Maple software                        |
| Attachment N.34 | Statically Indeterminate\Deformation_with_train_faze_4               | Calculation of statically indeterminate variant in Maple software                        |
| Attachment N.35 | Statically Indeterminate\Train_faze_4_normal_forces_nominal_stresses | Calculation of statically indeterminate variant in Maple software                        |
| Attachment N.36 | Statically Determinate\Normal_forces_self-weight_s=0_A               | Normal forces and nominal stresses result in self-weight load for S=0. Analytically      |
| Attachment N.37 | Statically Determinate\Normal_forces_TRAIN_1_-weight_s=0_A           | Normal forces and nominal stresses result with train phase 1 load for S=0. Analytically  |
| Attachment N.38 | Statically Determinate\Normal_forces_TRAIN_2_-weight_s=0_A           | Normal forces and nominal stresses result with train phase 2 load for S=0. Analytically  |
| Attachment N.39 | Statically Determinate\Normal_forces_TRAIN_3_-weight_s=0_A           | Normal forces and nominal stresses result with train phase 3 load for S=0. Analytically  |
| Attachment N.40 | Statically Determinate\Normal_forces_TRAIN_4_-weight_s=0_A           | Normal forces and nominal stresses result with train phase 4 load for S=0. Analytically  |
| Attachment N.41 | Statically Determinate\copmarisem_A_N_s=0_normal_forces              | Comparison of the normal forces between analytical and numerical 2D statically Determine |
| Attachment N.42 | Statically Determinate\compairsem_A_N_s=0_Deformation                | Comparison of the Displacement between analytical and numerical 2D statically Determine  |
| Attachment N.43 | Statically Determine\Ansys_self_wight                                | Calculations in Ansys Workbench  |

|                 |   |   |
|-----------------|---|---|
| Attachment N.44 | Statically<br>Determinate\Ansys_Train_faze_1_s=0                                      | Calculations in Ansys Workbench                                 |
| Attachment N.45 | Statically<br>Determinate\Ansys_Train_faze_2_s=0                                      | Calculations in Ansys Workbench                                 |
| Attachment N.46 | Statically<br>Determinate\Ansys_Train_faze_3_s=0                                      | Calculations in Ansys Workbench                                 |
| Attachment N.47 | Statically<br>Determinate\Ansys_Train_faze_4_s=0                                      | Calculations in Ansys Workbench                                 |
| Attachment N.48 | Statically<br>Determinate\urcita_soustava_self_wight_deformation                      | Calculation of statically determinate variant in Maple software |
| Attachment N.49 | Statically<br>Determinate\urcita_soustava_self_wight_normal_forces_nominal_stresses   | Calculation of statically determinate variant in Maple software |
| Attachment N.50 | Statically<br>Determinate\urcita_soustava_Train_faze_1_deformation                    | Calculation of statically determinate variant in Maple software |
| Attachment N.51 | Statically<br>Determinate\urcita_soustava_Train_faze_1_normal_forces_nominal_stresses | Calculation of statically determinate variant in Maple software |
| Attachment N.52 | Statically<br>Determinate\urcita_soustava_Train_faze_2_deformation                    | Calculation of statically determinate variant in Maple software |
| Attachment N.53 | Statically<br>Determinate\urcita_soustava_Train_faze_2_normal_forces_nominal_stresses | Calculation of statically determinate variant in Maple software |
| Attachment N.54 | Statically<br>Determinate\urcita_soustava_Train_faze_3_deformation                    | Calculation of statically determinate variant in Maple software |
| Attachment N.55 | Statically<br>Determinate\urcita_soustava_Train_faze_3_normal_forces_nominal_stresses | Calculation of statically determinate variant in Maple software |
| Attachment N.56 | Statically<br>Determinate\urcita_soustava_Train_faze_4_deformation                    | Calculation of statically determinate variant in Maple software |
| Attachment N.57 | Statically<br>Determinate\urcita_soustava_Train_faze_4_normal_forces_nominal_stresses | Calculation of statically determinate variant in Maple software |
| Attachment N.58 | S=0, released nodes   | Relaced nodes and equations of static determinate structure     |
| Attachment N.59 | S=0, 3D   | Calculations in Ansys Workbench, for 3D model                   |
| Attachment N.60 | Train_Faze_4_s=10, 3D   | Calculations in Ansys Workbench, for 3D model                   |